C.P. No. 1093

C.P. No. 1093

MINISTRY OF TECHNOLOGY

AERONAUTICAL RESEARCH COUNCIL

CURRENT PAPERS

An Investigation of the Scatter in Constant Amplitude Fatigue Test Results of Aluminium Alloys 2024 and 7075

by

A. M. Stagg

Structures Dept., R.A.E., Farnborough

LONDON: HER MAJESTY'S STATIONERY OFFICE

1970

PRICE £2 17s 0d [£2·85p] NET

U.D.C. 620.178.3 : 539.431 : 669.715

C.P. No. 1093*
April 1969

AN INVESTIGATION OF THE SCATTER IN CONSTANT AMPLITUDE FATIGUE TEST RESULTS OF ALUMINIUM ALLOYS 2024 AND 7075

by

A. M. Stagg

Structures Dept., R.A.E., Farnborough

SUMMARY

A brief review of some of the investigations that have been conducted in the past into the form of the distribution of constant amplitude fatigue test results is presented and is followed by an analysis of a large amount of constant amplitude data for 2024 and 7075 materials collected from a variety of sources. This analysis, in terms of a log-normal distribution of life, confirms that the amount of scatter obtained in fatigue results increases with a decrease in the alternating stress amplitude. Further, a comparison of the scatter for the two materials is made and the effects on the scatter of such parameters as notch acuity and mean stress are investigated. The discussion is in terms of a simplified model of the fatigue mechanism and indicates a possible correlation between the amount of scatter and the number of crack nuclei present in a specimen.

---

* Replaces R.A.E. Technical Report 69075 - A.R.C. 31800.

CONTENTS

1 INTRODUCTION

The efficiency of a structural design is as dependent on the accuracy and precision of the available knowledge about the properties of the materials employed as on the method of design. However, by no means all material properties exhibit a strict one to one relationship with the imposed macroscopic test conditions. The internal microscopic conditions within nominally identical specimens depend not only on the external macroscopic restraints but also on such inherent factors as the size, shape and orientation of grains, dislocation density and precipitate dispersion. The degree of sensitivity of a property to these inherent characteristics decides the method of treatment of the property.

Provided there is a sufficient degree of accuracy of measurement all the properties can be related to the microscopic rather than the macroscopic conditions. Some properties, e.g. density, are relatively insensitive to the changes in microscopic conditions caused by the inherent material characteristics and so, unless very precise measurements are taken, a unique value is assigned to these properties for each set of macroscopic conditions. Other properties on the other hand, e.g. tensile strength, are more sensitive to the microscopic conditions and a distribution of values of the property, one for each set of microscopic conditions, is obtained for each combination of macroscopic restraints. A detailed knowledge of this distribution is then necessary for efficient design, where a 'detailed knowledge' is understood to mean a knowledge not only of the form of the distribution but also of all the parameters necessary to define the distribution for each set of macroscopic conditions.

Fatigue endurance, or strength, is one of the many properties that are sensitive to microscopic conditions and so the results of macroscopic fatigue tests always exhibit a degree of scatter that is inherent in the material, whilst additional scatter, caused by the testing procedure, increases the final observed scatter of a set of fatigue test results. By analysing the 'apparent' scatter for results obtained from different sources, for various types of specimens under diverse forms of loading and a variety of loading conditions, the varying amounts of scatter obtained might help in pinpointing the chief sources of scatter and the degree of scatter that can be attributed to each source. To this end a large amount of data on the fatigue test results of simple laboratory specimens of two aluminium alloys under constant

amplitude loading conditions was collected from a number of sources. The two aluminium alloys considered, 7075 and 2024 materials*, were selected primarily because the former is a zinc bearing alloy whilst the latter is copper bearing and it was thought that this might cause differences in behaviour of the two types. Also, however, these two alloys are the materials most commonly used in aircraft and a large amount of data was available from research programmes into their fatigue properties. The only criterion adopted in the collection of this data was that a sufficient number of specimens had been tested under the same conditions to allow a meaningful statistical appraisal. The analysis of this data is presented below.

2 A REVIEW OF PREVIOUSLY USED FATIGUE FAILURE DISTRIBUTIONS

The form of the distribution function of times to fatigue failure under constant amplitude loading has been investigated by many experimenters, one of the earliest studies being that by Muller-Stock in 1938 [1]. The frequency distribution of his results for the fatigue life of ST-37 steel specimens in rotating bending is decidedly skew with respect to the number of cycles to failure (Fig.1), but if analysed in terms of the logarithm of the life to failure, the results conform to a symmetric normal distribution[2]. The same data is analysed by Weibull[3] according to his own distribution, and comparison between the expected and observed values show his distribution also to provide a good fit with the experimental data.

Since 1938 several forms of distribution have been applied to constant amplitude fatigue results, but of these the log normal distribution, whereby the logarithm of the life to fatigue failure is assumed to have a normal probability density function, is by far the most commonly adopted. Stepnov[4] goes one step further and considers the distribution of the logarithm of $(N - N_o)$ to be normal, where N is the life of a specimen and N_o is a threshold life below which the probability of failure is zero. In comparison the threshold life for a simple log-normal distribution is at zero cycles, whilst a normal distribution can theoretically lead to negative lives for low probabilities of failure.

A finite lower life limit also appears in the distribution derived empirically by Weibull[5] that was mentioned earlier, but the basic shape is no longer normal. This same distribution occurs in Refs.6 and 7 as well, where Gumbel establishes theoretically the distribution of the extreme values from any parent population. In this case it appears as Gumbel's third

---

* The composition and specification of these two alloys are given in the table at the end of the Appendix.

asymptotic probability distribution of smallest values, the most general form of which requires three parameters for its definition, one parameter corresponding to the threshold life. In the earliest application of this distribution to fatigue lifing, however, Freudenthal and Gumbel[8] reduced the number of parameters to two, thereby eliminating the threshold life.

Several distributions other than those mentioned above have been developed (e.g. Refs.9, 10 and 11) but these in general require additional parameters for their definition and thus the analysis of experimental results becomes more complex and further degrees of freedom are absorbed. A brief review follows of some of the investigations that have been made into the form of the probability density function of lives to fatigue failure, whilst Fig.2 presents a comparison of representations of the data for one stress level from Ref.12 in terms of four different distributions each defined by two parameters, i.e. the normal and two parameter Gumbel distributions of both cycles and log-cycles. The results from Ref.12 were chosen as being the largest available set of results for a homogeneous sample of specimens of which all the members failed. It is of interest to note in Fig.2 that in the range of probabilities of survival between 90% and 10% all four representations give good agreement and that outside this range the log-normal distribution appears, in this case, to give the best fit to the data.

Plunkett[13]; Stulen[14]; Pope, Foster and Bloomer[12]; Liu and Corten[15]; Sinclair and Dolan[16] and Freudenthal[17] are amongst those who found that over the central portion at least the log-normal distribution provides a good fit for constant amplitude fatigue data, the range of this central portion being defined as between failure probabilities of 0.01 and 0.09 in Ref.16 and between 0.05 and 0.95 in Ref.17. Sinclair and Dolan[16] also analyzed their results for 174 specimens of 7075 alloy at six stress levels in terms of the Gumbel two parameter and Weibull three parameter distributions and found that Weibull's three parameter distribution gave the best fit throughout the stress range, whilst of the distributions defined by two parameters the Gumbel form gave a better fit than the log-normal distribution at the lowest stress level but a worse fit at the higher stress levels. In all cases extrapolations of the distributions to the low probability end intersected one another thus producing the anomaly that below this probability those specimens tested at a low stress would have a shorter life than those specimens under a high stress level.

Swanson[18,19] and Impellizzeri[20], who provides a review of the results of Refs.21, 22 and 23, both found that the log-normal distribution was

satisfactory at all but the low stresses and that the use of an extreme value distribution produced no benefit. Swanson reanalyzed his low stress results and those of Webber and Levy[24] in terms of two log-normal distributions at each stress level and obtained a good fit, as did Cicci[25] using the same procedure. Cicci went on to compare the representations of his data in terms of the log-normal, extreme-value and Maxwell-Boltzman distributions and concluded that two log-normal distributions gave the best fit with his test results.

A difference in the form of the distribution of life for notched and unnotched results was suggested by Plantema[26] who claimed that a normal distribution of either life or log life fitted his unnotched data equally well, whilst his notched data conformed to neither representation. No alternative function was suggested for these latter results, but Bastenaire[27] considered the distributions of log-life, of the reciprocal of life and of powers of the reciprocal of life in fitting other experimenters' results, and decided that the distribution of stress at constant life could be considered normal (Fig.3) whilst the distribution of log life at the higher stresses is very nearly normal. Although the conversion of conventional fatigue data into a form suitable for analysis in terms of a distribution of stress at constant life required the assumption of a mean S-N curve shape this approach was also adopted by Westland Aircraft Ltd[28] and by Albrecht[29], who decided that the distribution of stress at constant life was normal for smooth, non-fretted components, but log-normal for concentrated, fretted components. Westland's[28] initially considered the distribution of stress at constant life to be log-normal and then in an addendum to Ref.28 examined the possibility of a truncation both of this distribution and of that of endurance at constant stress, in the region around three standard deviations below the mean. More recently[30] they have compared the normal, log-normal and three parameter Weibull representations of the distributions of stress at constant life obtained from a series of fibre glass specimens but no decision was reached as to which was the most suitable form. Weibull himself[31] compared four distributions of cycles namely (a) normal, (b) log-normal, (c) three parameter Weibull and (d) three parameter Weibull for log-cycles and concluded that the log-normal distribution did not provide a good fit, whilst a choice as to which of the others was the best was impossible without increasing the number of specimens tested. In the many reports he has written Weibull sometimes analyzed his results in terms of a distribution of stress[5,32,33,34] whilst at other times his analysis was in terms of a distribution of cycles[31,33,35], but

in either case he claimed a better fit for his own three parameter distribution than for the log-normal distribution with its two parameters, without deciding whether the Weibull shape should be applied to a distribution of cycles or to a distribution stress[33]. Unfortunately the results of tests on 1088 specimens of 24S-T alloy presented by Weibull[36] do not lend themselves to analysis in terms of a distribution of life, as the variation in specimen axis with respect to the direction of rolling separates the specimens into four distinct populations in each of which only about half were tested to failure, the rest being run outs. Other experimenters, e.g. Pope, Foster and Bloomer[12] and Freudenthal and Gumbel[8,37,38,39] have also analysed their results in terms of the three parameter Weibull-Gumbel shape of distribution and found good agreement with their data as is provided by the log-normal distribution as well, but as in all the previous reports the sample sizes were not large enough to reach definite conclusions.

A number of investigators realizing this need for a larger population to define the form of distribution more accurately have contrived by various means to collect and standardize data from different sources for various types of specimens and loading levels. Examples of this method are provided by Refs.21, 40, 41 and 42 in all of which a log-normal distribution of life was shown to be a good approximation even for the 1157 specimens collected in the first of these references. Kaechele[43] also used this approach of data standardisation and his resulting distribution for 163 specimens approximated to the log-normal distribution in the central range but tended to pull away from it into the higher probability region towards the lower tail of the distribution, whilst the shape derived by Abelkis[11] was definitely not log-normal, a fact which, in view of the method of grouping and standardization of data employed in its derivation, is perhaps not surprising.

3 SELECTION OF A DISTRIBUTION

Whilst not as closely obeyed as some workers in the fatigue field believe, the log-normal distribution of life at constant stress was adopted as the foundation of this analysis for several reasons:

(1) The data reviewed above indicated that the discrepancies between practice and the log-normal distribution are small in the range $0.95 > P > 0.05$.

(2) The mean and variance of a log-normal distribution provide the basis for a readily comprehensible comparison of the positions and extents of

the distributions obtained under different loading conditions using various forms of specimen.

(3) The use of a normal form of distribution, rather than any other basic type, considerably eases the analysis of the data without impairing the validity of the conclusions.

(4) The analysis in terms of a log-normal distribution of life at constant stress involves no graphical procedures and thus is exactly reproducible.

These four arguments in its favour, together with the fact that the review of data that starts this publication showed no tendency for any one particular frequency distribution defined in terms of only two parameters to give a consistently better fit with observed values than any other, led to the adoption of the log-normal distribution of life at constant stress as the basis of the analysis that follows.

4 DEFINITION AND DERIVATION OF TERMS

The normal distribution is defined by the probability density function

$$p(x)\,dx = \frac{1}{\sqrt{2\pi\sigma^2}} \exp - \tfrac{1}{2}\left(\frac{\mu - x}{\sigma}\right)^2 dx$$

where $p(x)\,dx$ is the probability of occurrence of the event between conditions x and $x + dx$ and μ and σ are the population mean and standard deviation respectively. When a normal distribution of the logarithm of the number of cycles to failure is used, the above expression must be replaced by

$$p\,(\log N)\,d\,(\log N) = \frac{1}{\sqrt{2\pi\sigma^2}} \exp - \tfrac{1}{2}\left(\frac{\mu - \log N}{\sigma}\right)^2 d\,(\log N)$$

where μ and σ are now the mean and standard deviation of log(life) and N is the number of cycles to failure of a randomly selected specimen.

The best estimates of μ and σ that can be obtained from a sample of n test specimens are given by

$$m = \overline{\log(N)} = \frac{\sum_{r=1}^{n} \log N_r}{n}$$

and

$$s = \left\{ \frac{\sum_{r=1}^{n} (\log N_r)^2 - n\,(\overline{\log N})^2}{n - 1} \right\}^{\frac{1}{2}}$$

where it is to be noted that the unbiassed estimate of the standard deviation is used as the number of specimens tested under one set of conditions is generally small. These two parameters are enough by themselves to define the normal distribution, but sometimes another parameter, the coefficient of variation v is used. Any two of those three parameters μ, σ and v are sufficient to define the normal distribution, for the coefficient of variation is defined by the expression

$$v = \frac{\sigma}{\mu}$$

while the estimated coefficient of variation as used in this publication is defined as the ratio of the estimated standard deviation to the estimated mean, i.e. $v_{estimate} = \frac{s}{m}$.

In the course of this publication confidence limits on the estimated standard deviation will be required. These limits are derived using Table 8 'The percentage points of the χ^2 distribution' from 'Biometrika Tables for Statisticians' edited by E. S. Pearson and H. O. Hartley, Vol. I and the levels used will be 90% and 95%.

5 DEPENDENCE OF SCATTER ON STRESS LEVEL

Perhaps the most basic parameter in constant amplitude fatigue testing is the magnitude of the alternating stress at which the test is conducted. Many components are tested at only one constant amplitude stress level, the results providing an estimate of the mean life and the scatter about the mean life at that stress level. The mean life can then be related to the mean life at any other stress level by the adoption of a standard stress-cycle curve shape. But what relationship exists between the scatter at one stress level

and that at any other stress level? The first part of the analysis that follows investigates this question.

5.1 General trend

In this section the overall trend of the magnitude of the scatter associated with constant amplitude testing is studied to determine whether the magnitude of the scatter (a) increases, (b) decreases or (c) is unaltered with an increase in the test stress level. A comparison is made within the results of each experimenter to decide whether there is any statistically significant change in the amount of scatter obtained under different levels of constant amplitude loading.

The variance ratio F defined as $F = \frac{(\sigma_1)^2}{(\sigma_2)^2}$, where σ_1, σ_2 $(\sigma_1 > \sigma_2)$ are the two sample estimated standard deviations, is taken as the basis of this test, (the two samples applying to two different stress levels). The null hypothesis tested is that the two samples were drawn at random from normal populations of equal variance. Table 4 (Ref.44) gives values of F at various levels of significance such that if the appropriate value of F is exceeded the null hypothesis is contradicted and the two samples of which the standard deviations are being compared can be said at the appropriate level of significance to be taken from different parent populations.

The comparisons are restricted to be within each experimenter's results in order to reduce the possible causes for any trend observed. The factors minimised by this restriction are

(1) Changes in material composition from one laboratory to another. The changes in material composition from specimen to specimen taken from the same billet or batch, which are one of the possible causes of scatter in fatigue, are not affected by this restriction.

(2) Differences in specimen configuration from one laboratory to another. Such factors as surface finish, machining direction, and the shape of the specimen itself are likely to vary more between laboratories than within the one laboratory.

(3) The specimen test method. No comparisons are made between two different methods of loading, e.g. tension-tension is not compared with rotating bending or unclamped with clamped etc.

The individual results of each comparison are too numerous to be printed here, however the general picture obtained is as follows:-

Over 700 comparisons were made at the 5% level of significance. Of these 322 gave significantly larger variances for the lower stress, 26 gave significantly lower variances for the lower stress and the remainder were undecisive. The reason for this large number of undecisive cases is that in general the sample size is statistically small, down to 4 and 5 at times. This means that the values of F required to be significant were on occasion as high as 9 and 10.

These results indicate that the general trend is an increase in the standard deviation with a decrease in alternating stress level. The 26 cases that contradict this trend were restudied and it was found in 23 cases that the lower of the standard deviations in the comparison is below the general level of the surrounding standard deviations, whilst the greater of the two standard deviations fits in with the general trend. This indicates the possibility that these 23 cases were caused by the results being too consistent and could be purely fortuitous events. Three cases are still left unexplained, in none of which is the number of specimens in a sample greater than 5. These results could be indicative of a real discrepancy in the general trend or alternatively it is possible that they, forming such a small fraction of the total number of comparisons, might be expected, being extreme values of a stochastic variable.

This general increase in the amount of scatter with a decrease in the alternating stress was observed by Sinclair and Dolan[16] and by Kaechele[43], who analysed the results of Ref.15 into a suitable form. Schjve and Jacobs[45] also noted this effect although their analysis used the coefficient of variation as a measure of the scatter present rather than the standard deviation.

5.2 Form of stress-scatter relationship

The analysis in the above section gives encouragement to the idea that there is a general trend, whereby the standard deviation of the distribution of fatigue lives to failure increases with a decrease in stress level. Assuming that this trend is present the next step is to attempt to generalise this trend by finding an analytical expression that describes the relationship between the magnitudes of the standard deviation and the alternating stress level throughout the stress range.

Sinclair and Dolan[16] indicated that an expression of the form $\sigma = \sigma_o S^{-k}$ fitted their results for 75S-T6 unnotched specimens in rotating bending (in this case σ and σ_o are standard deviations, S is the alternating stress level). However, an expression of the form $\sigma = ae^{-bS}$ was thought to be an equally likely alternative to the form employed by Sinclair and Dolan (a and b are constants, whilst e is the base of the natural logarithms).

The aim of this part of the analysis is to decide if either of these forms fitted the results that had been accumulated and to note any possible trends in the values of a and b or σ_o and k discernible from the results. It must be appreciated that either of these expressions, if suitable at all, can apply only over a limited range of values of stress. Consider a value of stress just below the upper boundary of the fatigue limit band, at which the probability of failure is p. If 100 specimens are tested, approximately $100p$ will fail at this stress whilst the others will remain unbroken for however long the test is continued. It is thus impossible to assign a meaningful value to the mean or the standard deviation of the distribution of fatigue lives in this zone. Despite this limitation it was thought that the analysis might prove fruitful.

The analysis takes the form of a simple linear regression of the results into the forms

(1) $\log \sigma = \log \sigma_o - k \log S$

(2) $\log \sigma = \log a - bS$.

The scatter of the plotted points about the regression line, determined by the method of least-squares, is taken as a basis for an approximate comparison of the two representations. In both cases stress is taken as the independent variable and so both scatter values are in terms of $\log \sigma$ and are thus directly comparable.

If the true line of regression is given by $y = A + Bx$ then the best estimates of A and B, α and β respectively are given by Ref.46 as

$$\beta = \frac{n\sum_{i=1}^{n}(X_i Y_i) - \sum_{i=1}^{n}(X_i)\sum_{i=1}^{n}(Y_i)}{n\sum_{i=1}^{n}(X_i)^2 - \left(\sum_{i=1}^{n}X_i\right)^2}$$

$$\alpha = \frac{1}{n} \sum_{i=1}^{n} (Y_i) - \beta \cdot \frac{1}{n} \cdot \sum_{i=1}^{n} (X_i)$$

and the best estimate of the deviation from the regression (treating x as the independent variable) is given by

$$s^2_{YX} = \frac{1}{n-2} \left\{ \sum (Y_i)^2 - \alpha \sum (Y_i) - \beta \sum (X_i\ Y_i) \right\}$$

where n is the number of points under consideration.

The values of the standard deviation of the fatigue failure times being used in this analysis are only the best unbiassed estimates that can be obtained from samples of very limited size and are not population values. Thus even if one of the stress-scatter forms tried were exact the values of standard deviation derived in this analysis would not be expected to lie on the regression line. However, if the same estimates of scatter are assumed to be true population parameters, 90% confidence limits can be calculated for the gradient of the linear regression line to provide some idea of the possible variation that might be present in this gradient. These confidence limits are given by

$$b - t_{s_b} < B < b + t_{s_b}$$

where $S_b = \sqrt{\frac{s^2_{YX}}{\Sigma x^2}}$ and t is the value of Student's 't' distribution at the appropriate probability level and with (n-2) degrees of freedom. When these limits are interpreted the original assumption that the sample estimated standard deviation is the true population parameter must be borne in mind.

The results of this analysis are presented in Tables 1, 1a, 2 and 2a where they have been grouped as much as possible in terms of material, type of test and form of specimen. The most general point to note from these tables is that the gradients are mostly (with two exceptions) negative, thus confirming the trend noticed in section 5.1. The two exceptions to this rule both come from the results of Ref.47 in Tables 1 and 1a which have positive gradients. The values of stress and standard deviation for these two sets of results are given below:-

Ref.47 7075T Stress	Notch radius=0.094 in Standard Deviation	Ref.47 7075T Stress	Notch radius=0.0032 in Standard Deviation
36 ksi	0.506	22 ksi	0.142
32 ksi	0.627	18 ksi	0.136
28 ksi	0.621	13 ksi	0.225
25 ksi	0.165	10 ksi	0.089
22 ksi	0.615	9 ksi	0.136

It can be seen that the standard deviations at the two stresses underlined in the above tables are below the general level of the surrounding standard deviations. If these two values were increased (to the general level) then the gradient of each of the two plots would become negative. Thus a possible explanation of these two positive gradients is the purely fortuitous occurrence of a closely packed set of fatigue results, which is quite possible with only ten results from which to estimate a standard deviation of the fatigue life distribution.

The results from some of the references quoted are presented in Figs.4 to 12, each of which gives four representations of the same data, being respectively:-

(a) Log-standard deviation against log stress level (analysis in sections 5.2 and 5.3).

(b) Log-standard deviation against stress level (analysis in sections 5.2 and 5.3).

(c) Log-standard deviation against log life (analysis in section 6).

(d) Standard deviation against log life (analysis in section 6).

The plots in Figs.4 to 12 were chosen from the total available selection to illustrate the following points:-

(1) The two forms of representation apply to both axial and rotating bending load data.

(2) The two forms of representation apply to both unnotched and notched data under both forms of loading.

The results Sinclair and Dolan obtained in their report[16] are shown in Figs.8a and 8b. Fig.8a is the plot that led them to suggest the form of relationship $\sigma = \sigma_o S^{-k}$, whilst Fig.8b presents their results plotted on a linear-log plot showing the equal validity of the relationship $\sigma = ae^{-bS}$.

The 90% and 95% confidence limits for the standard deviations are shown plotted in all these figures, as is the regression line obtained from a least-squares analysis. The confidence limits for the notched specimen tests are in general broader than for the unnotched specimens simply because fewer notched than unnotched specimens were tested at any stress level.

A comparison of the two methods of representation is made possible by the use of $\log \sigma$ scales in both methods thus making the values of s^2_{YX} directly comparable. Points to be noted in this comparison are:-

(1) The range of gradients in the linear-log plot for 7075 material in rotating-bending is 1:3.52 whilst in the log-log plot it is 1:4.6.

(2) The range of gradients in the linear-log plot for 2024 material in rotating-bending is 1:1.9 whilst in the log-log plot it is 1:1.7.

(3) The scatter about the regression line, as shown by the s^2_{YX} column, are of very much the same order in both representations.

(4) The range of variation of the constant is large in both the representations.

The results of this comparison are neither sufficiently definite nor sufficiently numerous to enable us to reach a conclusion on the relative merits of the two representations. Points (1) and (2) above indicate that possibly a linear-log plot is more suitable for a uniform representation of 7075 data, whilst a log-log plot is more suitable for 24S-T material.

5.3 Effects of other parameters on stress-scatter relationships

Before leaving the results of this analysis of the effect of stress level on scatter, one or two other points are to be noted. Firstly the gradients listed in Tables 1 and 1a, 2 and 2a are of very much the same order for the zinc bearing alloy 7075 as for the copper bearing material 2024. The average gradient for the 7075 material results in unnotched rotating beam testing was -1.85 and the corresponding figure for 2024 material -1.75. However, it is to be noted that whilst the range of gradients for the zinc bearing alloy was 1:4.6, the range for the copper bearing alloy was only 1:1.7, where the range is defined as the ratio of the minimum to the maximum value. This difference in the ranges for the two materials might be attributed to either

(1) the fact that more estimates of the gradient for the zinc than for the copper bearing alloy were available, or,

(2) the fact that the minimum value for the 7075 material happened to be a low estimate, or the maximum value high etc., or,

(3) a fundamental difference between the two materials.

Unfortunately insufficient data are available to test for the origin of the discrepancy.

Secondly, an increase in mean load at constant notch acuity appears to produce a large increase in the negative gradient of a scatter-versus-stress plot (see results for Ref.48 in both 2024 and 7075 material). In Table 1, it can be seen that the 90% confidence ranges on the gradients derived for the results of Ref.48 for mean stresses of 10 ksi and 20 ksi and 0 ksi and 20 ksi do not overlap. This indicates that this apparent trend is most probably not caused by the method of analysis adopted here. It does not show, however, that the effect is not caused by a chance disposition of fatigue results, though this seems unlikely bearing in mind the number of standard deviations that were involved in each gradient determination.

A study of Figs.4 to 12, (a) and (b) shows that there is a tendency in each plot for the standard deviation to reach a limiting value at the higher stress levels. The value of the apparent lower limit thus placed on the standard deviation varies from data source to data source. This tendency to level off is shown in Figs.13a and 14a, in which all the available data on unnotched 7075 and 2024 respectively are combined on a linear-log plot. Two other points are to be noted from Figs.13a and 14a. They are:-

(1) The results from Ref.15 are noticeably lower than the results from the other data sources. There are three possible causes of this phenomenon,

(a) better experimental procedure,
(b) size effect,
(c) less inherent material scatter.

The diameters of the test pieces used by each data source are indicated in the legend to each plot and Ref.15 can be seen to use the smallest diameter.

(2) Also noted in the legend to each plot is the basic form of loading employed, i.e. whether rotating bending or axial loading. In Fig.13a, only one set of axial results is shown and it is to be noticed that these occur at the top of the band of other results. In Fig.14a, two sets of axial results are plotted and here again, though not as markedly as in Fig.13a, the axial results appear generally towards the upper part of the band of results.

A linear regression analysis using the method of least squares was carried out on several groupings of results within Fig.13a and the lines so obtained are shown plotted in that figure. As can be seen the regression line for axial loading is higher than that for rotating bending; both of these lines being higher than the line for Ref.15. The relative positions of these lines are unaltered in the two representations of the data given in Figs.13a and 13b (the latter figure is dealt with later).

A linear regression analysis was similarly carried out on Figs.14a and 14b, although it was recognised that the data contained therein did not comply very well with a linear law. The results obtained are thus of less validity than those for Figs.13a and 13b. However, the lines are in the same relative positions in Figs.14a and 14b again as in Figs.13a and 13b, although the spacing between the lines is not as great.

From these results it appears that the effect of axial loading is to give higher scatter than rotating bending, whether the comparison be made at the same stress level or at the same value of $\log_{10} N$ (under constant amplitude loading).

In Figs.15a and 15b, and 16a and 16b, all the constant amplitude notched data collected for 7075 and 2024 are plotted in the form of log (standard deviation) against stress. The stress used for these notched specimens in an effort to obtain uniformity was the product of the nominal stress and the theoretical elastic stress intensity factor K_t. Points to be noted from these figures are:

(1) There is a tendency for values of σ to level off with increasing stress.

(2) The results fall within a band which includes both the results for 7075 and for 2024.

No trends with notch acuity or form of loading can be inferred from these diagrams.

The tendency of scatter-stress level curves to level off at the higher stress levels and the inability to cope with several different notch acuities on the same stress scale resulted in other forms of scatter relationships being tried, but this in no way detracts from the trends noted in the above stress-scatter analysis.

6 STANDARD DEVIATION - CYCLE RELATIONSHIP

In an effort to obtain a form of plot that was more general in its format than our previous representations (i.e. log σ against stress, and log σ against log stress) it was decided to plot the data in the form of log σ against log N (the log of the number of cycles to failure). The main advantage of a plot of this type is that it is applicable not only to constant amplitude loading but also to all forms of variable amplitude loading, and clearly this form of plot can also cope equally readily with notched as well as unnotched data.

The data already presented in Figs.4 to 12, (a) and (b), are plotted in this new form in Figs.4 to 12, (c), whilst Figs.4 to 12, (d), contain the same data plotted as standard deviation against log N. This latter type of plot was tried when it was found that the log σ against log N plots were reaching a limit for the high values of $\log_{10}N$ as well as for the low values of $\log_{10}N$. The lower limit has already been noticed in the log σ/stress plot for high stress. From the log σ against log N plots, it appeared that the rate of increase of log σ was decreasing rapidly at higher values of log N. It was thought that σ itself might not level off and so plots of σ against log N were tried. It can be seen, however, from these plots, Figs.4 to 12, (d), that there is a tendency for σ itself to level off at high values of log N.

Figs.13 to 16, (b), show the combined results for 7075 and 2024, notched and unnotched, plotted as log σ against log N. In these plots the levelling off at low values of $\log_{10}N$ can be seen clearly, but the limit at high values of log N is lost. It is to be noted that the bands covered in Figs.13 to 16, (b), are similar, thus indicating that the scatter in the zinc based alloy (7075) is similar in magnitude and disposition to that in the copper based material (2024) as was shown in the previous section.

Although an increase in the generality of the plot was achieved by matching standard deviation against cycles to failure, the tendency of the standard deviation to level off at both high and low values of log N suggested that at least one limit would be eliminated if the standard deviation was divided by the mean life, i.e. log N, giving the coefficient of variation.

7 COEFFICIENT OF VARIATION

7.1 The inability to obtain a straight line plot with any of the above forms led to the trial of such plots as log σ against the reciprocal of the

stress, and log σ against the logarithm of log N. Lack of success resulted in the adoption of a different method of attack. In all the earlier plots the value of the standard deviation of a set of fatigue results increases rapidly with the logarithm of the number of cycles to failure. It was thought that perhaps the coefficient of variation as used by Schijve and Jacobs[45] could be more constant with $\log_{10}N$, which was taken as the abscissa on account of its generality of application.

Figs.17 to 27 inclusive give the collected plots in this form for the data presented in Figs.4 to 12, grouped as to material (7075 and 2024), type of loading (axial or rotating bending), notch acuity (notched or unnotched) and form of specimen (bar or sheet).

A cursory inspection of these plots shows that the coefficient of variation increases with an increase in log N. This type of plot does not ameliorate the situation at large values of log N. The coefficient of variation does not necessarily tend to infinity at the upper limit of the endurance limit band, because although the standard deviation becomes infinite in this range so does the mean, and the coefficient of variation itself is meaningless. However, it might well (theoretically) reach a limiting value just above the endurance limit. The apparent trend from these plots is that v (the coefficient of variation) does tend to infinity at large values of log N and reaches a lower limit at low values of log N.

Besides revealing the increase in the coefficient of variation at larger values of log N, Figs.17 to 27 also show that the range of values taken by the coefficient of variation for 2024 material is very much the same as that taken by the coefficient of variation for 7075 material as we concluded from Figs.13 and 14. Again Figs.17 to 27 indicate that axial loading tests seem to entail a greater coefficient of variation at longer lives than is produced by rotating bending tests for both the zinc and copper based alloys in unnotched bar form, while the scatter for axially loaded sheet is the same as that for rotating bending bar tests, both being unnotched. The notched data for both materials appears to give greater scatter at the longer lives than the unnotched data but at short lives the two amounts of scatter agree approximately. The results of Ref.49, Figs.20 and 25, also indicate that possibly an increase in notch acuity leads to a slight decrease in the coefficient of variation, a trend also supported in part by the results of Ref.47, Fig.20.

8 ADDITIONAL RESULTS

Besides the data plotted in Figs.17 to 27 results have been obtained from other references. These results were thought not to be suitable for inclusion in Figs.17 to 27 on the basis that either, (a) very few specimens were tested under each condition, or, (b) the number of stress levels at which the experimenters tested, under otherwise identical conditions, were too few to show any trend with stress level. An analysis of this data in terms of the effects of individual parameters is presented in the Appendix and in the relevant Figs.28 to 46, whilst a synopsis of some possible trends noted is given below.

A little further support is given to the trend indicated in section 7 whereby an increase in notch acuity results in a slight decrease in the coefficient of variation and, in addition, sets of tests in which periods of heating are applied to the specimens give low scatter, as do the few tests of lug specimens analysed. Although the mean stress in the range of values covered by this data produced no marked effect on the amount of scatter present, there was an apparent increase in scatter for lives below 10^4 cycles for some specimens tested under conditions at a constant ratio of minimum to maximum stress. Larger specimens may produce less scatter than smaller ones under the same conditions, whilst the effect of surface finish is not clear, though covering the surface with vaseline and thus keeping more control on the moisture at the crack reduces the scatter, as do various methods of presorting the specimens according to their magnetic, electrical or mechanical properties.

9 DISCUSSION

9.1 The basic fatigue model

The discussion that follows of the results obtained in this Report is based upon a very simplified model of the mechanism of the fatigue process as applied to aluminium alloys. The basic concepts of the fatigue process differ from those advocated by Epremiam and Mehl[2], because their report was concerned with fatigue in steels in which inclusions are known to play a very much more important role in crack initiation than is the case for the aluminium alloys considered here. However, the resultant ideas are similar if the concept of imperfections in Ref.2 is replaced by that of 'sites' developed below. The model adopted seems to be the most likely and in fact its use explains several of the trends noted in the Report, but in one

particular situation, the comparison of the scatter of axial test results with the scatter of rotating bend tests, this model forecasts a trend opposite to that which is observed. Despite this failure, these concepts were adopted in this discussion, because there is a fair amount of evidence, though some of it is indirect, to support the proposed model.

In general, the fatigue life of a metal has until recently been defined in terms of two stages; (1) the initiation or nucleation of the crack, and, (2) the propagation period, in which the length of the crack increases, leading to final failure. This separation into two stages, although arbitrary in that no definition or determination of the boundary between the two periods is possible, is sometimes useful as it provides a method of distinguishing between two apparently different physical phenomena. However, Forsyth[50] defines the growth of a crack in terms of two stages in which two quite distinct growth mechanisms are employed. In Stage 1 the crack growth takes place in the shear mode (the mechanism of initiation belongs to this stage) whilst in Stage 2 growth follows the tensile mode. The relative amounts of Stage 1 and Stage 2 growth mechanisms depend upon the stress applied and the specimen configuration, and in some cases Stage 1 is either so short as not to be distinguishable or it does not take place at all.

The most common mechanism of crack initiation in the two aluminium alloys considered in this Report, 2024 and 7075, at room temperature and in unnotched form, is thought to be related to the occurrence of cyclic slip along closely packed parallel planes within the grains of a metal. This cyclic slip, believed to be caused by dislocation or vacancy movement, results in the extrusion of thin tongues or the intrusion of hollows on the surface of the metal and these formations, of which the surfaces are planes of slip within the grain, then act as sites from which fatigue cracks may propagate. The mode of propagation of cracks from these sites can be either Stage 1 in which the crack continues along the slip band, or Stage 2 in which the crack changes direction, usually at an obstruction such as a grain boundary, a particle of precipitate or an inclusion, and then propagates approximately normally to the direction of stress.

In any metal the grains, of which the material is an aggregate, will be orientated in all directions, although due to some process in the production such as rolling or extrusion, one orientation may be favoured and the general trend will then be biassed in this direction. Thus the slip planes in those grains at or near the surface, which are the only grains in which

cracks will start, as in them cyclic slip will be less hindered than in the body of the material[51], will be orientated in various directions to the applied stress and so the shear components of stress resolved over the slip planes will vary from grain to grain. Similarly the strength of grains in this shear direction will be different for each grain as it will depend on such variables as the grain size, the presence of dislocations, vacancies and inclusions, the grain boundary shapes, the dispersion of different phases and the variation of chemical compositions within the grain. The result of all these variabilities will be a distribution of active sites, that is of planes on which slip will occur, over the surface of the metal, and also a distribution of the relative effectiveness of these active sites, where the effectiveness is to be taken as a measure of the quickness of initiation of a crack. For each apparently identical specimen these two distributions will be different and the fatigue life of these specimens will thus exhibit scatter.

Before the specific effect of various test parameters on this model is considered, the general result of increasing the number of active fatigue initiation sites in a specimen is discussed. Using the concept of the effectiveness of an initiation site, the fatigue life of a specimen will be governed by the most effective site present. The likely distribution of this most effective site could be calculated if the total number of sites present and the distribution of individual effectiveness were known. However, in general, the mean and standard deviation of the distribution of the 'best-of-n' will be higher and lower respectively than the corresponding parameters for the 'best-of-(n-1)' distribution, and so an increase in the number of active sites without any other accompanying changes will decrease the mean life, by increasing the mean effectiveness, and at the same time decrease the scatter of the fatigue life.

The basic mechanism of fatigue described above has been that developed from metallurgical research on unnotched specimens. The mechanism that occurs in notched specimens is not as well known, but it appears that in the presence of a notch the Stage 1 mode of crack growth is restricted, possibly by the adverse stress gradient introduced by the notch, and that the relative length of the Stage 1 mode is shortened, and in some cases this mode may not occur at all. However, the results of Heath-Smith and Kiddle[52] for notched specimens (K_t = 2.3, and K_t = 2.4) of an Al 6% Cu alloy show that even in notched specimens nucleation can occur at several points along the stress concentration in one specimen, or in other words that there is a

distribution of active sites in a notched specimen as well as in an unnotched specimen. Clearly, whatever the mechanism of initiation or growth employed in notched specimens, some grains whether by orientation or inherent weakness will be more susceptible to cracking than others and those grains at the root of the notch where the stress is considerably higher than elsewhere in the specimen are likely to produce the most effective positions or sites for crack growth. So the fatigue model can again be represented by a distribution of active sites, (in the notched case this is a distribution at or near the root of the notch), and a distribution of the relative effectiveness of these active sites. The same model thus applies to both notched and unnotched specimens, although the basic microscopic phenomena behind the model may or may not take different forms for the two cases.

9.2 Effect of stress amplitude

In terms of the above model of the fatigue process, an increase in the amplitude of the cyclic stress would be expected to increase the number of active sites. For any one particular specimen the resolved component of the applied stress on each and every slip plane, in unnotched specimens, and along or across every plane or direction, for notched specimens, will be increased and so more sites will become active. Not only that but each site would become more effective at the higher stress level because of faster dislocation and vacancy movement, more rapid strain-hardening etc. and the expected overall result would be a reduction in mean life accompanied by a reduction in scatter at the higher stress level as noted in section 5 of this Report. As the number of available sites becomes greater the effect of further increasing that number will become smaller in that those already present will be quite adequate to provide a quick failure usually. However, the increase in effectiveness of the sites at the higher stress level will still further reduce the mean, without appreciably diminishing the scatter. When the number of active sites available are few and of small effectiveness, as is the case at low stress levels, the addition of just one other active site would have a considerable effect on the scatter and on the mean life, and so we should expect the scatter to fall of rapidly with an increase in stress at low stress levels and also for the mean life to be very sensitive to stress at the lower stress level end of the S-N curve. The latter is a well known trend and the former is shown in the form of Figs.17 to 27.

The sites of crack nucleation or initiation produce areas which are recognisable by a macroscopic study of the final fracture surface, for they

have a distinctive metallurgical appearance. The increase in the number of active sites with an increase in stress amplitude has been noted experimentally by Heath-Smith and Kiddle[52] in HID 54 aluminium alloy, and in several other aluminium alloys (data yet to be published), by Swanson[18] in 2024 alloy and by Webber and Levy[24] in DTD 683 alloy. Although the most effective site causes failure, other sites may have been effective before final failure occurs, in that cracks may have originated at them after the crack that causes failure has originated at its source. This crack that produces the final failure will engulf the subsidiary cracks in its propagation but the distinctive appearance around the active site will remain and be visible after final failure. The results of Heath-Smith and Kiddle[52] and Swanson[18] are plotted in Fig.47, as standard deviation of logarithmic life against the average number of nuclei or sites per specimen measured after failure of the specimen. From this plot it can be seen that the axial constant amplitude data for 4 different aluminium alloys, for several different types of test specimen (lugs, unnotched and two notch severities) and even specimens that have had a period of heat applied, all correlate and that the scatter in the test results is only high when the number of nuclei present is small, as would be expected if the model adopted in this Report holds good. As soon as the number of nuclei present increases, the scatter decreases. Fig.48 is also of interest as it presents a plot of the number of nuclei per specimen found in Swanson's results[18] for axial unnotched 2024 against the log-life. The two other lines of this figure will be dealt with in the next section. It is of interest to note that the number of nuclei approaches 1 in the region of a life of 10^6 which is the life at which the scatter in Fig.24 suddenly increases and is also the region where the S-N curve produces some non-failures, i.e. specimens in which no sites are present. It is in this area that Swanson noted the bimodal phenomenon which might be explained in terms of those specimens having just one nuclei on the one hand and on the other those having more than one nuclei.

9.3 Effect of notch acuity

Fig.48, which was introduced above in connection with unnotched data, also contains two plots of the number of nuclei per specimen for axially loaded notched specimens (K_t values 2.3 and 3.4) of 2024 material from Kiddle (unpublished as yet). A comparison between the three lines on the figure shows that for the same life, below 10^5 cycles, the $K_t = 3.4$ notch produces most sites, with the unnotched specimen having fewest. In this region of lives, however, the sites are plentiful and so the effect on scatter of the various number of nuclei would be expected to be small.

Above 10^5 cycles it appears that the sharper notch still produces more nuclei than the blunter notch although both produce few nuclei above 5×10^5 cycles, whilst the number of sites produced in unnotched specimens appears to reduce more slowly than in notched specimens and in fact there may be more sites per specimen in an unnotched than in a notched specimen at lives between 5×10^5 and 10^7 cycles.

A possible explanation of this phenomenon could be that in the notched specimens only a few grains are in the area of the stress concentration and so could produce cracks, but of these few because the stress is high in this area a large proportion will be suitable for starting a crack. In an unnotched specimen, however, the number of grains available for crack initiation is larger but in only a few of these will the stress be large enough. As the stress level decreases the number of active sites will fall off more rapidly in the notched specimen because there are fewer suitable sites and because the stress at the root of the notch decreases more rapidly than in the unnotched specimen, and eventually the unnotched specimen may have more active sites than the notched specimen. Clearly the number of available sites is the same for two different notch acuities if the design of the specimen is such that the length of the root of the stress concentration is equal in the two cases, but because the sharper notch involves a higher stress the number of nuclei would be expected to be greater than for the blunter notch as is the case of Fig.48.

So a sharper notch will always give more nuclei than a blunter notch, whilst an unnotched specimen will give fewest nuclei at low lives but as the length of life increases the number of sites will gradually approach that for the notched specimens and indeed may become larger. The blunter notches, provided the notch is sharp enough to restrict the area affected by the stress concentration, will thus reach the condition of having only 1 or 2 nuclei at the shortest lives. The sharper notches will achieve this condition next and the unnotched specimens, last of all. Assuming a correlation between the number of nuclei and the amount of scatter this would result in the scatter being indistinguishable between notched and unnotched specimens for mean lives up to about 10^5 cycles and after that the blunter notch would be slightly more susceptible to scatter than the sharper notch until about 10^6 cycles when all notch acuities would be equally susceptible. The unnotched specimen, however, would be less likely to exhibit a large amount of scatter than the notched specimens above about 5×10^5 cycles but eventually the scatter in the unnotched specimens would be likely to be equally as high as for the notched specimens. These trends agree with those shown in Figs.17 to 27 and

presented more simply in Figs.49 and 50 for a comparison between notched and unnotched data and also with the effect of notch acuity noted in section 7.

The evidence in the literature on the effect of a notch on the scatter in fatigue is very meagre and inconsistent. Albrecht[29] and Petersen (in Ref.2) both found that the coefficient of variation of stress is higher for notched than for unnotched specimens which implies that the coefficient of variation for log-life will also be higher. Ford, Graff and Payne[21] on the other hand say that there is a highly significant difference between the standard deviations of plain and notched specimens, with more scatter in the fatigue life of plain specimens. Values of standard deviation

$$= 0.2995 + 0.1442\ (\overline{\log N} - 5.72) \quad \text{(plain)}$$

and

$$= 0.132 - 0.042\ (\overline{\log N} - 5.17) \quad \text{(notched)}$$

are quoted in Ref.21 showing a slight decrease in standard deviation with an increase in log-life for notched specimens but an increase for unnotched specimens.

9.4 Effect of the method of application of the load

From Figs.49 and 50, it appears that tests on unnotched bar specimens of both 2024 and 7075 under a rotating cantilever form of loading produce less scatter than tests under axial loading on bar specimens, whilst axial tests on sheet material give much the same scatter as rotating beam tests on bar specimens. For 7075 material, notched rotating beam bar specimens give the same scatter as notched axial sheet with no data available on notched axial bar, whilst for 2024, notched axial bar and sheet give the same scatter but notched rotating beam appears to give less scatter, although only a few points are available to substantiate this trend. As no difference has been noted in the trends in scatter followed by these two materials so far, it seems not unlikely that, in fact, all three configurations give the same scatter as one another in notched form. This might be expected, for in the presence of a notch only those grains at the root of the notch could become active sites and from Fig.48 it was seen that in notched specimens the number of active nuclei falls off rapidly with a slight increase in life. Thus the difference in length of the root of the notch with the possibly smaller number of associated sites between the sheet specimens and the bar specimens would be expected to have little discernible effect on the scatter, as the lives for which the scatter would be expected to increase rapidly would differ only slightly for the two cases.

However, this does not explain the difference in scatter noticed between axial and rotating beam tests of unnotched specimens. In these two forms of test the stresses at the surface of similarly shaped specimens are inversely proportional respectively to the square and to the cube of the cross-sectional dimension. This implies that a longer length of a specimen would be highly loaded in an axial rather than in a rotating bend test. Also, whereas the cross-sectional area was constant throughout the gauge length for all the axial test specimens the results for which are presented in Figs.17 to 27, the radius of the rotating bend tests varied continually along the specimen reaching a minimum at one position only. It would thus be expected that at the same stress level more sites would be active in axial than in rotating bending testing, producing a lower mean life and less scatter. The lower mean life in axial than in rotating bending tests has been verified experimentally, e.g. Templin[53], and Heywood[54], but the smaller scatter expected in the axial type of test disagrees with the trend indicated in this Report. Unfortunately, no data on the number of nuclei obtained in rotating bending unnotched material could be found and so no comparison of the relative number of nuclei present in the two forms of loading is possible.

The two types of unnotched test differ in several particulars, examples of which are:-

(1) Initiation in rotating bending takes place in a stress gradient, which does not exist in an uncracked axial specimen.

(2) In axial tests the dispersion of the nuclei along the specimen is much greater than in rotating bending tests, cf. Refs.18 and 24, because a greater length of an axial specimen experiences a high load.

(3) The intrinsic accuracy of the loading, which depends on such parameters as specimen machining, chuck alignment and load control method, may be different for the two types of tests, though it is not readily apparent that one form of test would be more accurate than another.

It is possible that such factors could affect the scatter in the two types of testing, but at this stage not enough information is available to pinpoint the actual cause of the discrepancy.

9.5 The effect of mean stress

The average number of nuclei per specimen measured by Swanson[18] on axial specimens tested at an alternating stress level of 34 ksi, but at 4 different mean stresses is shown in Fig.51, from which it can be seen that, whilst the test in alternating compression gave by far the most nuclei

per specimen, of those tests in which the mean stress was positive the specimens tested with the greatest mean (+34 ksi) gave most nuclei. It is interesting to note that the values of the number of nuclei obtained for these tests with a positive mean stress lie on or near to the suggested line in Fig.48 which presented results with a mean of 16 ksi, whereas the value for the tests in alternating compression (mean = -34 ksi) is quite distinct from the general pattern shown in the figure. Thus although the tests in alternating compression produced by far the most nuclei per specimen of all the tests in Ref.18, their mean life was the largest and their scatter was not the smallest. A possible explanation of this effect is that the propagation stage of a test in alternating compression occupies a very large proportion of the total life, during which time a large number of cracks other than the one that causes failure have the chance to nucleate. In such a case it seems likely that the scatter obtained in the final life would be dependent not on the number of nuclei present at failure, but on the number present within a short period of the start of the test, which might be similar to the number present in a test with a positive mean stress.

The chief effect of mean stress may thus be to alter the relative duration of the initiation and propagation stages, and thereby to change the number of nuclei apparent at failure, without any obvious effect on the measured scatter.

9.6 The effect of specimen configuration, finish and mechanical properties

It is often quoted that lug specimens with the associated fretting produce more scatter than conventional test specimens and yet the two groups of lug specimens data presented in this Report, Fig.38, both give low scatter and are associated with a large number of nuclei, Fig.47. This large number of nuclei is obviously partly due to the fact that in the specimens tested both ends were lugs with equal diameter holes etc. and so there were, in fact, 4 positions of maximum stress in each specimen, each associated with its own nuclei. However, there may be something in the fretting process that causes a large number of nuclei to be found, although the number of nuclei per area under maximum loading in notched and lug specimens did not appear to differ much in the two cases considered.

It is suggested in the Appendix, that the introduction of an interference fit fastener into a hole in a specimen reduces the scatter more than the introduction of a clearance fit bolt and that a smaller specimen possibly produces more scatter. No explanation for the former possibility can be found as it

would be thought that variations in the degree of interference would increase the scatter in the final life, but it might be expected that the larger the specimen the more nuclei present and so the smaller the scatter.

As mentioned in the Appendix, several experimenters have correlated fatigue performance with some other property of the material, Smith[55], Weibull[3] and Gassner[56] with yield strength, Bastenaire[27] with magnetic permeability and with damping capacity, Ravilly[57] with magnetic properties and Heath-Smith and Kiddle[52] with percentage elongation. The fact that these correlations, however indirect, were found and that presorting the specimens according to some of the characteristics reduced the scatter obtained, e.g. Refs.55 and 57, shows that some. at least, of the scatter is caused by material variation, which whilst not confirming the model of fatigue adopted here shows that material variation is important.

9.7 Effect of heat

Another effect noticed in Ref.52, was that the number of nuclei present in a specimen on failure increased if the specimen was heated before the crack nucleation of the specimen was complete. The scatter for four sets of tests conducted with heat applied before the fatigue test on both notched and lug specimens fits in well with the shape of Fig.47. However, it must be appreciated that the four sets of data in Fig.47 for tests with heat applied were all conducted at a stress level high enough to give low scatter anyway. The number of nuclei does show a large increase between tests with and without heat for these stress levels and it would seem reasonable to expect the lower stress levels as well to produce more nuclei after heat, in which case the scatter with heat would be lower than the scatter without heat throughout the range, a trend that is indicated by Dunsby's results presented in the Appendix.

9.8 Effect of water content of the air

The deleterious effect of water vapour molecules on the fatigue of metallic specimens has been known for some time and clearly variations in the amount of water vapour present during a test will affect the result of that test. Thus unless all tests are conducted at the same temperature and at the same specific humidity the results from those tests will exhibit a scatter caused by the variations of the environment on top of the scatter caused by metallurgical phenomena, as indicated in the Appendix to this Report.

9.9 General

The model of fatigue crack nuclei discussed above is obviously a very much simplified concept of the mechanism of fatigue but none the less a number of the trends exhibited by the scatter in fatigue life of sets of light alloy specimens have been explained in terms of this model in this Report. In practice, however, all fatigue tests will suffer from variations in numerous other quantities, such as specimen and notch dimensions, machine loading level, axiality of loading and environment, and the scatter produced by these variations in the test conditions will be additional to that derived from metallurgical variations. From the data presented in this Report it is impossible to distinguish between these two general sources of scatter and in fact, from the point of view of the application of fatigue data to engineering problems, this separation is not necessary provided the inherent scatter is the predominant factor, as appears to be the case from the data presented in this Report.

10 CONCLUSIONS

This Report presents the results of an analysis in terms of the log-normal distribution of lives obtained in constant amplitude fatigue tests of 2024 and 7075 aluminium alloy materials conducted in a large number of laboratories. A brief synopsis of the trends which have been noticed follows, but it must be understood that these conclusions are only tentative in nature, some being based on very few observations.

(1) The coefficient of variation increases with an increase in the life of a specimen above a value of log N of about 4.

(2) The coefficient of variation increases with a decrease in the value of log N below a value of 4. This trend is by no means as well supported as (1) above.

(3) Axial loading fatigue tests of bar specimens seem to entail a larger coefficient of variation at the longer lives than is produced in rotating bending tests.

(4) The coefficients of variation at the same value of log N for the two materials considered, i.e. the zinc based 7075 and the copper based 2024 aluminium alloy, cover very much the same range of values as one another.

(5) The effect of the mean stress on the coefficient of variation, if it exists at all, is small enough not to be discernible in these results.

(6) The effect of the degree of notch acuity is small, and the difference in coefficient of variation between two different sharpnesses of crack is not easily distinguishable. However, it appears that notched specimens in general give a greater range of coefficients of variation than the unnotched specimens for both materials, thereby possibly indicating that the results from notched specimens are less consistent between experiments than those for unnotched specimens.

(7) The effect of specimen size is thought to be small, but, from the results given, a decrease in specimen size appears to give higher values of the coefficient of variation (very little evidence).

(8) There did not appear to be any effect of surface finish on the coefficient of variation although possibly a finer finish gives a longer life at which the coefficient of variation tends to infinity (1 report only).

(9) The effect of a period of heat soaking before fatigue testing appeared to reduce the coefficient of variation at the lower stress levels (1 report only).

(10) The effect of fretting on the coefficient of variation is not decipherable from the analysis. However, the lug specimen of Ref.52 gave low scatter.

(11) The effect of Taper Lok fasteners in the specimens of Ref.55 was to reduce the scatter of the fatigue results for the specimen.

Appendix

As mentioned in section 8, additional data was available that was not suitable for inclusion in Figs.17 to 27 on the basis that either, (a) very few specimens were tested under each condition, or, (b) the number of stress levels at which the experimenters tested, under otherwise identical conditions, were too few to show any trend in scatter with stress level. An analysis of this data, in terms of the effects of various test parameters on the scatter in fatigue life that each produces, is presented here and comparisons are made with any trends noted in the main body of the Report. The figures to which this analysis refers and in which the data is plotted are Figs.28 to 46, inclusive. With one or two notable exceptions, e.g. Figs.30 to 33, it can be seen that the points in these figures conform generally to the boundaries of scatter defined by Figs.17 to 27. The confidence that can be placed in any trends which are suggested by these additional results and not supported by data in the main part of the Report is limited but some of the effects may nevertheless be real.

A.1 Effect of mean stress

Figs.28 and 29 present the results of an investigation reported in Ref.58 into the effect of mean stress on notched alclad aluminium alloys 7075 and 2024 tested under axial loading, but no effect of the mean stress on scatter is easily discernible in the range +20 ksi to -20 ksi, from these results. The effect of a change of mean stress is also studied by Schijve and Jacobs[41], in which the specimens used were riveted joints of 24S-T clad sheet 0.032 inch thick. Again the results (Fig.37) show no marked trend with mean although the coefficient of variation for the higher mean is slightly larger than for the lower mean in both cases, whilst of 3 comparisons possible in the data from Ref.19 a higher mean gives less scatter on two occasions but more in the third case. It is to be noted that the results from the above references all conform to the general range of Figs.17 to 27, but a study of Figs.20 to 33 shows that the coefficients of variation for the 7075-T6 notched coupons tested in Ref.59 cover a wide range and are generally much higher than the values from other reports. No effect of mean stress at any notch acuity can be deciphered from these figures for the results are altogether very confused.

The tests conducted in the investigation reported in Ref.55 on unnotched 7075-T6 were at constant amplitude but under three different values of R, where R is defined as the minimum stress divided by the maximum stress. The mean stress thus varies from test set to test set. The chief point of interest

from the results, Fig.40, is the apparent increase in the coefficient of variation at low values of log N. There is a minimum value for the coefficient when log N is 4.0, but no trends with the magnitude of R are discernible. This apparent increase in the coefficient of variation at small values of log N is also shown, to some extent, in Figs.30 and 32, for the 7075-T6 notched coupons of Ref.59.

Taking all these references together there does not appear to be a discernible effect of the mean stress on the magnitude of the scatter involved in constant amplitude fatigue testing, although in section 5.3 it was noted that an increase in mean load appeared to produce a more rapid decrease in the scatter with an increase in stress level. It must be stated here that although no effect of mean load on scatter magnitude was observed this may have been because the effect is small and was masked by the paucity of fatigue test results.

A.2 Effect of notch acuity

Unnotched and notched (K_t = 2.85) data for 2024 sheet axially loaded are presented in Ref.42 and compared in Fig.34, where no distinction in the amount of scatter obtained can be made between the two types of test. Similarily, Fig.36 contains the results obtained from Ref.60 on 2024-T4 in rotating bending tests on both notched and unnotched specimens (notch acuity K_t = 5.2) and again no effect is noticeable as in Fig.35 for axial sheet results for 7075 and 2024 from Ref.61. The results for 7075-T6 notched coupons of Ref.59, Fig.30 to 33, which as mentioned in section A.1 cover a wide range of values of the coefficient of variation and generally appear higher than values from the other reports, correspond to notch acuities of K_t = 3, 4, 7 and 10. Any trend in scatter with notch acuity that may exist is hidden in the general confusion of the results on these plots, which appear to be a haphazard display of parts.

However, Ref.52 contains results for HID 54 which is an Al 6% Cu alloy and is similar in constitution to 2024 material, and this and other unpublished data from the same author on 2024 is presented in Fig.38. From this figure it is to be noted that the scatter lies in the general band for 7075 and 2024 materials of Fig.17 to 27, and also that there is an apparent effect of notch acuity, whereby the sharper notch appears to give slightly less scatter.

These additional results therefore do not unanimously confirm the possible trend indicated in section 7, whereby an increase in notch acuity

might result in a small decrease in the coefficient of variation at constant life. Neither, however, are they sufficiently numerous or reliable to contradict it, for any trend, if small, could quite easily be lost amongst the general scatter of results.

A.3 Effect of specimen configuration, finish and mechanical properties

Fretting and interference fit fasteners

Besides those results, reported in section A.2, from Ref.52, the experimenters also tested two sets of lug specimens of HTD 54 material, and it can be seen, Fig.38, that in both sets of tests the scatter resulting was low even though fretting was present which might be thought likely to increase the scatter, Ref.62. Unfortunately no more results with fretting are available, but Ref.55 provides the results shown in Figs.42 and 43. Fig.42 relates to the effect, on the scatter in life of a simple specimen with a 3/16 inch countersunk hole, of filling the hole, firstly with a NAS-333 bolt (0.001 clearance) and secondly with a Taper-hole TL 100-3 bolts (0.003 interference). There are very few points from which to deduce any trend although it is perhaps noticeable that the interference fit gives least scatter, the clearance fit next lowest and the open hole most. Fig.43 presents the results for single shear butt joints, with NAS-333 and Taper Lok fasteners, showing no obvious difference between the two.

A.4 Effect of size

The effect of specimen size is studied in Ref.63, for a riveted single lap joint of 2024-T alclad material at a mean stress of 9.0 kg/mm^2. The scatter obtained for three different sizes of the same specimen configuration (ratio of sizes 3:5:8) were not greatly different from one another, Fig.39, though, if anything, the smallest specimen gave a larger coefficient of variation than the two larger sizes, between which it was impossible to differentiate, whilst the results in Figs.17 to 27 do not give a consistent picture of size effect.

A.5 Effect of surface finish

Ref.40 studies the effect of surface finish on the fatigue properties of a 2024S-T, rotating cantilever, unnotched specimen. The results, Fig.41, show no sensible trend in the coefficient of variation with a change in the finish, although they conform to the boundaries of Figs.17 to 27. The surface finish does, however, seem to have an effect on the fatigue life at which the coefficient of variation starts increasing rapidly, the finer finishes having a

longer life at which the coefficient of variation tends to infinity. Swanson[19], however, compared the fatigue lives of 18 unprepared specimens of 2024-T4 material with the lives of 18 specimens which had been electropolished in a perchloric acid-ethyl alcohol solution bath and then lightly polished. The electropolished specimens had a lower mean life, 61400 cycles against 83000 cycles, and significantly less scatter at the 5% level of significance, $\sigma = 0.065$ electropolished and $\sigma = 0.123$ as received.

The steel specimens tested by Laurent[64], although showing an increase in mean fatigue life with the degree of polish of the surface, produced very little variation in scatter with the five different surface finishes tried.

A.6 Effect of mechanical property

Ref.55, in addition to the results discussed above, also includes results for 7075 alloy double shear riveted butt joints, the material for which had been previously categorised in terms of the yield strength into three specific ranges $\sigma_{YS} > 77$ ksi or $74 < \sigma_{YS} < 77$ or $\sigma_{YS} < 74$ ksi. As can be seen from Fig.43 the specimens with the highest yield strength ($\sigma > 77$ ksi) have a considerably higher coefficient of variation than the other specimens with no effect on the mean life.

Weibull[3] also noticed an indirect correlation between yield strength and fatigue life. The frequency curve of the yield strength of the Sb.37 steel considered showed two distinct maxima, indicating that the parent material could be split up into two components, 30% of the material belonging to one and 70% to the other component. The fatigue results for the same material of which 235 specimens were tested also showed this double distribution, for which the percentage proportions were again 30% and 70%, and so a correlation between fatigue life and yield strength seemed likely for this material.

Similar effects were noted by Gassner[56] who found that specimens whose fatigue lives brought them to the longer side of the scatter band had low yield strengths in general, whilst the endurance of Fisher's joints[65] in a light alloy was longer the smaller the value of the ratio of the yield strength to the ultimate strength. In spite of these results, though, no correlation between the proof strength, the ultimate strength, the proof-ultimate ratio or the elongation with fatigue life could be seen in the analysis in Ref.45 from the results for 2024 and 7075 specimens.

A.7 Effect of time and temperature of annealing

Dunsby[66] studied the effect of periods of heat on the fatigue properties of 24S-T unnotched specimens in simple reversed bending. Initially he compared the fatigue lives of the specimens in the 'as supplied' condition and in the '100 hours at 400°F soak' condition. As can be seen, Fig.44, the scatter in all these sets of tests is small but in general the scatter in the 'soaked at 400°F' condition appears to be smaller than that in the 'as supplied' condition. The mean after 400°F soak also appears to be considerably lower than the 'as supplied' mean at the same stress level. The scatter at stress level 32.5 ksi is almost identical for the two conditions, whilst at 22.5 ksi the scatter for the 'as supplied' specimens is the smaller but not statistically so. For the other three stress levels involved, the 'soaked' tests have less scatter than the 'as supplied' test; in two of these three cases the difference is statistically significant at the 10% level but not at the 5% level.

Dunsby also conducted two series of tests in which the length of application of the soak was varied and the run out stress was kept constant. The two series are accounted for by different soak temperatures of 400°F and 300°F. At a soak temperature of 400°F increases in the soak time in the range 1.5 hours - 100 hours decrease the mean steadily, but the scatter, which was universally small, shows no definite trend although the longest soak gives the largest scatter and the shortest soak the smallest scatter. The two points in between, however, are in inverted order. At 300°F the mean life decreases with an increase in soak time from 1.5 hours - 4 hours and from 4 hours - 30 hours, but experiences an increase from 30 hours - 100 hours; however 4 hours soak time gives a longer life than 100 hours. 30 hours soak gives the largest scatter, being statistically greater at the 10% level than the scatter for 100 hours and 4 hours but the difference is not significant at the 5% level.

A.8 The effect of water content of the air and of protective surface coatings

Liu and Corten[15] studied the effect of the two variables, water content of the air and surface coating, on the fatigue life of 7075 and 2024 wire specimens under constant amplitude loading. From their results, Figs.45 and 46, it is clear that the water content of the air had less effect on the mean fatigue life of the 2024 material than of the 7075 material, whose mean life was halved by an increase in water content from 12 to 120 grains per pound

of dry air. No sensible trend in scatter with a change in water content is noticeable, but the scatter in those groups of tests of 7075 material in which the specimens were coated with vaseline or oil appear to have markedly less scatter than the uncoated tests. The results of these coated tests also appear more consistent, for when the results of groups of uncoated specimens were amalgamated the standard deviation of the pooled data was larger than that of any of the constituent groups, whilst for the coated specimens the overall standard deviation was very nearly the same as the member standard deviations.

No difference in scatter between coated and uncoated 2024 material specimens is apparent, but the coefficient of variation for all these sets of results is very small, being less than 0.017.

The nominal chemical composition by weight of 2024 and 7075 aluminium alloys

Alloying element / Material	Cu	Mg	Mn	Fe	Si	Sn	Ni	Pb	Sn	Cr	Ti	Others		Al
												Each	Total	
2024	3.8 – 4.9	1.2 – 1.8	0.3 – 0.9	0.50 max	0.50 max	0.25 max				0.10 max		0.05 max	0.15 max	Remainder
7075	1.2 – 2.0	2.1 – 2.9	0.30 max	0.70 max	0.50 max	5.1 – 6.1				0.18 – 0.40	0.20 max	0.05 max	0.15 max	Remainder

The specification for each of these two alloys varies to a great extent with the condition or temper of the material considered. In general however the ultimate tensile strength of the 2024 alloy lies in the range 55-70 ksi and the 0.2% yield stress in the range 35-60 ksi. Comparable values for the 7075 material are 65-85 ksi and 55-70 ksi.

Table 1

RESULTS OF THE LINEAR REGRESSION ANALYSIS OF SECTION 5.2

7075 Material log standard deviation/log stress analysis

Reference number	Type of loading	Notch description	Mean stress	90% lower limit on gradient	Gradient (β)	90% upper limit on gradient	Constant (α)	S^2_{XY}
Unnotched								
15	Rotating beam	None	0	- 2.345	-1.712	-1.079	22.22	0 0479
15	Rotating beam	None	0	- 1.942	-1.629	-1.315	17.53	0.0366
16	Rotating beam	None	0	- 4.065	-3.190	-2.316	23400.0	0.0574
47	Rotating beam	None	0	- 4.104	-1.992	1.193	384.0	0.0635
49	Rotating beam	None	0	- 2.625	-0.701	1.223	2.23	0.138
34	Axial	None	S_{min} = 0	- 3.891	-3.202	-2.512	52170.0	0.0106

$\frac{\sum_{r=1}^{n} b_r}{n}$ { Mean gradient of rotating beam results = -1.845

Mean gradient of rotating beam + axial results = -2.071

Riveted joints								
45	Axial	-	8.96 ksi	- 3.053	-1.649	-0.245	1.88	0.0849
Notched								
47	Rotating beam	0.094" radius	0	- 3.151	0.732	+4.616	0.0397	0.413
47	Rotating beam	0.010" radius	0	- 2.561	-1.546	-0.531	2.750	0.357
47	Rotating beam	0.0032" radius	0	- 0.905	0.2223	1.349	0.0782	0.132
49	Rotating beam	0.0625" radius	0	- 5.106	-0.866	3.375	3.639	0.380
49	Rotating beam	0.025" radius	0	- 4.001	-1.446	1.115	9.954	0.204
48	Axial	K_t = 4.0	0	- 1.454	-0.530	0.394	0.505	0.141
48	Axial	K_t = 4.0	10 ksi	- 2.767	-1.27	0.225	9.757	0.3399
48	Axial	K_t = 4.0	20 ksi	-18.37	-8.85	-6.73	9.718	0.336
67	Axial	K_t = 4.0	S_{min} = 7 ksi	- 2.342	-1.536	-0.732	2.086	0.562

Table 1A

RESULTS OF THE LINEAR REGRESSION ANALYSIS OF SECTION 5.2

7075 Material log standard deviation/stress analysis

Reference number	Type of loading	Notch description	Mean stress	90% lower limit on gradient	Gradient (β)	90% upper limit on gradient	Constant (α)	S^2_{XY}
Unnotched								
15	Rotating beam	-	0	-0.0734	-0.0512	-0.0291	0.327	0.0629
15	Rotating beam	-	0	-0.0500	-0.0393	-0.0286	0.233	0.0679
16	Rotating beam	-	0	-0.0876	-0.0729	-0.0583	3.626	0.0318
47	Rotating beam	-	0	-0.119	-0.0530	+0.0134	2.119	0.0820
49	Rotating beam	-	0	-0.0838	-0.0207	+0.0424	0.391	0.149
34	Axial	-	S_{min} = 0	-0.0881	-0.0745	-0.0609	7.867	0.00774

$\frac{\sum_{r=1}^{n} b_r}{n}$ { Mean gradient of rotating beam results = -0.0474

Mean gradient of rotating beam + axial results = -0.0519

Riveted joints								
45	Axial	-	8.96 ksi	-0.696	-0.354	-0.0117	0.834	0.105
Notched								
47	Rotating beam	0.094" radius	0	-0.109	+0.0271	+0.163	0.211	0.410
47	Rotating beam	0.010" radius	0	-0.122	-0.0778	-0.0335	1.448	0.299
47	Rotating beam	0.0032" radius	0	-0.0665	0.0123	+0.0911	0.117	0.136
49	Rotating beam	0.0625" radius	0	-0.0593	-0.0340	-0.0087	0.544	0.350
49	Rotating beam	0.025" radius	0	-0.173	-0.0621	+0.0491	0.466	0.207
48	Axial	K_t = 4.0	0	-0.0809	-0.0306	+0.0196	0.201	0.135
48	Axial	K_t = 4.0	10 ksi	-0.0898	-0.0417	+0.0064	0.534	0.351
48	Axial	K_t = 4.0	20 ksi	-0.675	-0.328	+0.0197	154.0	0.328
67	Axial	K_t = 4.0	S_{min} = 7 ksi	-0.0641	-0.0392	-0.0144	0.412	0.672

Table 2

RESULTS OF THE LINEAR REGRESSION ANALYSIS OF SECTION 5.2

2024 Material log standard deviation/log stress analysis

Reference number	Type of loading	Notch description	Mean stress	90% lower limit on gradient	Gradient (β)	90% upper limit on gradient	Constant (α)	s^2_{XY}
Unnotched								
15	Rotating beam	-	0	-2.387	-1.500	-0.615	19.15	-0.108
49	Rotating beam	-	0	-3.613	-2.322	-1.031	617.2	-0.0856
68	Rotating beam	-	0	-2.272	-1.365	-0.458	15.5	-0.130
18	Axial	-	16 ksi	-4.514	-2.028	+0.458	164.5	-0.503
19	Axial	-	16 ksi	-1.524	-1.107	-0.691	8.804	-0.0872

$$\frac{\sum_{r=1}^{n} b_r}{n}$$

Mean gradient of rotating beam results = -1.729
Mean gradient of axial results = -1.568
Mean gradient of rotating beam + axial results = -1.664

Riveted joints								
45	Axial	-	12.8 ksi	-2.019	-1.33	-0.644	1.29	0.127
Notched								
49	Rotating beam	0.0625" radius	0	-4.243	-2.19	-0.130	406.0	0.331
49	Rotating beam	0.025" radius	0	-2.702	-1.605	-0.507	21.32	0.079
48	Axial	$K_t = 4.0$	0	-2.894	-1.000	+0.894	1.879	0.355
48	Axial	$K_t = 4.0$	17.4 ksi	-5.643	-3.105	-0.567	5401.0	0.872

Table 2A

RESULTS OF THE LINEAR REGRESSION ANALYSIS OF SECTION 5.2

2024 Material log standard deviation/stress analysis

Reference number	Type of loading	Notch description	Mean stress	90% lower limit on gradient	Gradient (β)	90% upper limit on gradient	Constant (α)	s^2_{XY}
Unnotched								
15	Rotating beam	-	0	-0.0593	-0.0340	-0.0088	0.316	0.150
49	Rotating beam	-	0	-0.099	-0.0650	-0.0310	1.665	0.0771
68	Rotating beam	-	0	-0.0693	-0.0401	-0.0110	0.530	0.146
18	Axial	-	16 ksi	-0.150	-0.0591	+0.0319	1.07	0.630
19	Axial	-	16 ksi	-0.0477	-0.0328	-0.0178	0.572	0.109

$$\frac{\sum_{r=1}^{n} b_r}{n}$$

Mean gradient of rotating beam results = -0.0463
Mean gradient of axial results = -0.0460
Mean gradient of rotating beam + axial results = -0.0462

Riveted joints								
45	Axial	-	12.8 ksi	-0.349	-0.186	-0.0236	0.440	0.294
Notched								
49	Rotating beam	0.0625" radius	0	-0.141	-0.0665	0.0080	1.94	0.413
49	Rotating beam	0.025" radius	0	-0.128	-0.0763	-0.0244	0.848	0.078
48	Axial	$K_t = 4.0$	0	-0.246	-0.0825	+0.0807	0.448	0.366
48	Axial	$K_t = 4.0$	17.4 ksi	-0.178	-0.0964	-0.0139	2.731	0.907

SYMBOLS

a, b	parameters in the expression $\sigma = ae^{-bS}$ relating the standard deviation to the alternating stress level
A, B	define the regression line $y = A + Bx$
e	the base of the natural logarithms
k	parameter in the Sinclair-Dolan expression $\sigma = \sigma_o S^{-k}$ relating the standard derivation to the alternating stress level
K_t	notch acuity
m	the best estimate of the mean of a sample of n specimens
n	the number of test specimens in a sample
N	the number of cycles to failure of a randomly selected sample
N_o	Stepnov's threshold life, below which the probability of failure is zero
N_r	the number of cycles to failure of the rth specimen
P	the probability of failure
p(x) dx	the normal probability density function of the variable x
S	the alternating stress level
s	the unbiassed estimate of the standard derivation of a sample of n specimens
s^2_{YX}	the best estimate of the variance from the regression line $y = A + Bx$ of points (X_i, Y_i) i = 1, 2 ... n
t	the value of Student's 't' Distribution
v	the population coefficient of variation $\left(= \frac{\sigma}{\mu}\right)$
$v_{estimate}$	the best estimate of the coefficient of variation $\left(= \frac{s}{m}\right)$
x, y	general variables
X_i, Y_i	sample values of the variables x, y
α, β	the best sample estimates of A and B that define the regression line $y = A + Bx$
μ	the population mean of the probability density function p(x) dx
σ	the population standard deviation of the probability density function p(x) dx
σ_o	a parameter in the Sinclair-Dolan expression $\sigma = \sigma_o S^{-k}$
σ_1, σ_2	the estimated standard deviations obtained from two different samples
σ_{YS}	the yield strength of a material

REFERENCES

No.	Author	Title, etc
1	H. Müller Stock	Der Einflüss dauernd und unterbrochen Wirkender, schwingender Überbeanspruchung auf die Entwicklung des Dauerbruchs. Mitt. Kohle und Eisenforsch, Vol 2, pp 83-107 (1938)
2	E. Epremian R.F. Mehl	Investigation of statistical nature of fatigue properties. NACA Technical Note 2719 (1952)
3	W. Weibull	A statistical distribution function of wide applicability. Journal of Applied Mechanics Vol 18 (1951)
4	M.N. Stepnov	The linear-regression analysis of the results of fatigue experiments with aluminium alloys. Zavodskaya Laboratoriya Vol 29, No.10 (1963)
5	W. Weibull	A statistical representation of fatigue failure in solids. Trans. of the Royal Inst. of Technology, Stockholm, No.27 (1949)
6	E.J. Gumbel	Statistics of extremes. Columbia University Press, New York (1958)
7	E.J. Gumbel	Statistical theory of extreme values and some practical applications. U.S. Dept. of Commerce, Applied Mathematics Series 33 (1954)
8	A.M. Freudenthal E.J. Gumbel	Statistical interpretation of fatigue tests. Proc. of the Royal Society A, 216 pp 309-332 (1953)
9	Z.W. Birnbaum S.C. Saunders R.C. McCarty R. Elliott	A statistical theory of life-length of materials. B.A.C. Document D2-1325 (1956)

REFERENCES (Contd)

No.	Author	Title, etc
10	Z.W. Birnbaum S.C. Saunders	A new family of life distributions. U.S.A. Washington University, Con. N-onr-477(38)
11	P.R. Abelkis	Fatigue strength design and analysis of aircraft structures. Part I: Scatter factors and design charts. U.S.A. A.F. Flight Dynamics Lab. TR-66-197 Pt. 1
12	J.A. Pope B.K. Foster N.T. Bloomer	Limited life design. A survey of the problem. University of Nottingham (1956)
13	R. Plunkett	Statistical analysis of fatigue data. Symposium on statistical aspects of fatigue. A.S.T.M. Spec. Tech. Publication 121 (1951)
14	F.B. Stulen	On the statistical nature of fatigue. Symposium on statistical aspects of fatigue. A.S.T.M. Spec. Tech. Publication 121 (1951)
15	H.W. Liu H.T. Corten	Fatigue damage under varying stress amplitudes. NASA Technical Note D-647 (1960)
16	G.M. Sinclair T.J. Dolan	Effect of stress amplitude on statistical variability in fatigue life of 75S-T6 aluminium alloy. Transaction of the A.S.M.E. Vol 75, No.5, pp 867-872 (1953)
17	A.M. Freudenthal	Planning and interpretation of fatigue tests. Symposium on statistical aspects of fatigue. A.S.T.M. Spec. Tech. Publication 121 (1951)
18	S.R. Swanson	An investigation of the fatigue of aluminium alloy due to random loading. University of Toronto UTIA-TN No.84 (1963)
19	S.R. Swanson	Systematic axial load fatigue tests using unnotched aluminium alloy 2024-T4 extruded bar specimens. UTIA Technical Note 35, A.F.O.S.R. 344 (1960)
20	L.F. Impellizzeri	Development of a scatter factor applicable to aircraft fatigue life. McDonnell Aircraft Corporation, St. Louis Missouri. Preprint for A.S.T.M. meeting in Seattle 31 October-5 November, 1965

REFERENCES (Contd)

No.	Author	Title, etc
21	D.G. Ford D.G. Graff A.O. Payne	Some statistical aspects of fatigue life variation from 'Fatigue of aircraft structures' edited by W. Barrois and E.L. Ripley. Published by Pergamon (1963)
22	W. Weibull	Scatter of fatigue life and fatigue strength in aircraft structural materials and parts from 'Fatigue in aircraft structures' edited by A.M. Freudenthal. Academic Press Inc., New York (1956)
23	A. Bender A. Hamm	The application of probability paper to life and fatigue testing. Internal Report, Delco-Remy Corporation
24	D. Webber J.C. Levy	Cumulative damage in fatigue with reference to the scatter of results. Ministry of Supply (1958)
25	F. Cicci	An investigation of the statistical distribution of constant amplitude fatigue endurances for a maraging steel. UTIA Technical Note 73, University of Toronto (1964)
26	F.J. Plantema	Some investigations on cumulative damage from 'Colloquium on fatigue', edited by W. Weibull and F.K.G. Odqvist, published by Springer-Verlag (1956)
27	F. Bastenaire	A study of the scatter of fatigue test results by statistical and physical methods from 'Fatigue of aircraft structures' edited by W. Barrois and E.L. Ripley, published by Pergamon, pp 53-85 (1963)
28	Westland Aircraft Ltd.	Statistical derivation of safety factors for use with mean S-N curves from fatigue tests. Report SD 753 (1961)

REFERENCES (Contd)

No.	Author	Title, etc
29	C.O. Albrecht	Statistical evaluation of a limited number of fatigue test specimens including a factor of safety approach. Vertol Division, The Boeing Co., Pennsylvania (1962)
30	Westland Helicopter Ltd.	Statistical analysis of the scatter of fatigue strengths of fibre glass bending specimens. Report SD 871 (1967)
31	W. Weibull	Basic aspects of fatigue from 'Colloquium on fatigue', edited by W. Weibull and F.K.G. Odqvist. Published by Springer-Verlag (1956)
32	W. Weibull	A new method for the statistical treatment of fatigue data. SAAB Technical Note 30 (1954)
33	W. Weibull	The statistical aspect of fatigue failures and its consequences. Conf. on Fatigue and Fracture of Metals. Mass. Inst. Tech. (1950)
34	W. Weibull	Static strength and fatigue properties of unnotched circular 75S-T specimens subjected to repeated tensile loading. F.F.A. Meddelande 68 Stockholm (1956)
35	W. Weibull	Static strength and fatigue properties of threaded bolts. F.F.A. Meddelande 59 Stockholm (1955)
36	W. Weibull	Scatter in fatigue life of 24S-T alclad specimens with drilled holes. SAAB Technical Note 32 (1955)
37	A.M. Freudenthal E.J. Gumbel	Distribution functions for the prediction of fatigue life and fatigue strength. A.S.M.E. Proc. of ICAF (1956)
38	A.M. Freudenthal E.J. Gumbel	Minimum life in fatigue. American Statistical Association Journal (1954)

REFERENCES (Contd)

No.	Author	Title, etc
39	A.M. Freudenthal	The expected time to first failure. Technical Report AFML-TR-66-37 (1966)
40	A.K. Head	Statistical properties of fatigue data on 24S-T aluminium alloys. ARL/SM 180 (1950)
41	J. Schijve F.A. Jacobs	Research on cumulative damage in fatigue of riveted aluminium alloy joints. NLL Report M.1999 (1956)
42	J. Schijve F.A. Jacobs	Fatigue tests on notched and unnotched clad 24S-T specimens to verify the cumulative damage hypothesis. NLL Report M.1982 (1955)
43	L. Kaechele	Probability and scatter in cumulative fatigue damage. Rand Corporation Memo. RM-3688-PR (1963)
44	C.G. Paradine B.H.P. Rivett	Statistical methods for technologists. Published by English University Press Ltd. (1964)
45	J. Schijve F.A. Jacobs	Program fatigue tests on notched light alloy specimens of 2024 and 7075 material. NLL Report M.2070 (1960)
46	E.C. Bryant	Statistical analysis. Published by McGraw-Hill Book Co., 2nd edition (1966)
47	H.F. Hardrath E.C. Utley D.E. Guthrie	Rotating beam fatigue tests of notched and unnotched 7075-T6 aluminium alloy specimens under stresses of constant and varying amplitudes. NASA Technical Note D-210 (1959)
48	E.C. Naumann H.F. Hardrath D.E. Guthrie	Axial load fatigue tests of 2024-T3 and 7075-T6 aluminium alloy sheet specimens under constant and variable amplitude loads. NASA Technical Note D-212 (1959)

REFERENCES (Contd)

No.	Author	Title, etc.
49	J.A. Bennett J.G. Weinberg	Fatigue notch sensitivity of some aluminium alloys. Bureau of Standards Journal of Research, Vol 52, p 235 (1954)
50	P.J.E. Forsyth	Crack Propagation Symposium, Cranfield (1961)
51	J. Schijve	Fatigue crack propagation in light alloys. NLL Technical Note M.2010 (1956)
52	J.R. Heath-Smith F.E. Kiddle	Influence of ageing and creep on fatigue of structural elements in an Al 6% Cu alloy. R.A.E. Technical Report 67093 (A.R.C. 29543) (1967)
53	P.L. Templin	Fatigue of aluminium. A.S.T.M. Proc. Vol 54 (1954)
54	R.B. Heywood	Designing against fatigue. Published by Chapman and Hall (1962)
55	C.R. Smith	A method for estimating the fatigue life of 7075-T6 aluminium alloy aircraft structures. ASL Report NAEC-ASL-1096 (1965)
56	E. Gassner	Preliminary results from fatigue tests with reference to operational statistics. NACA Technical Memorandum 1266 (1950)
57	E. Ravilly	Contribution à l'étude de la rupture des fils métalliques soumis à des tensions alternées. Pub. Sci. et tech. du Ministère de l'air, No.120 (1938)
58	I.E. Wilks D.M. Howard	Effect of mean stress on the fatigue life of alclad 24S-T3 and alclad 75S-T6 aluminium alloy. WADC Technical Report 53-40 (1953)
59	W.J. Crichlow A.J. McCulloch L. Young M.A. Melcom	An engineering evaluation of methods for the prediction of fatigue life in airframe structures. ASD-TR-61-434 (1962)
60	W.S. Hyler E.D. Abraham H.J. Grover	Fatigue crack propagation in severely notched bars. NACA Technical Note 3685 (1956)

REFERENCES (Contd)

No.	Author	Title, etc
61	A. Hartmann	An investigation on the notch sensitivity of cladded 24S-T and 75S-T alloys under pulsating cyclic loads in tension. Ministry of Supply TIB/T4096 (1953)
62	S.E. Larssen	The development of a calculation method for the fatigue strength of lugs and a study of test results for lugs of aluminium. SAAB Technical Report KHU-O-2294R (1965)
63	A. Hartmann F.A. Jacobs P. de Rijk	Tests on the effect of the size of the specimen on the fatigue strength of 2024-T alclad double row riveted single lap joints. NLR Technical Note M2104 (1962)
64	P. Laurent	Les Travaux récents de l'Institut de Recherches metallurgiques de Sarrebruck dans le donaine de la fatigue, from 'Colloquium on fatigue', edited by W. Weibull and F.K.G. Odqvist. Published by Springer-Verlag 1956
65	W.A.P. Fisher	Experimental correlation between the endurance of a wing spar joint and ratio between 0.1% proof and ultimate tensile strengths of the material. A.R.C. C.P. 371 (1956)
66	J.A. Dunsby	Some experiments on the effect of time at temperature on the room temperature reversed bending fatigue characteristics and on the tensile strength of 24S-T alclad Al alloy. NLR Report MS 102 (1960)
67	E.C. Naumann R.L. Schott	Axial load fatigue tests using loading schedules based on manoeuvre load statistics. NASA Technical Note D-1253 (1962)
68	H.F. Hardrath E.C. Utley	An experimental investigation of the behaviour of 24S-T4 aluminium alloy subjected to repeated stresses of constant and varying amplitudes. NACA Technical Note 2798 (1952)

REFERENCES (Contd)

No.	Author	Title, etc
69	A.M. Freudenthal R.A. Heller P.J. O'Leary	Cumulative fatigue damage of aircraft structural materials Part 1: 2024 and 7075 Al alloy. WADC Technical Note 55-273 Part 1 (1955)
70	T.J. Dolan H.F. Brown	Effect of prior repeated stressing on the fatigue life of 75S-T aluminium. Proceedings of the American Society for testing materials Vol 52 p 733 (1952)
71	H.W. Liu H.T. Corten	Fatigue damage during complex stress histories. NASA Technical Note D-256 (1959)
72	R. Spitzer H.T. Corten	Effect of loading sequence on cumulative fatigue damage of 7075-76 aluminium alloy.
73	I. Smith D.M. Howard F.C. Smith	Cumulative fatigue damage of axially loaded Alclad 75S-T6 and Alclad 24S-T3 aluminium alloy sheet. NACA Technical Note 3293 (1955)
74	G.E. Dieter R.F. Mehl	Investigation of the statistical nature of the fatigue of metals. NACA Technical Note 3019 (1953)
75	Douglas Report	SM 9116 (1946)
76	E.C. Naumann	Evaluation of the influence of load randomization and of ground-air-ground cycles on fatigue life. NASA Technical Note D-1584 (1964)

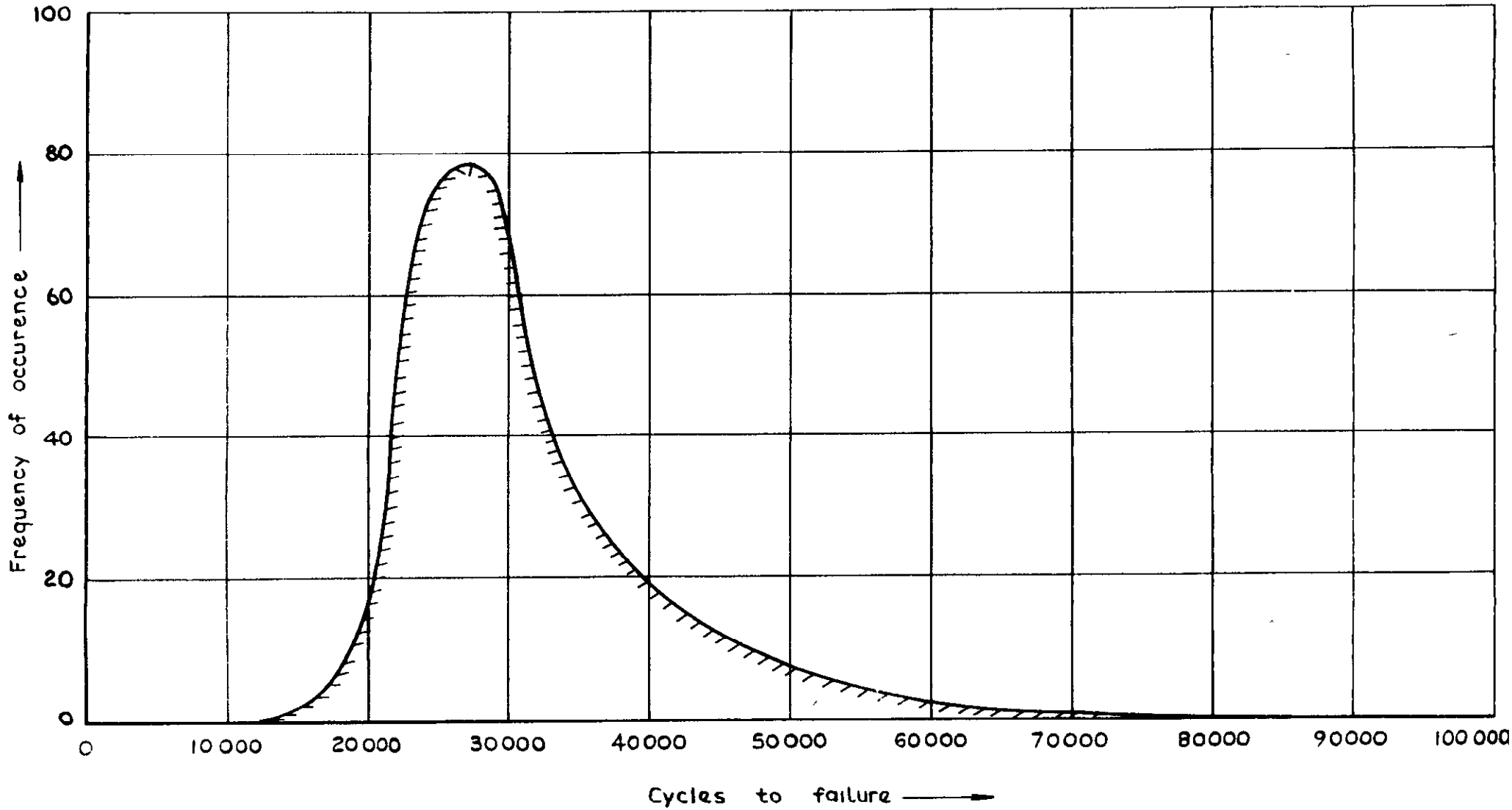

Fig.1 Fatigue tests of ST 37 at ± 45500 psi (235 specimens) from ref 1

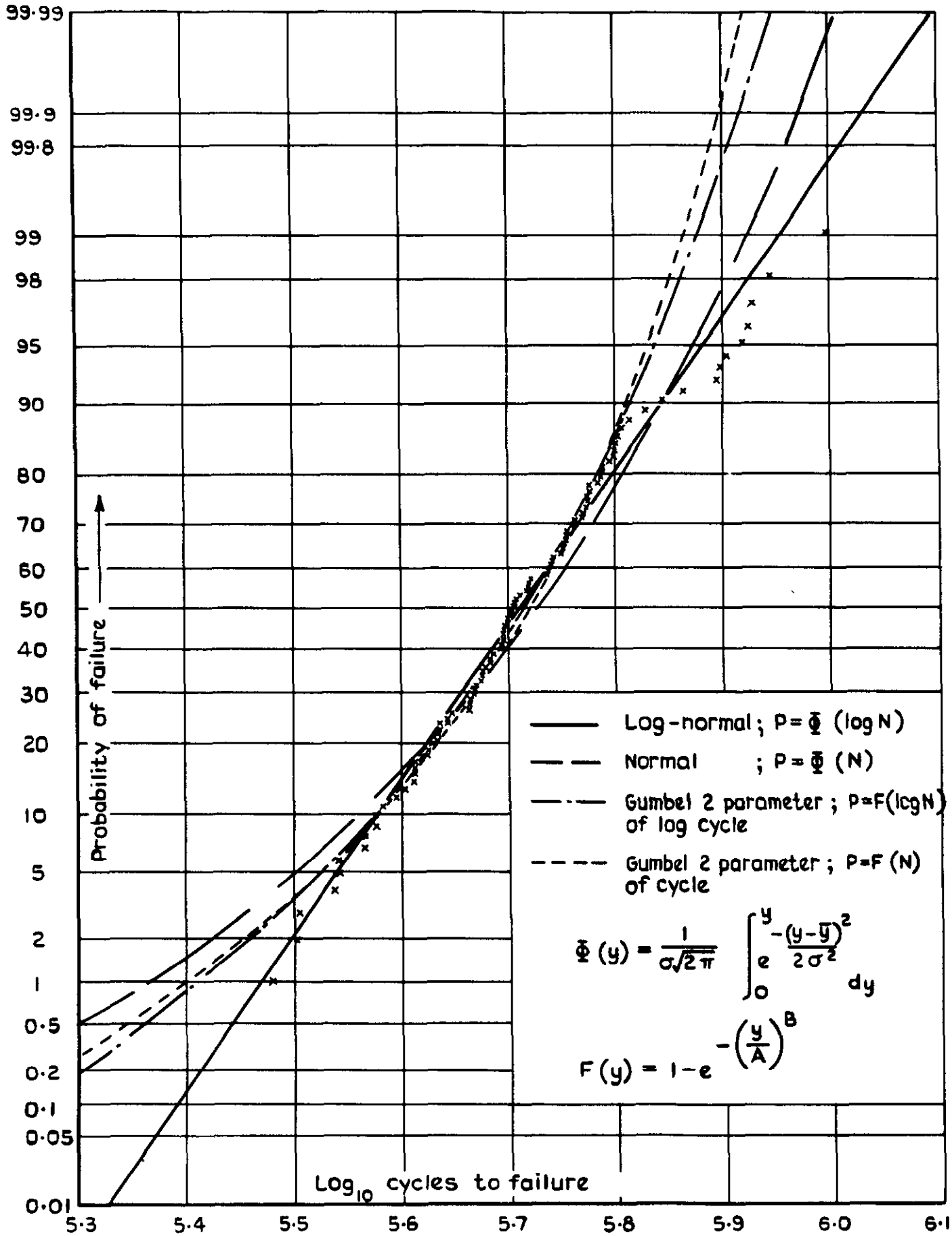

Fig. 2 Comparison of 4 two parameter representations of the fatigue test results of 100 specimens from ref(12) ±21 tsi. Rotating bending of 0·22% C steel

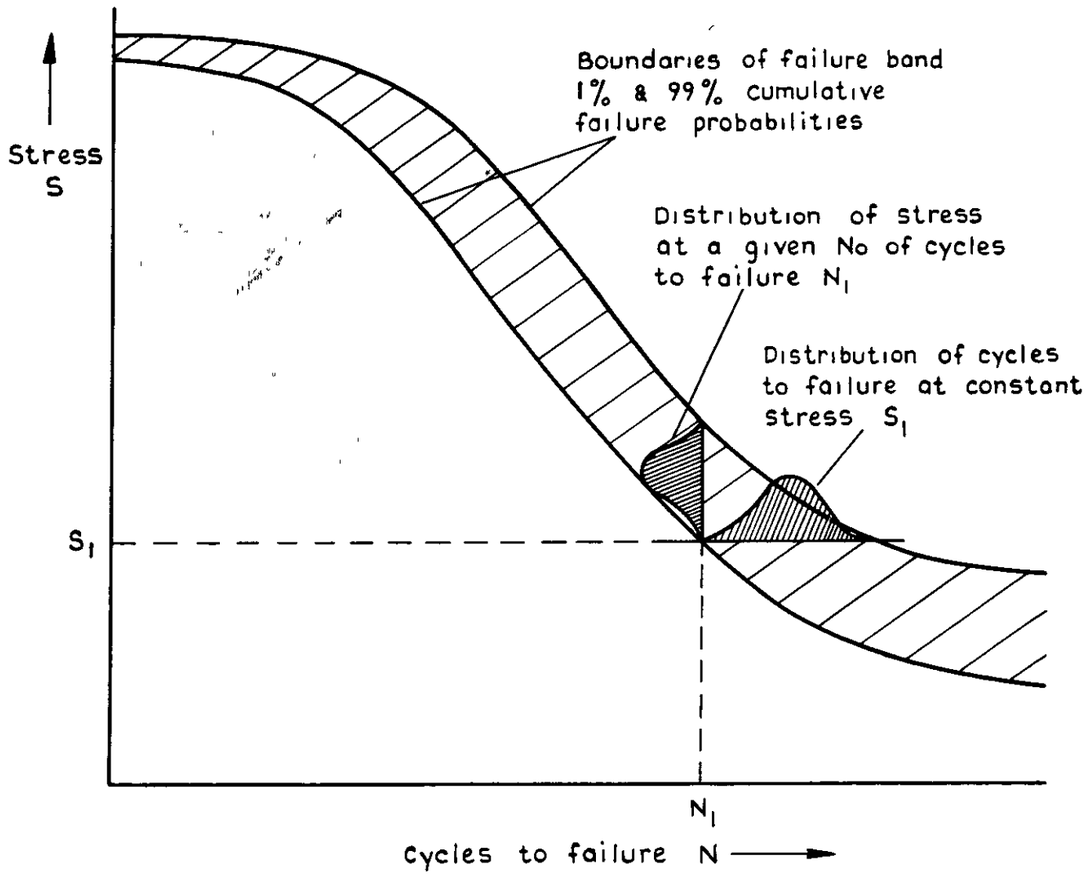

Fig.3 Distributions of fatigue failures

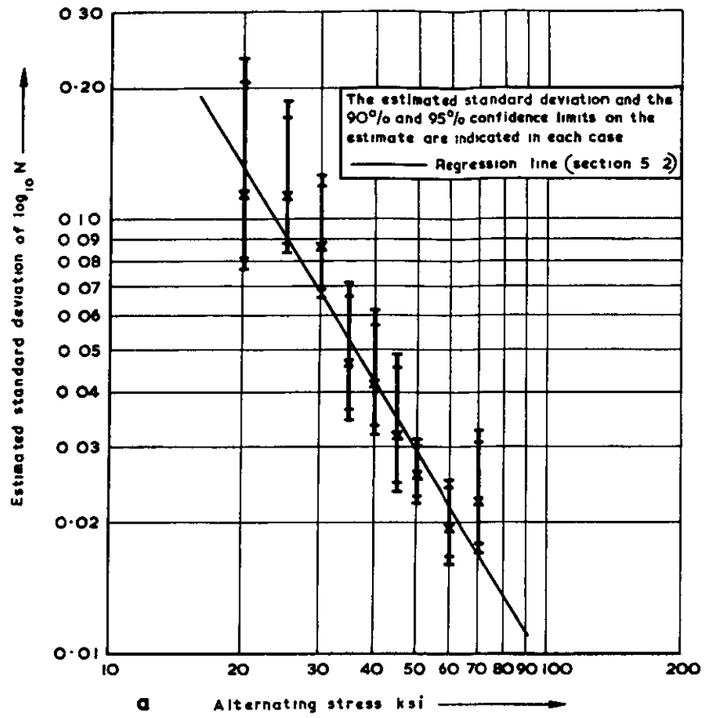

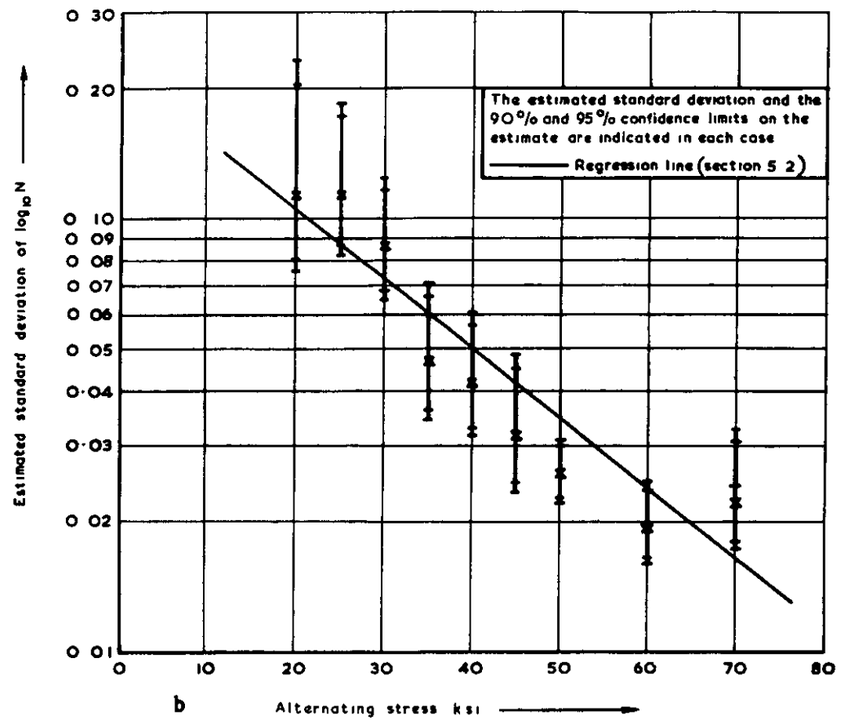

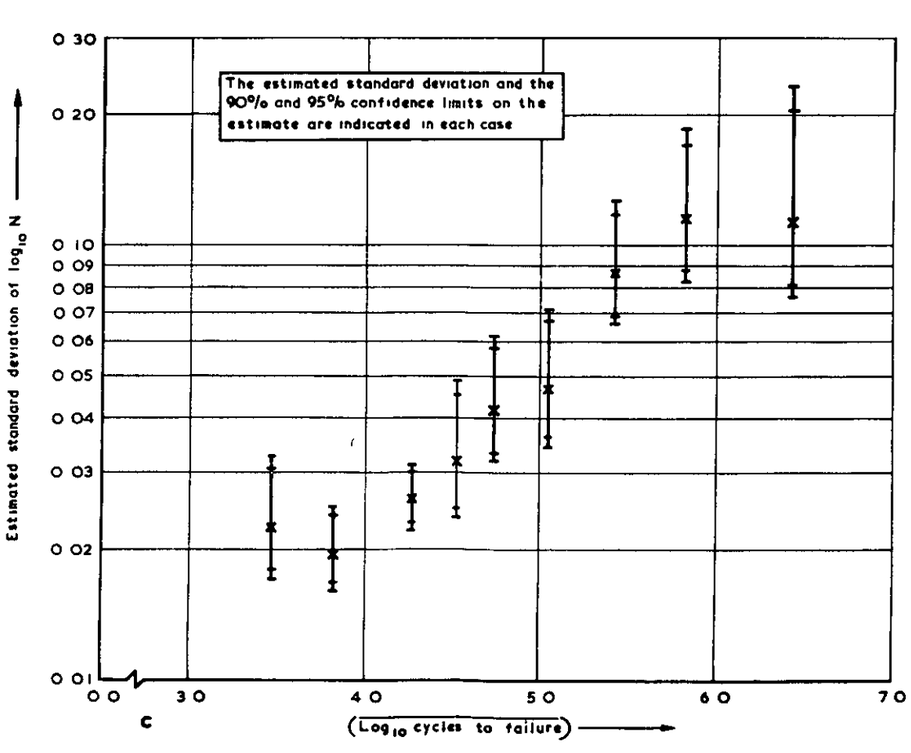

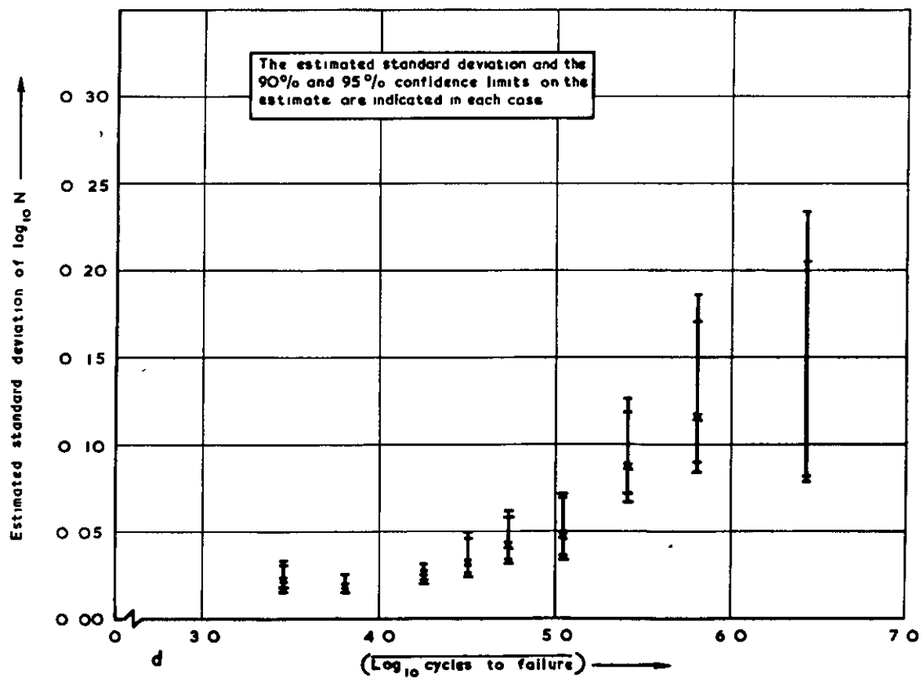

Fig.4 a - d Constant amplitude 7075 material ref (15)
Rotating bending All vaseline coated

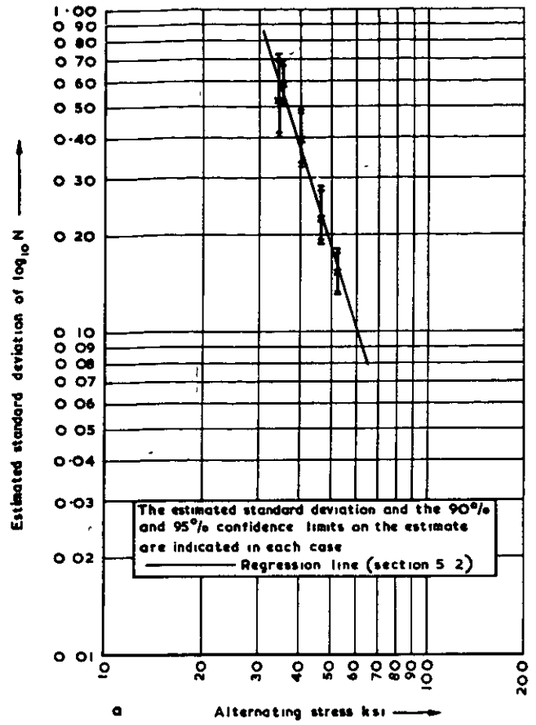

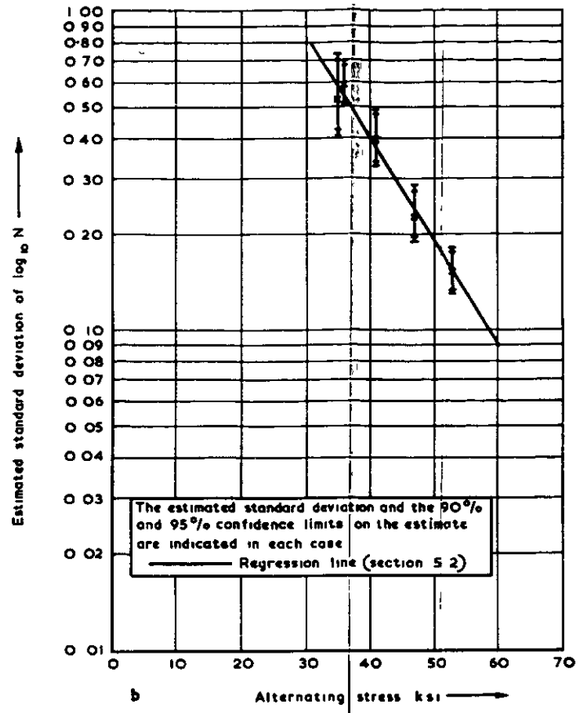

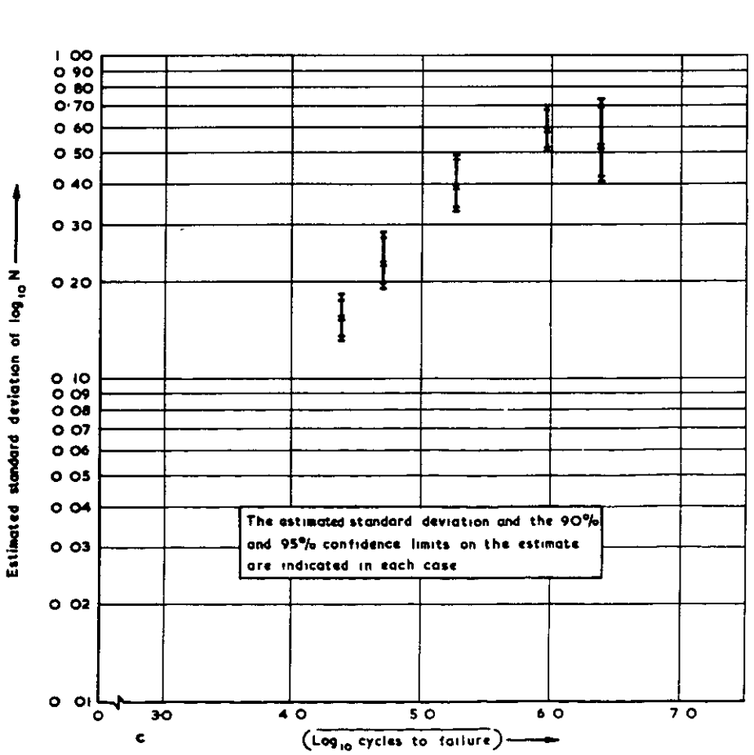

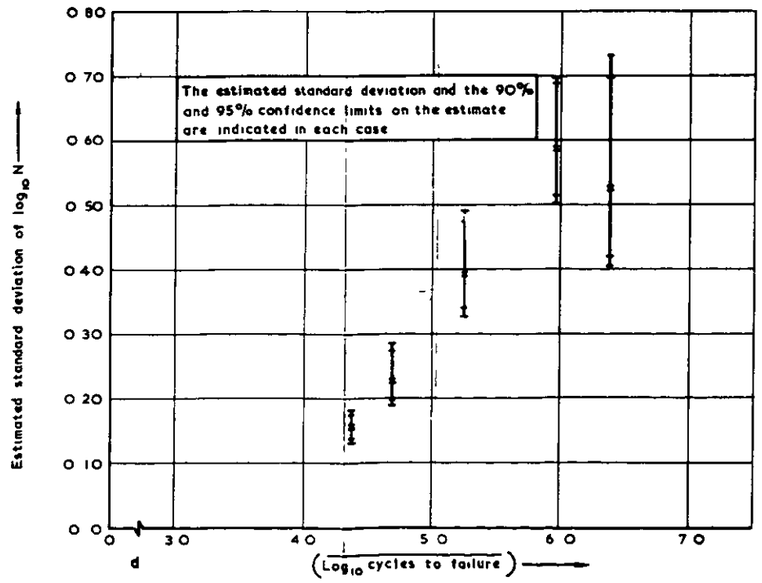

Fig.5 a - d Constant amplitude 7075 material ref (34)
Axial load Unnotched

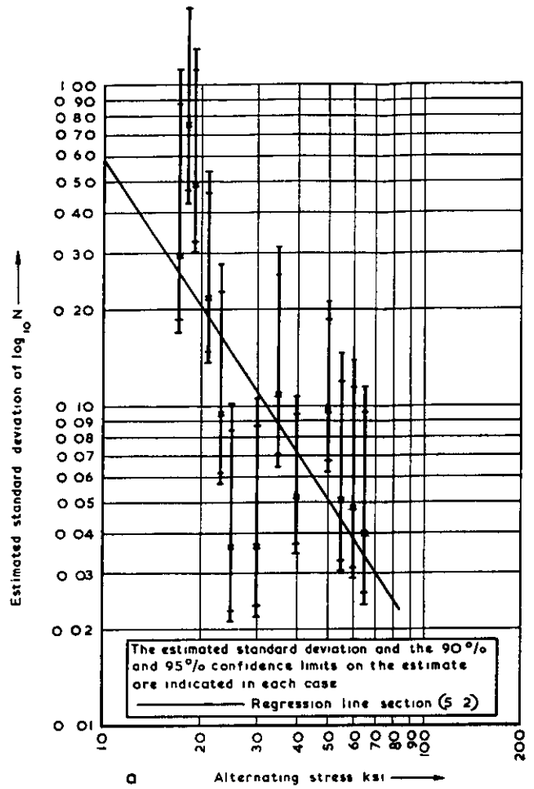

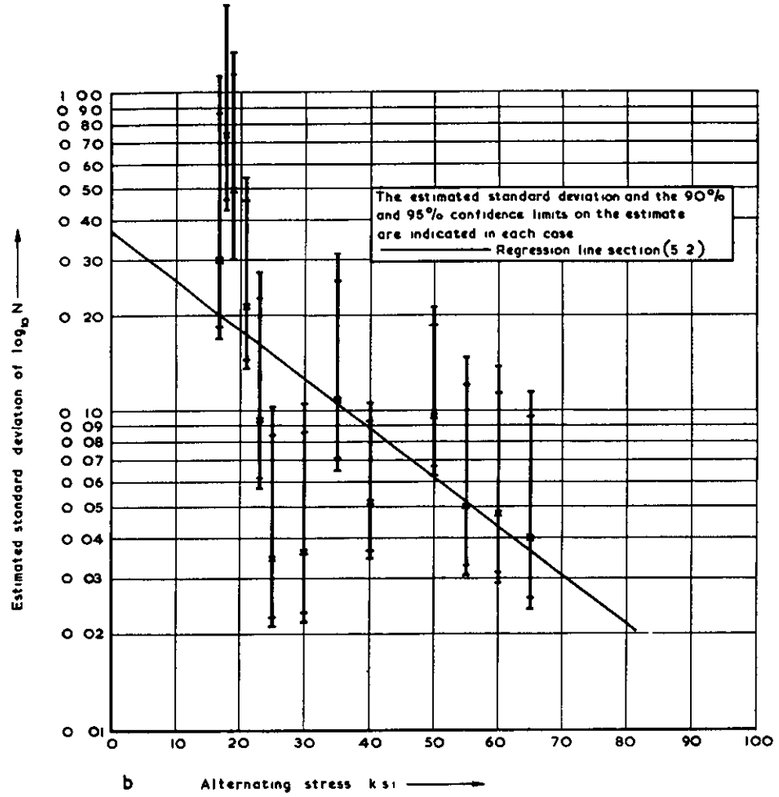

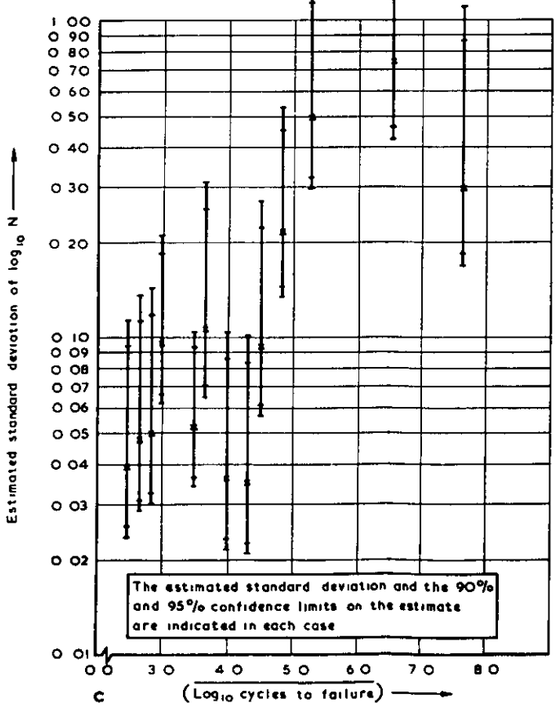

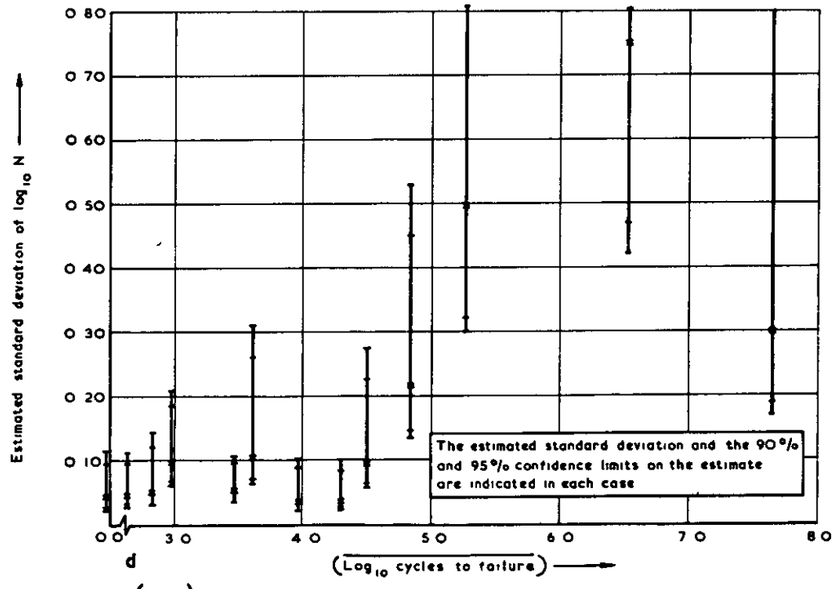

Fig.6a-d Constant amplitude 7075 material ref (67)

Axial load $K_t = 4 \cdot 0$ Edge notched sheet

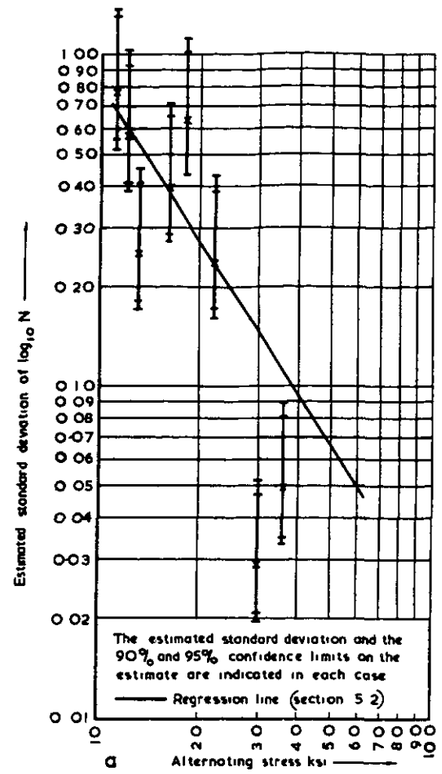

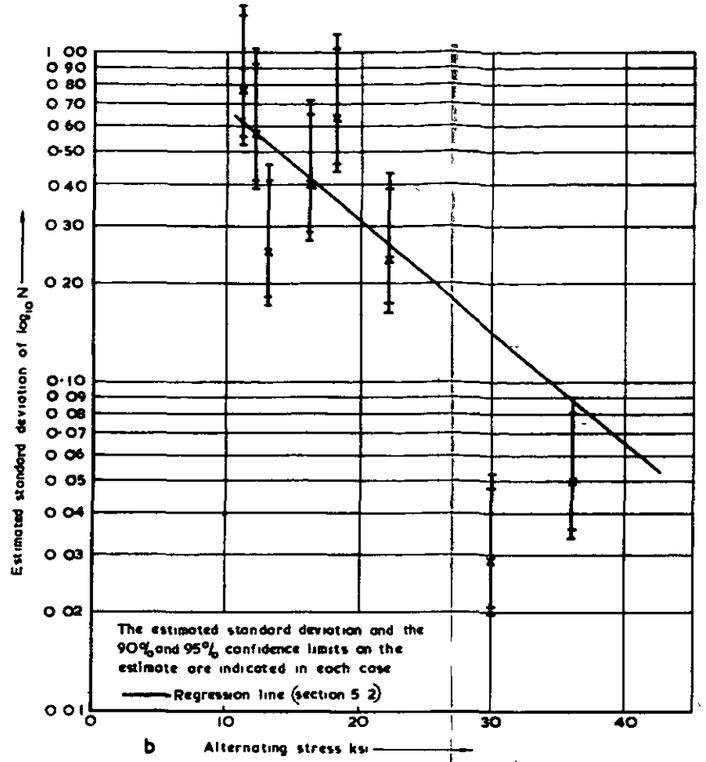

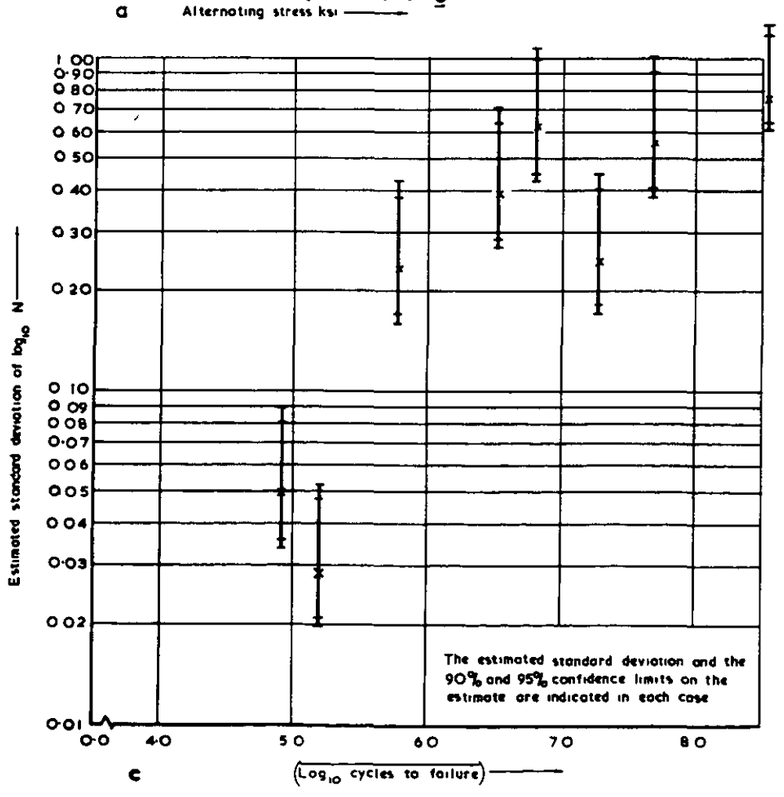

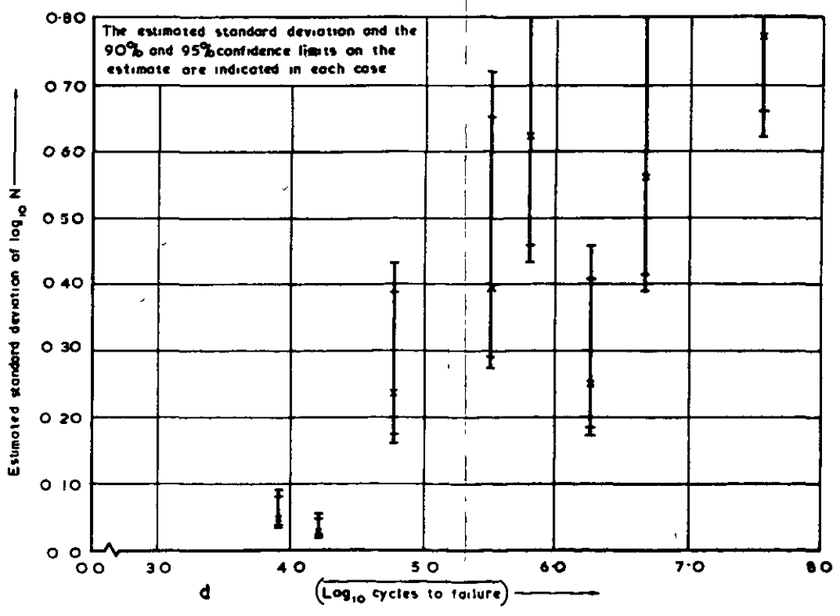

Fig. 7a-d Constant amplitude 7075 material ref (47)
Rotating beam Notched 0·01 inch radius

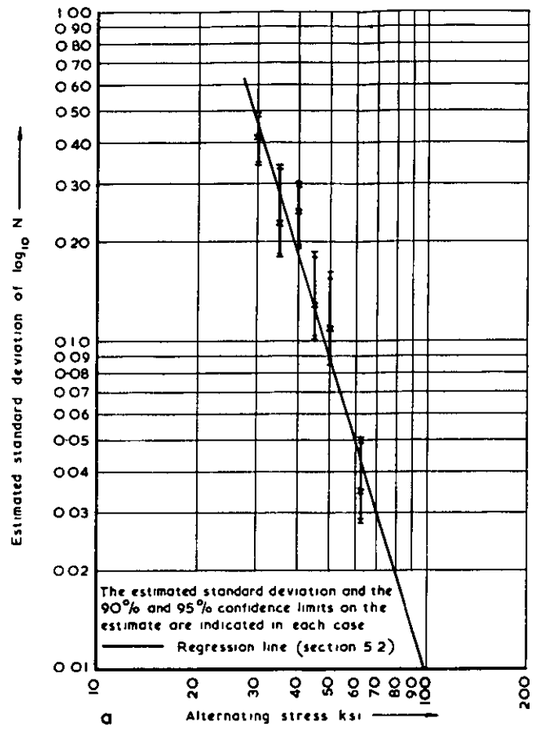

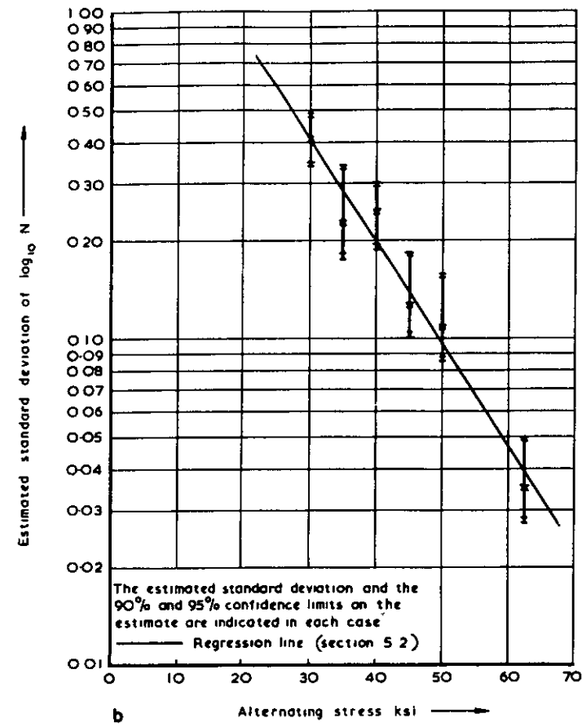

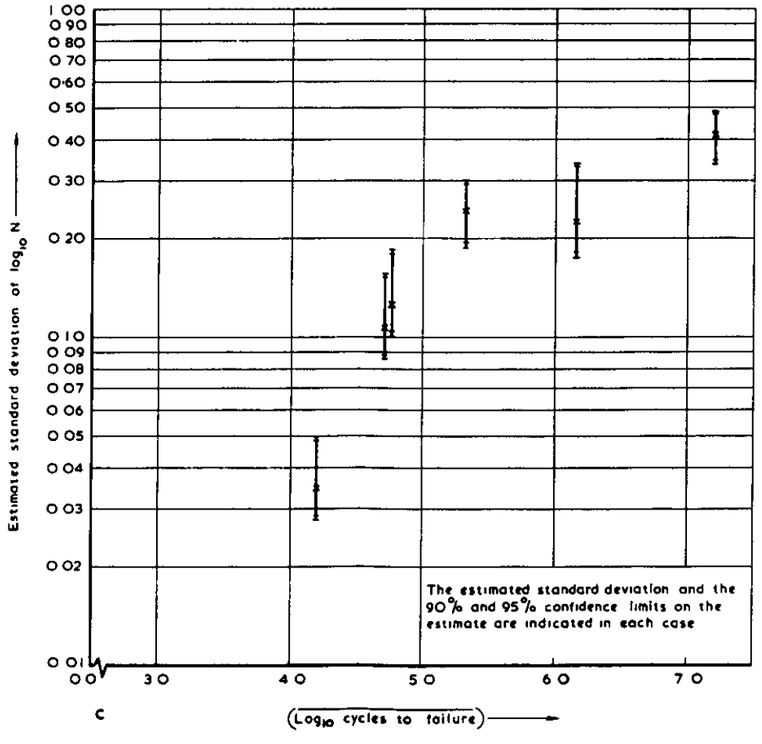

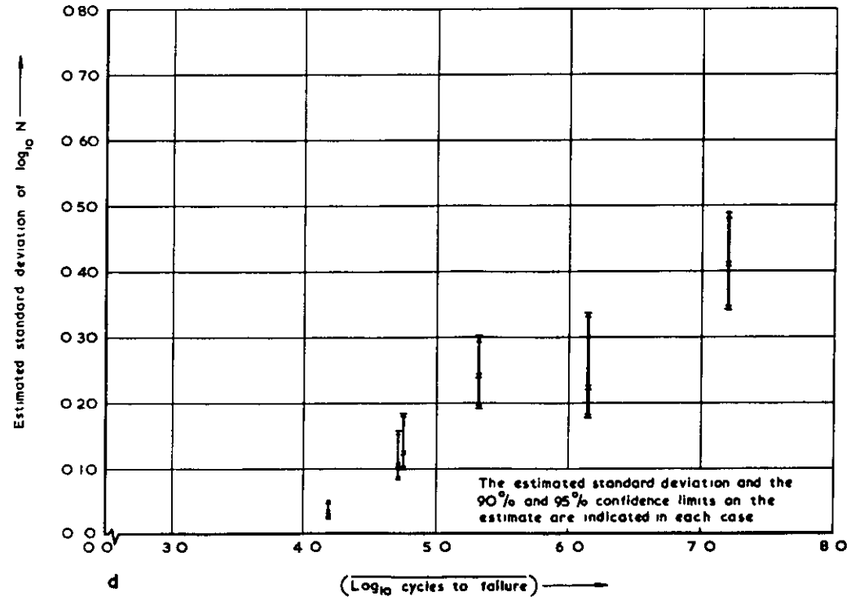

Fig 8 a–d Constant amplitude 7075 material. Bar form (ref 16)
Unnotched. Rotating bending

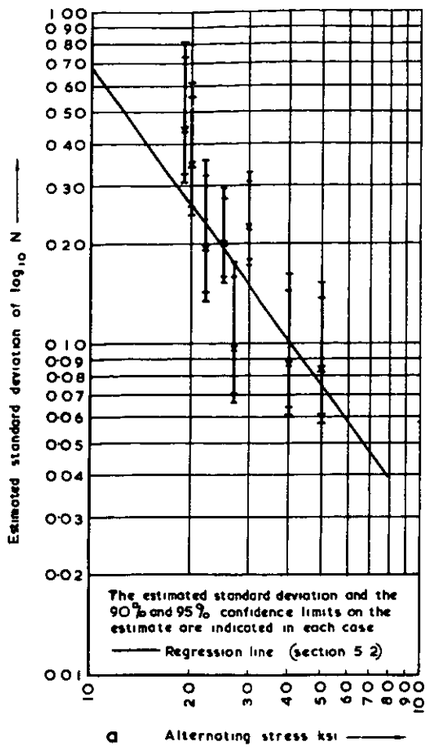

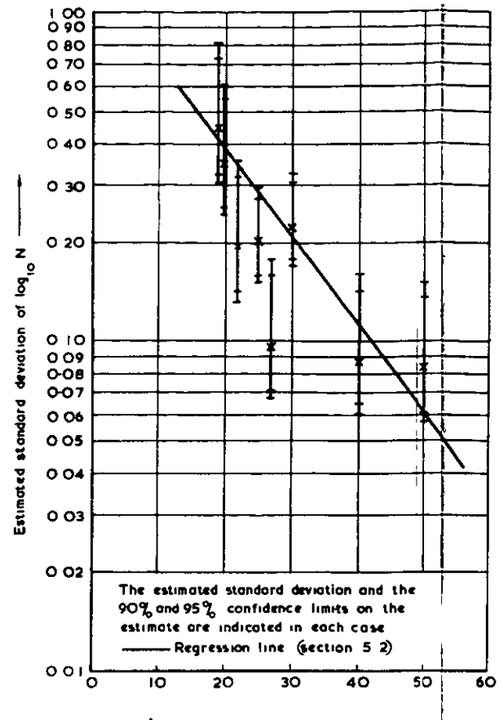

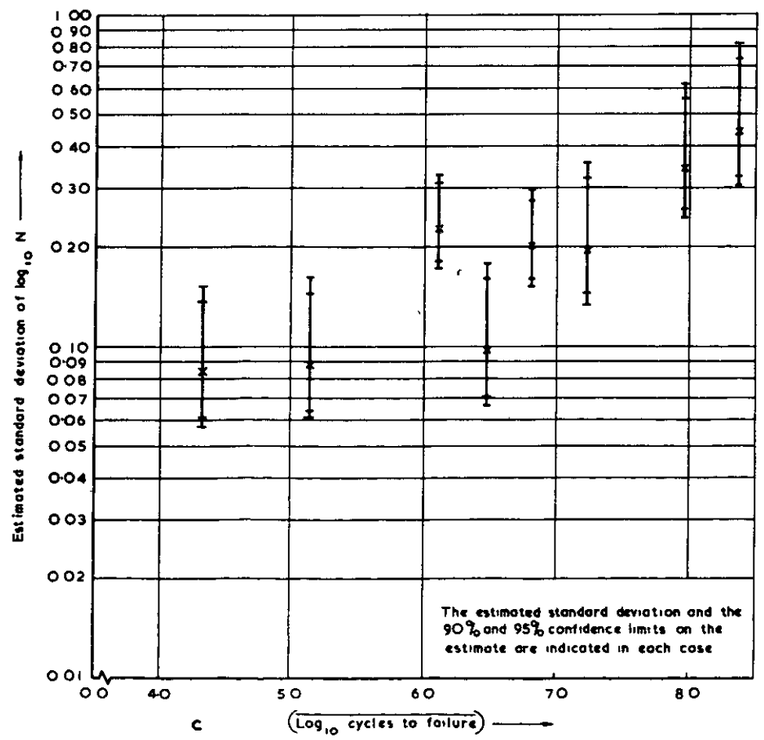

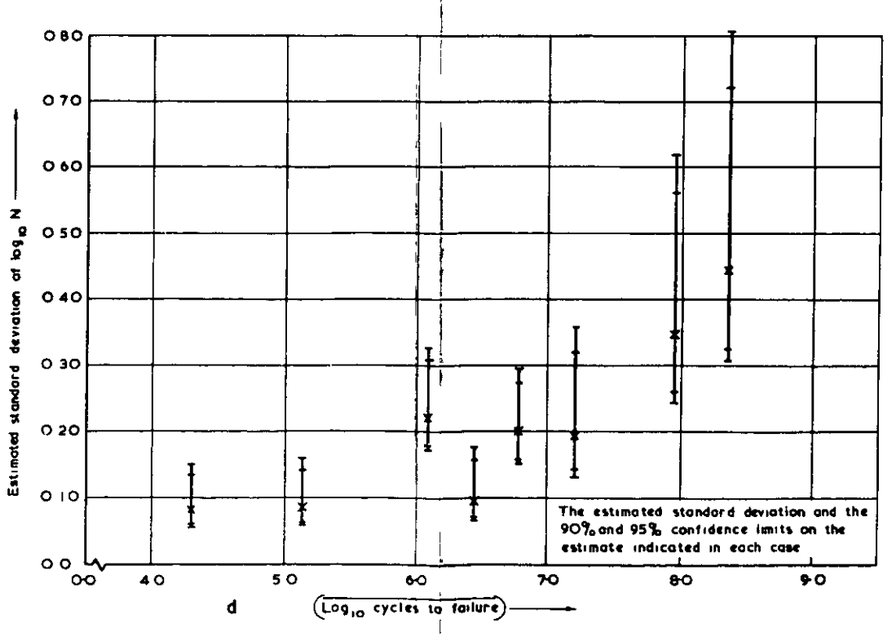

Fig. 9 a - d Constant amplitude 2024 material (ref 68)
Unnotched Rotating beam

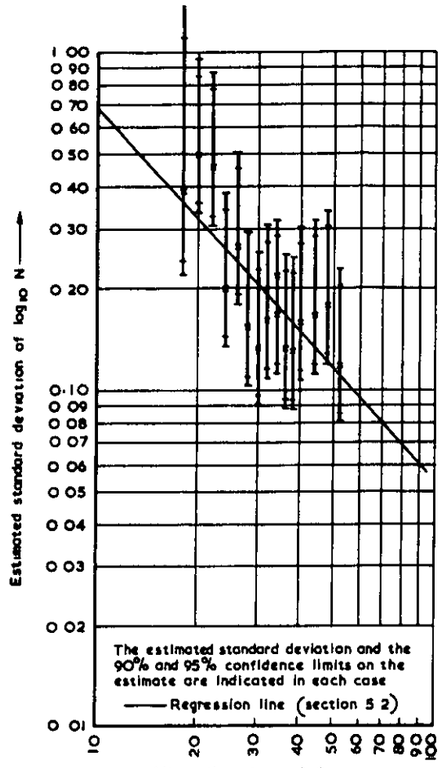

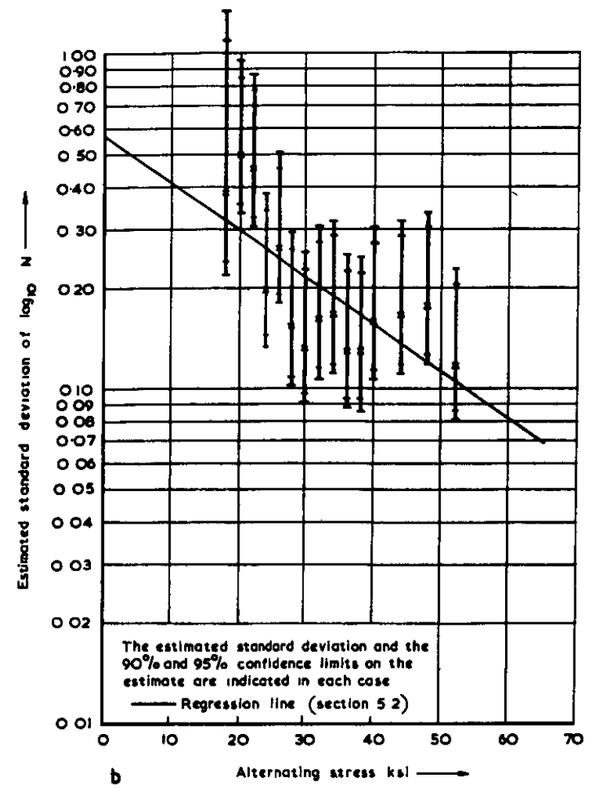

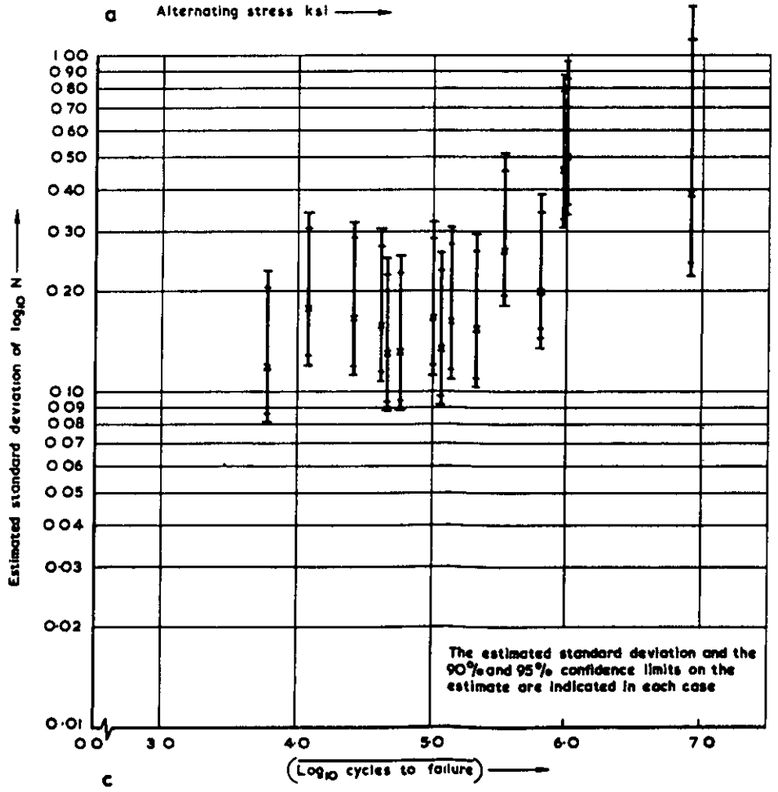

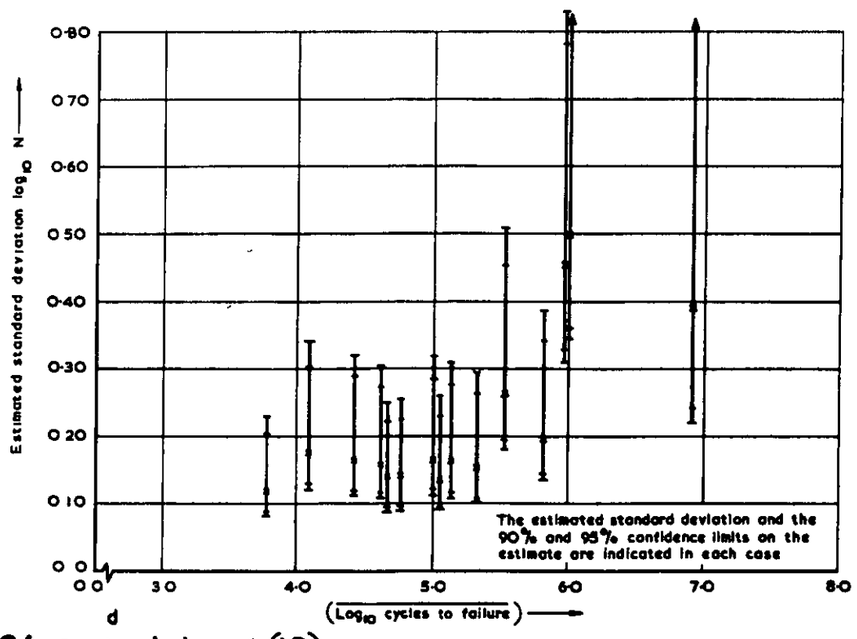

Fig. 10 a–d Constant amplitude 2024 material ref (19)
Unnotched. Axial load

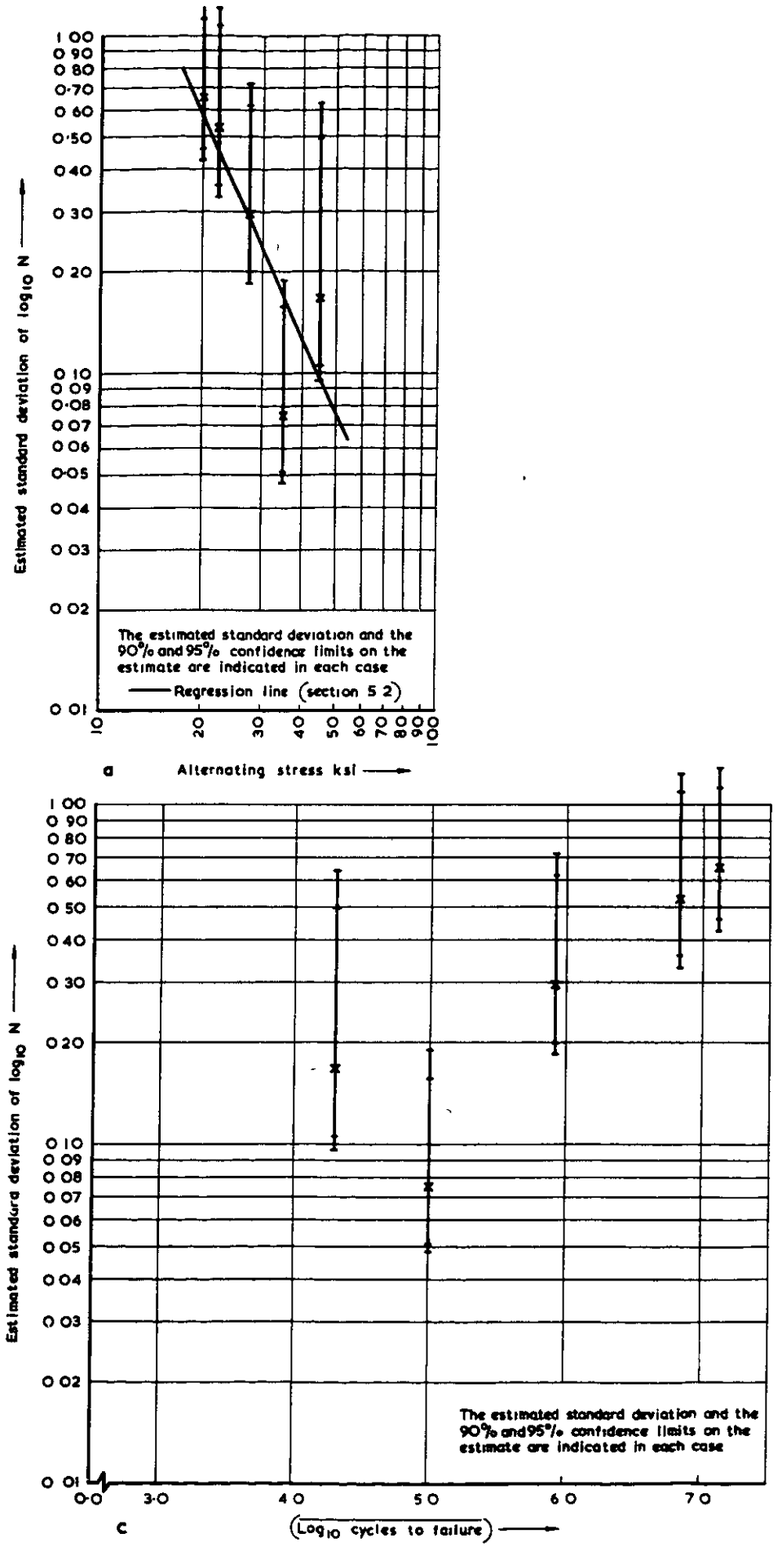

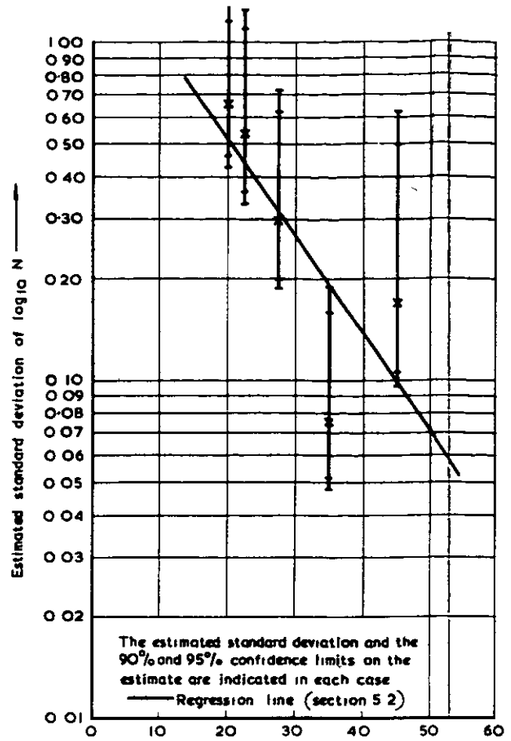

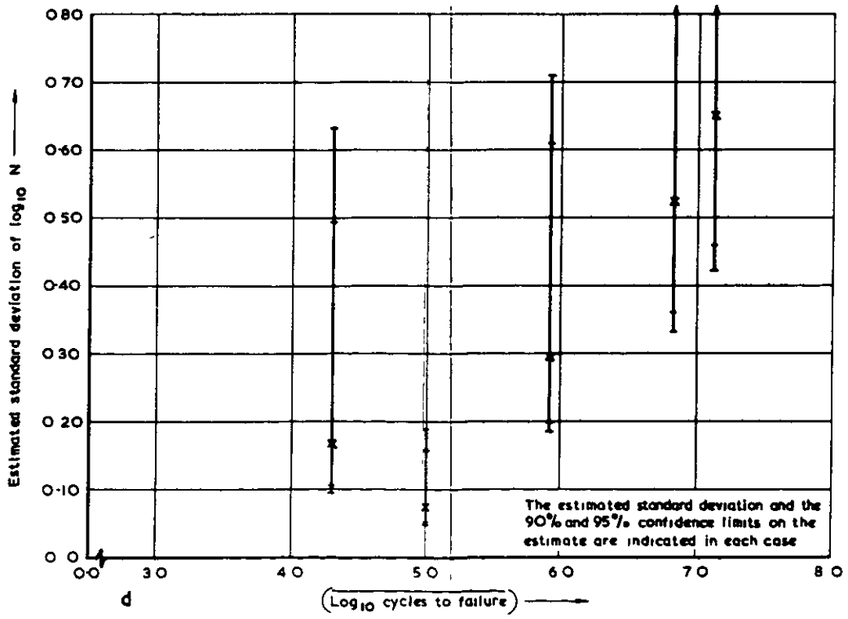

Fig. 11a-d Constant amplitude notch radius 0·0625 in 2024 material ref (49)
Notched. Rotating bending

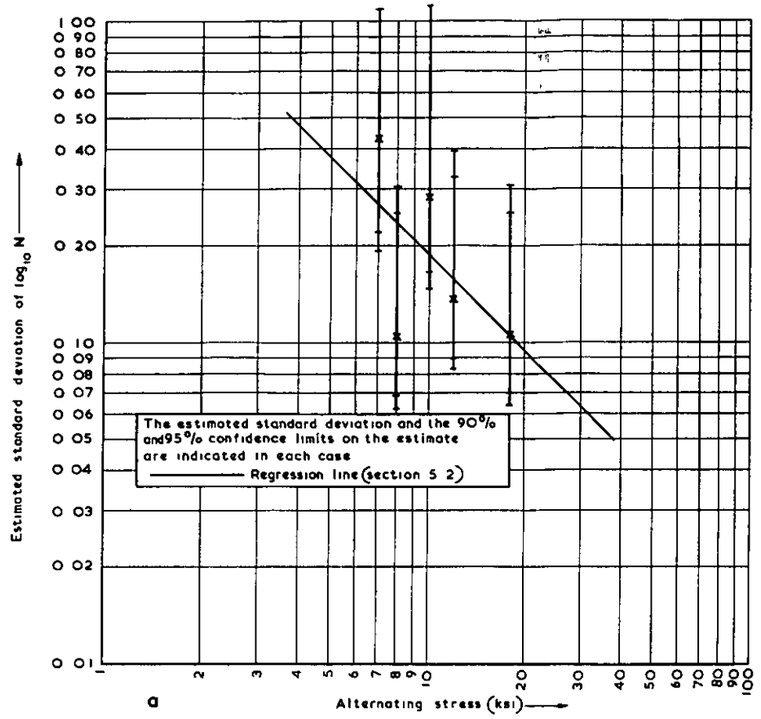

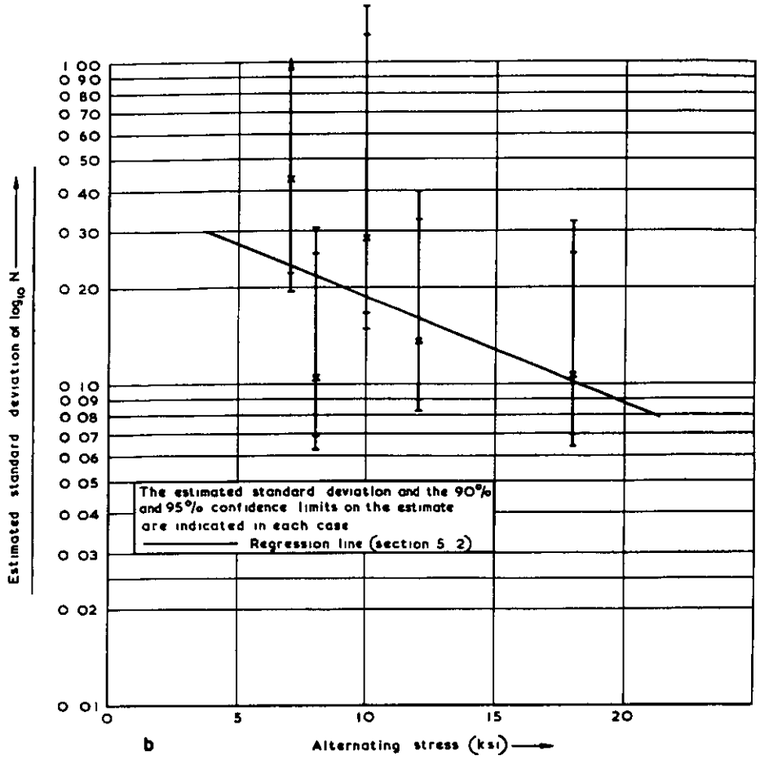

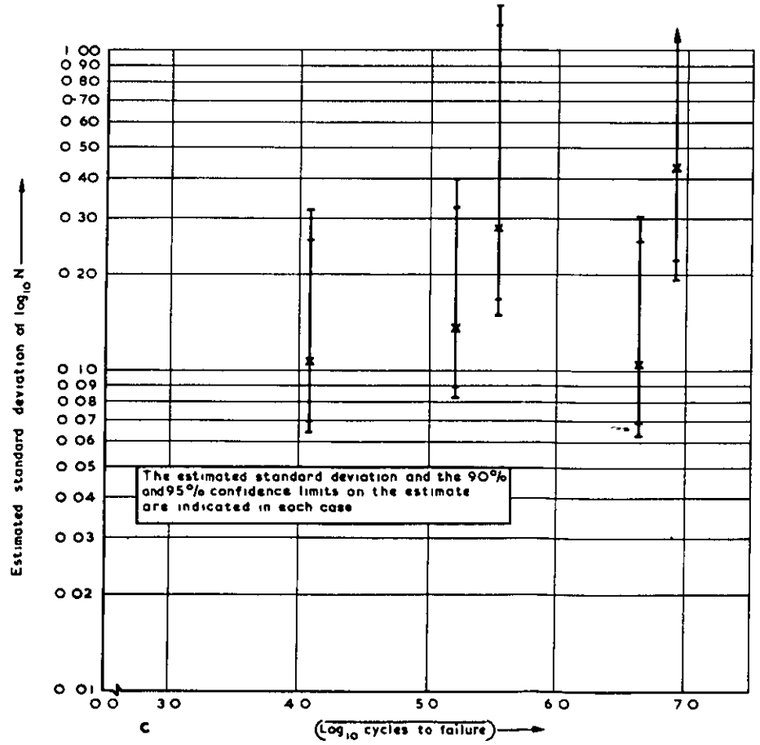

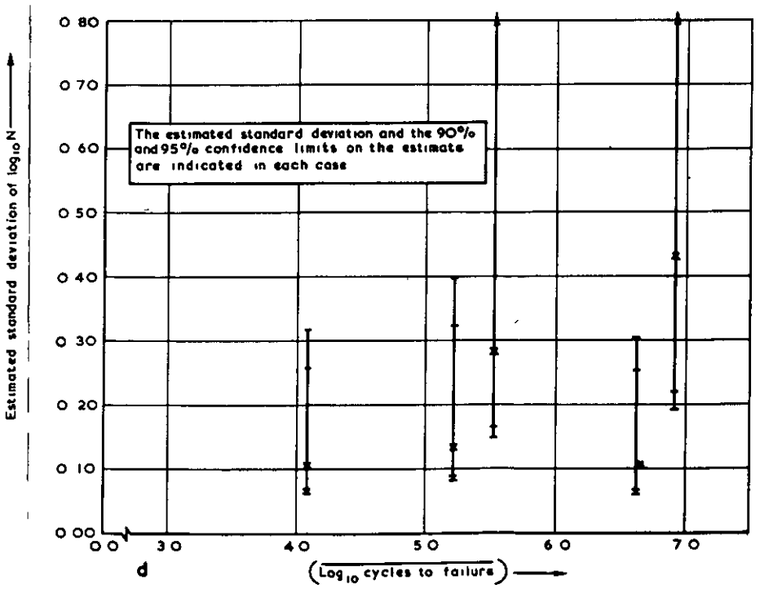

Fig.12a-d Constant amplitude 2024 material ref (48)
Notch. Axial. Edge notched sheet $K_t = 4{\cdot}0$

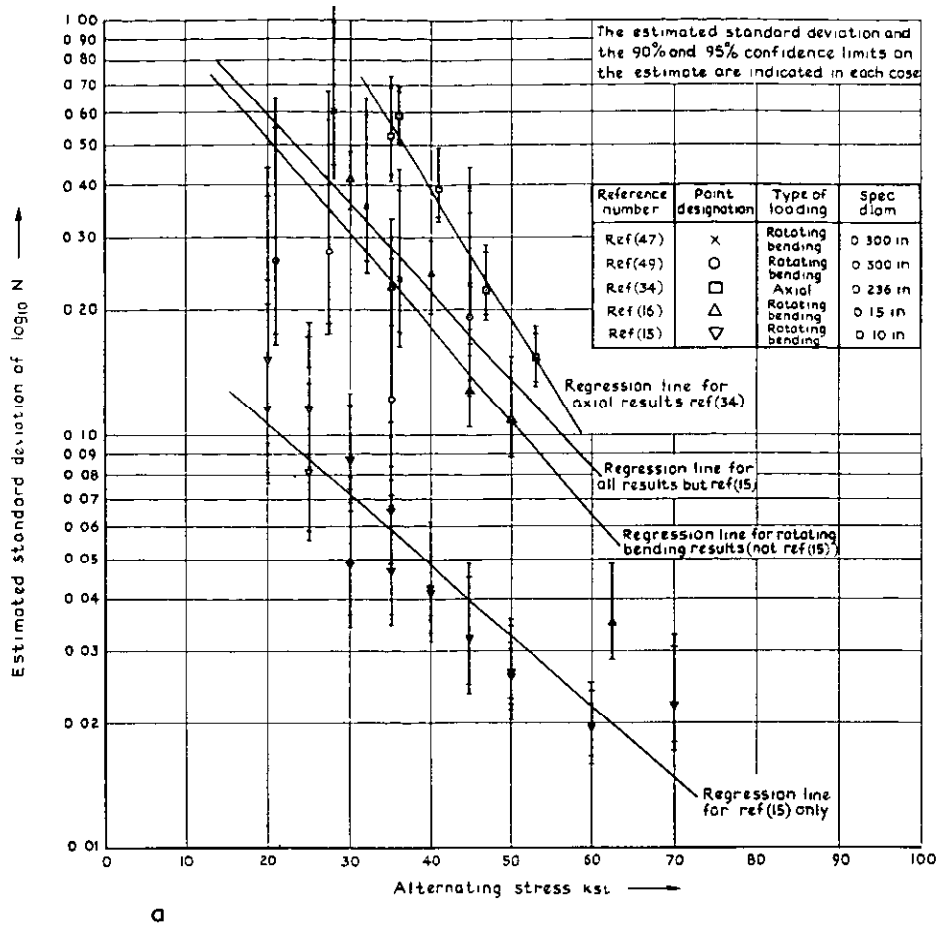

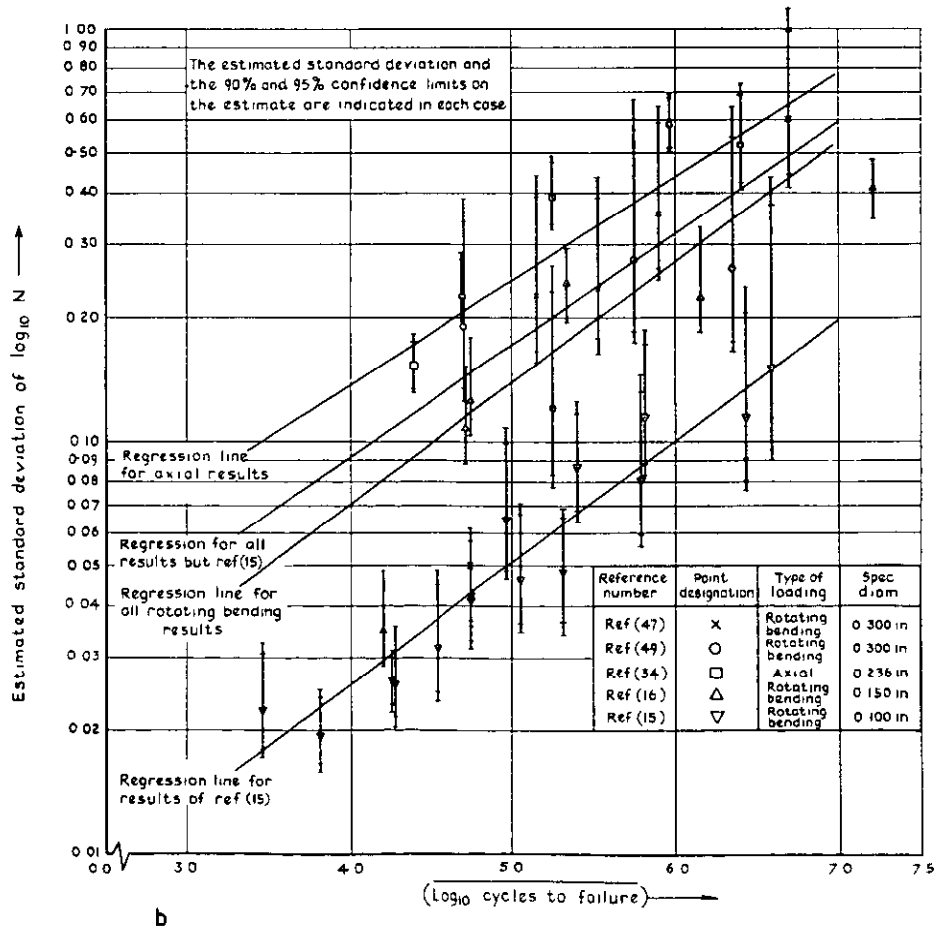

Fig 13 a&b Constant amplitude 7075 material Unnotched

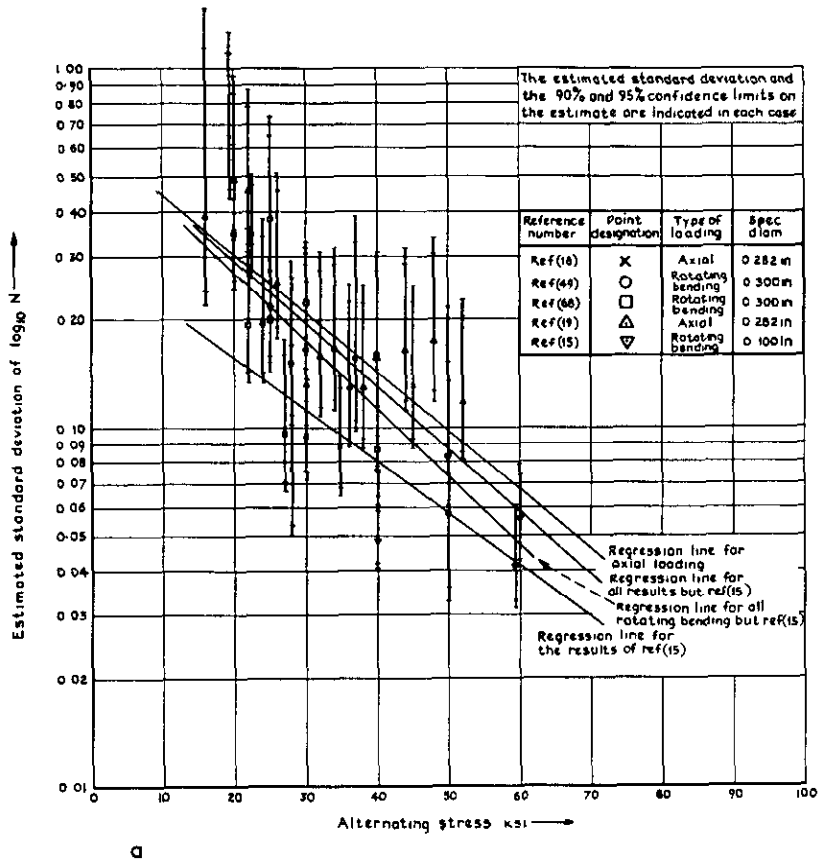

a

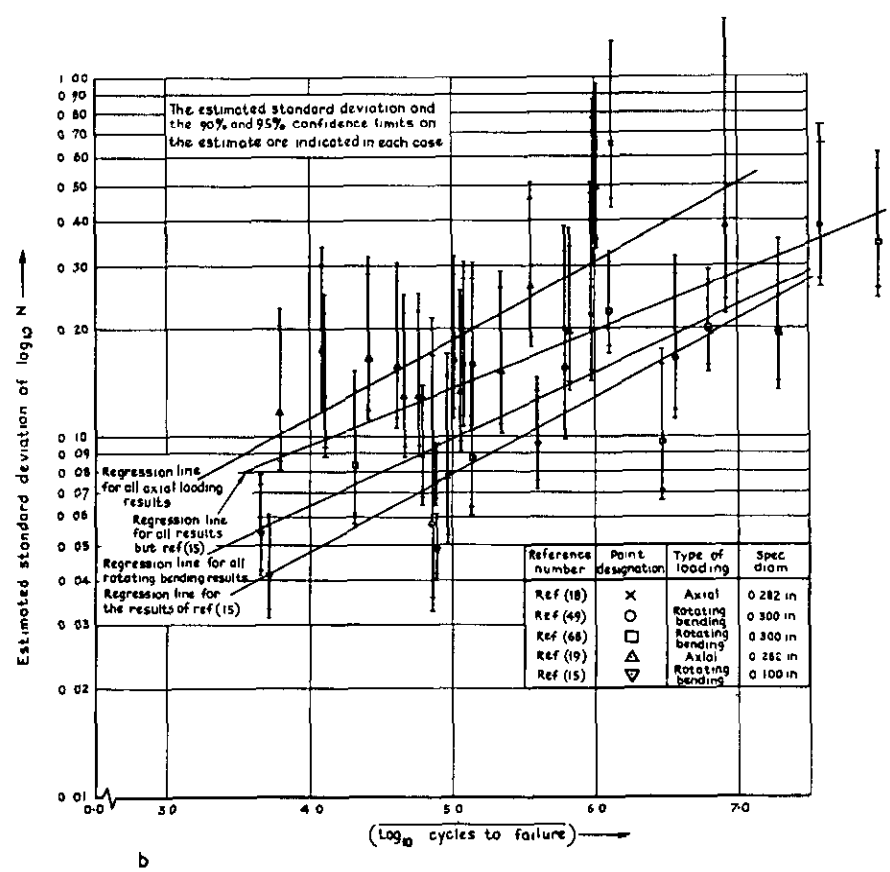

b

Fig 14 a & b Constant amplitude 2024 material Unnotched

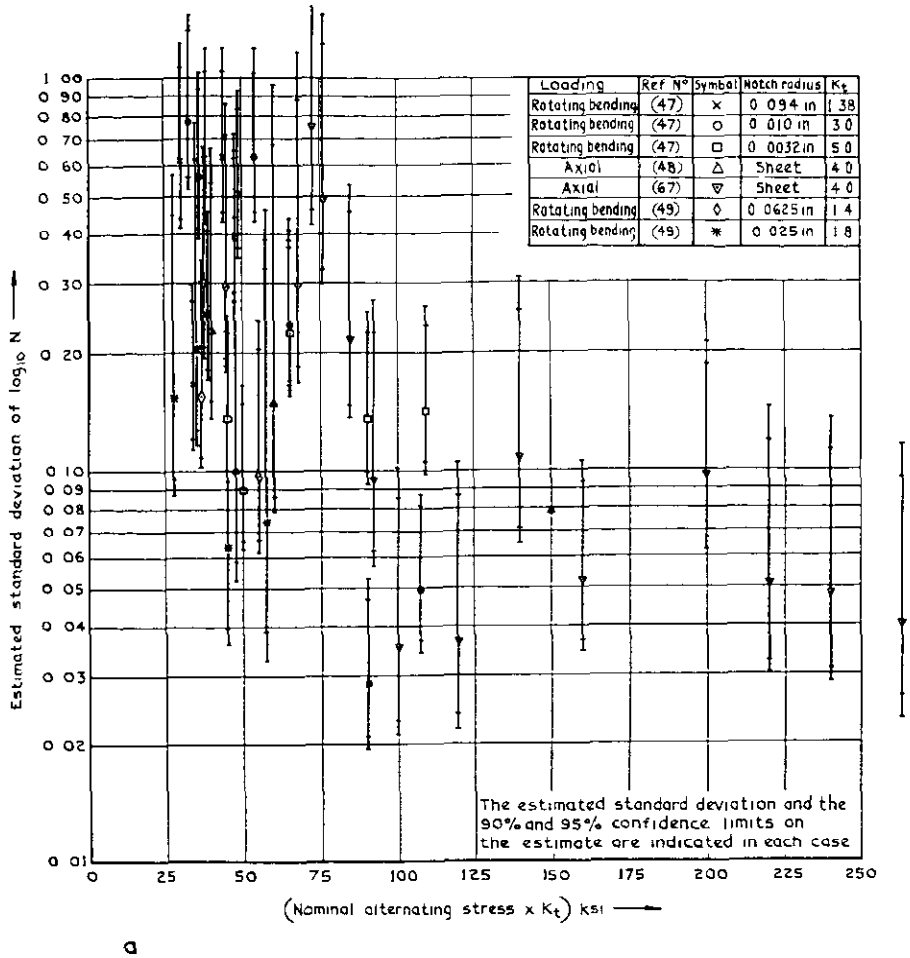

a

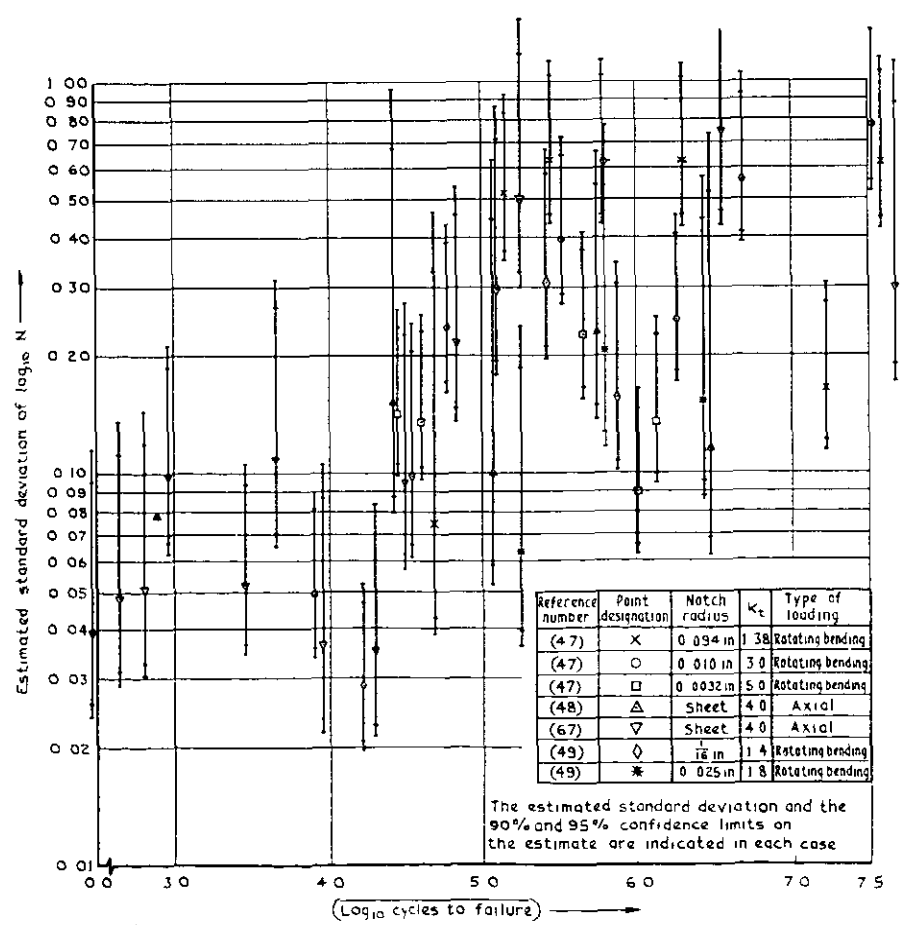

b

Fig 15 a & b Constant amplitude 7075 material Notched

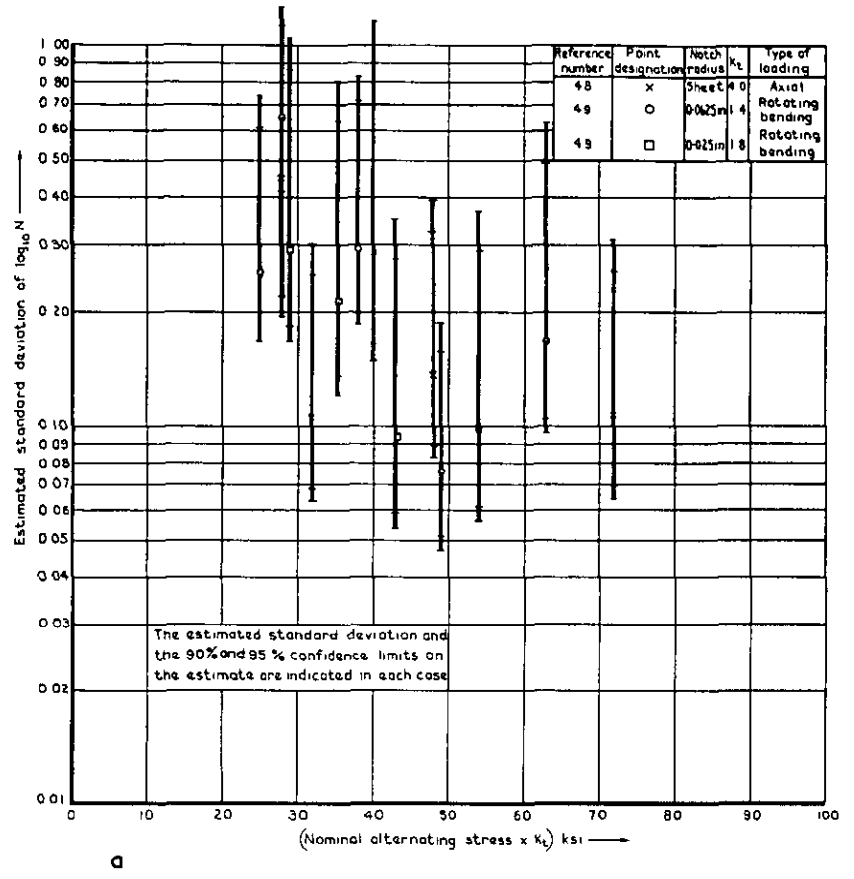

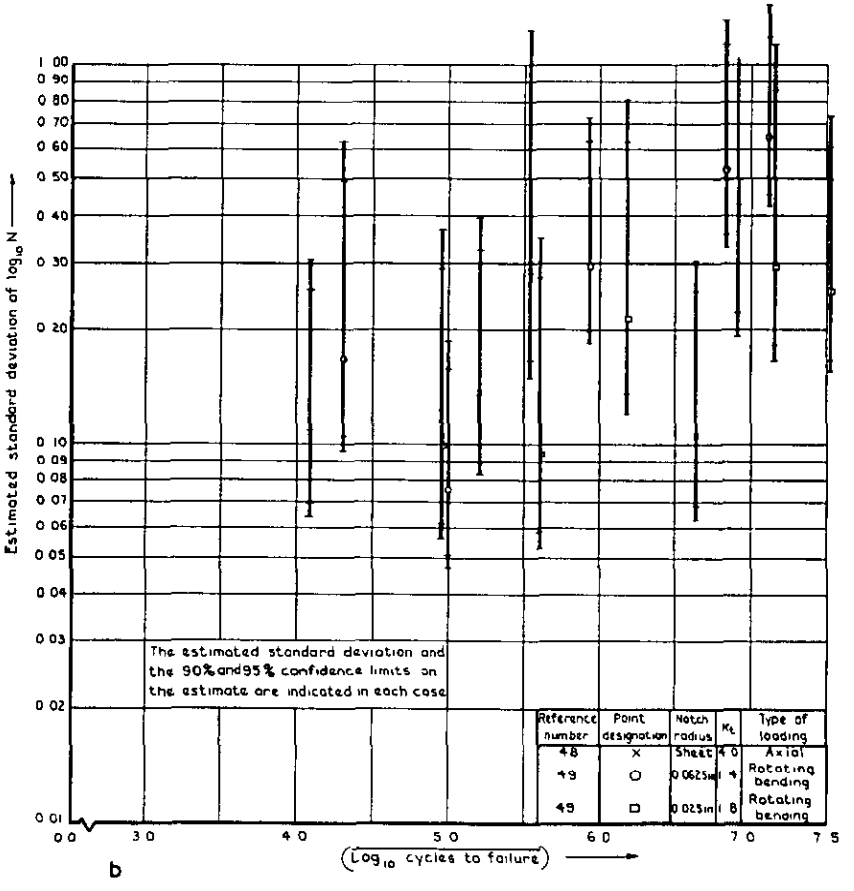

Fig. 16 a&b Constant amplitude 2024 material notched

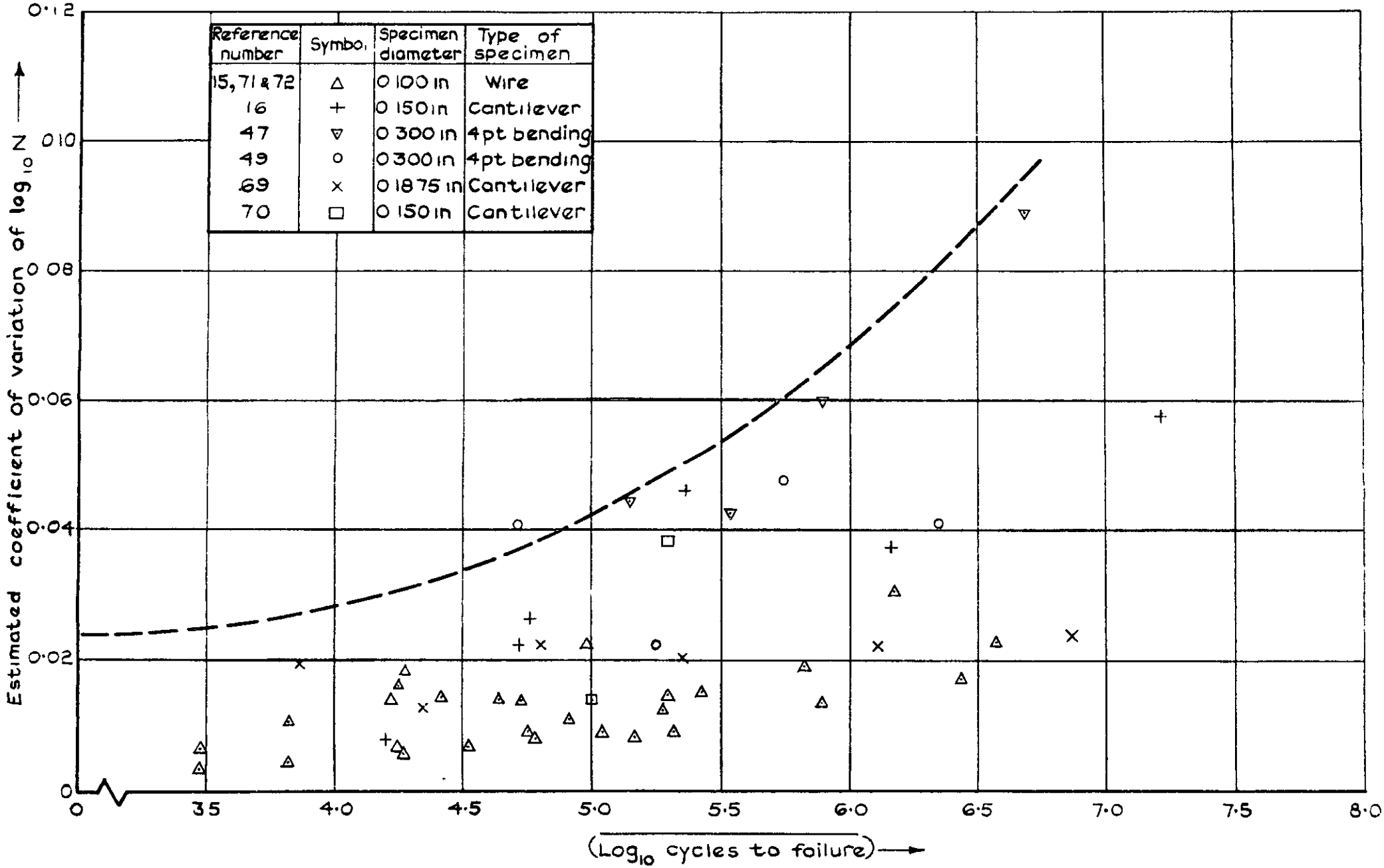

Fig. 17 Constant amplitude, rotating beam unnotched 7075 material bar form

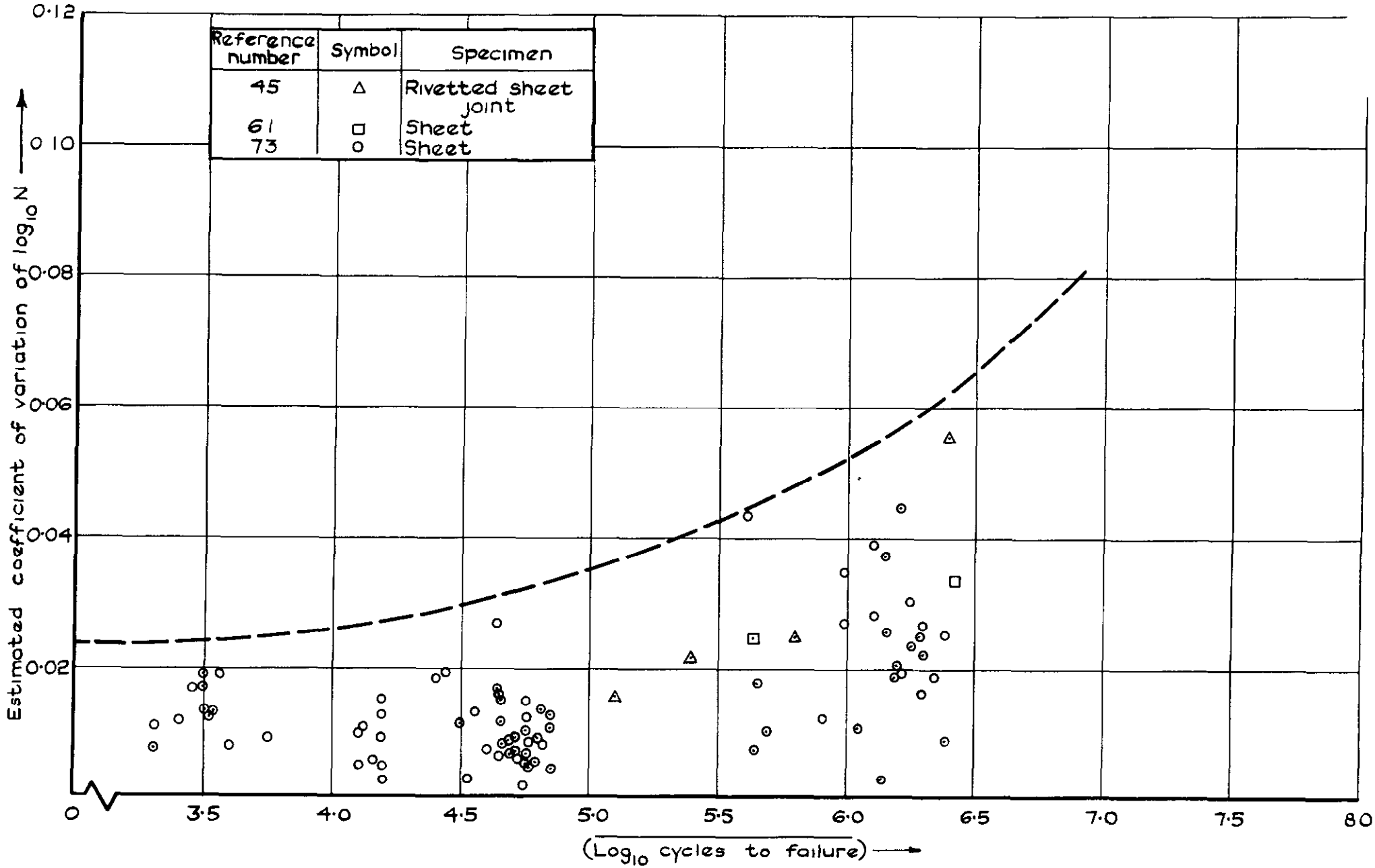

Fig.18 Constant amplitude, axial load unnotched 7075 material sheet form

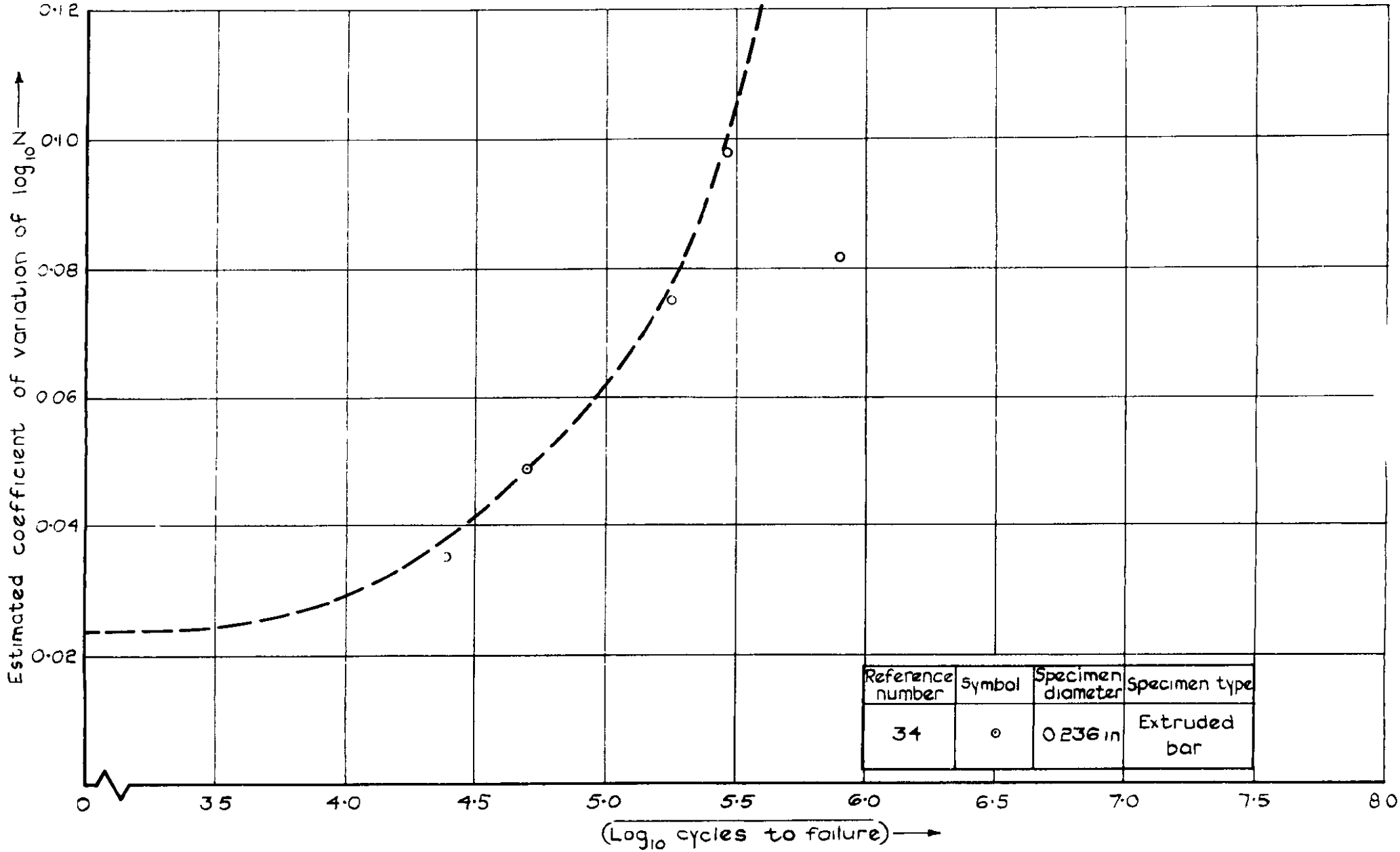

Fig. 19 Constant amplitude, axial load unnotched 7075 material bar form

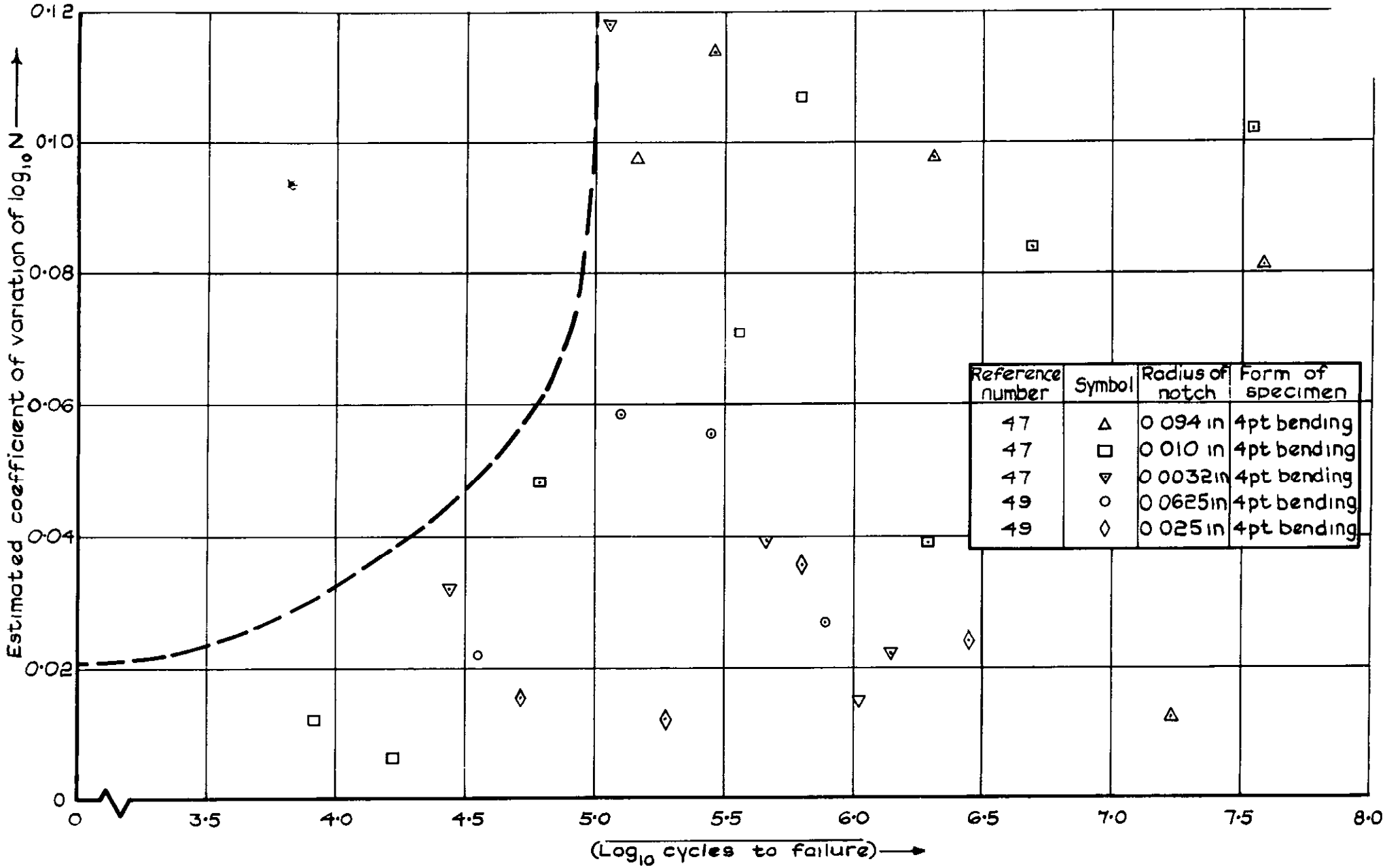

Fig. 20 Constant amplitude, rotating beam notched 7075 material bar form

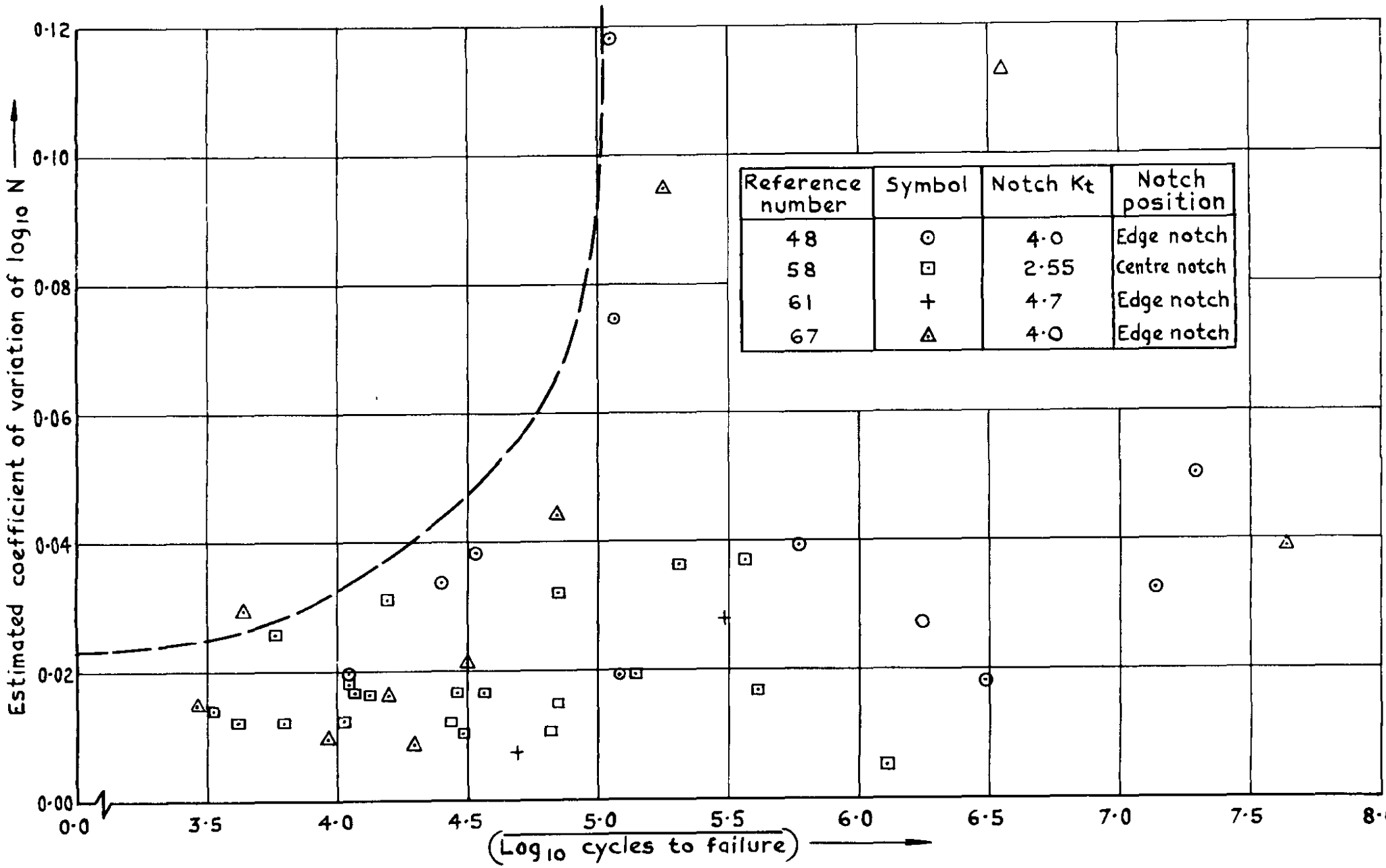

Fig. 21 Constant amplitude, axial load, notched 7075 material sheet form

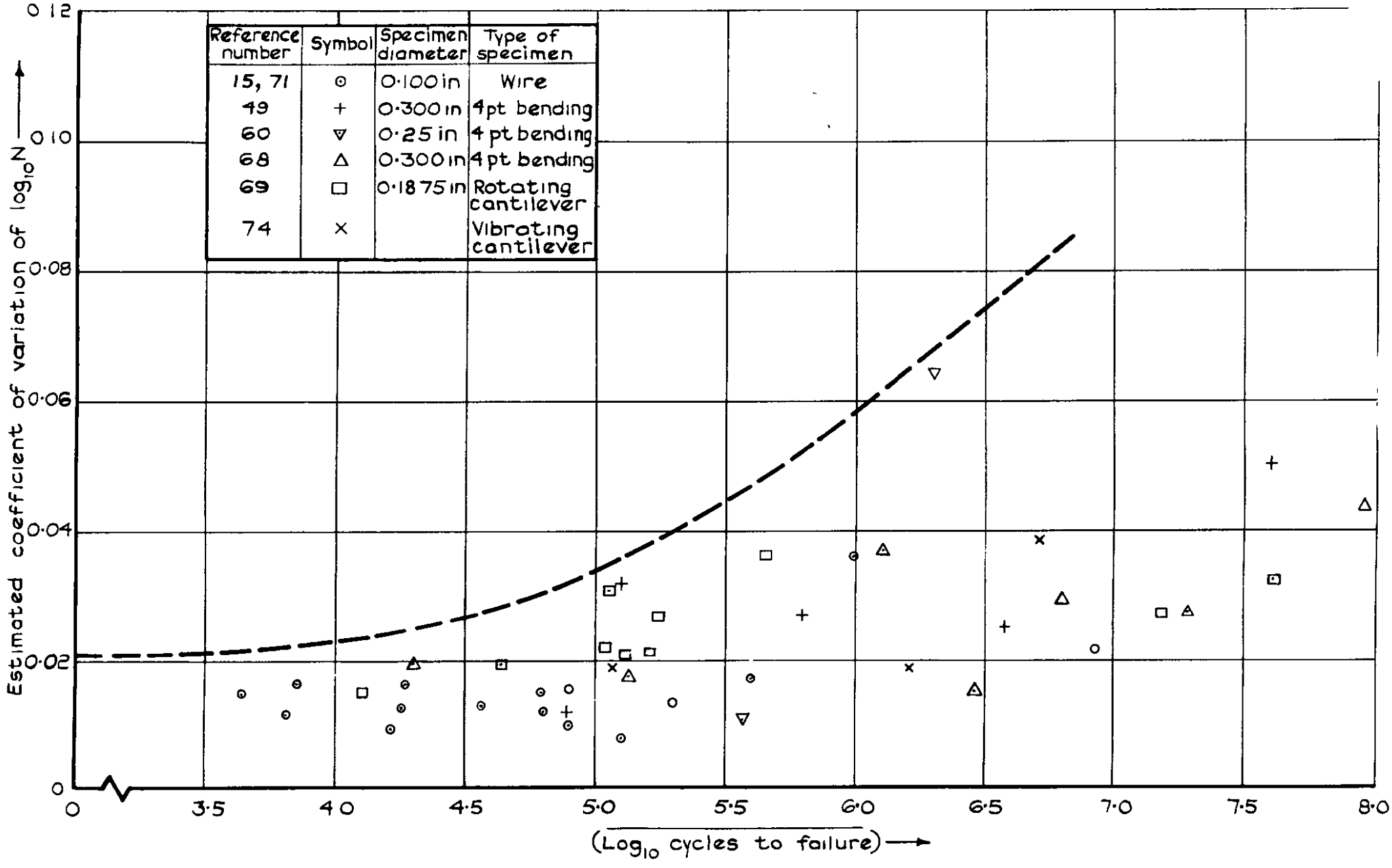

Fig. 22 Constant amplitude, rotating beam unnotched 2024 material bar form

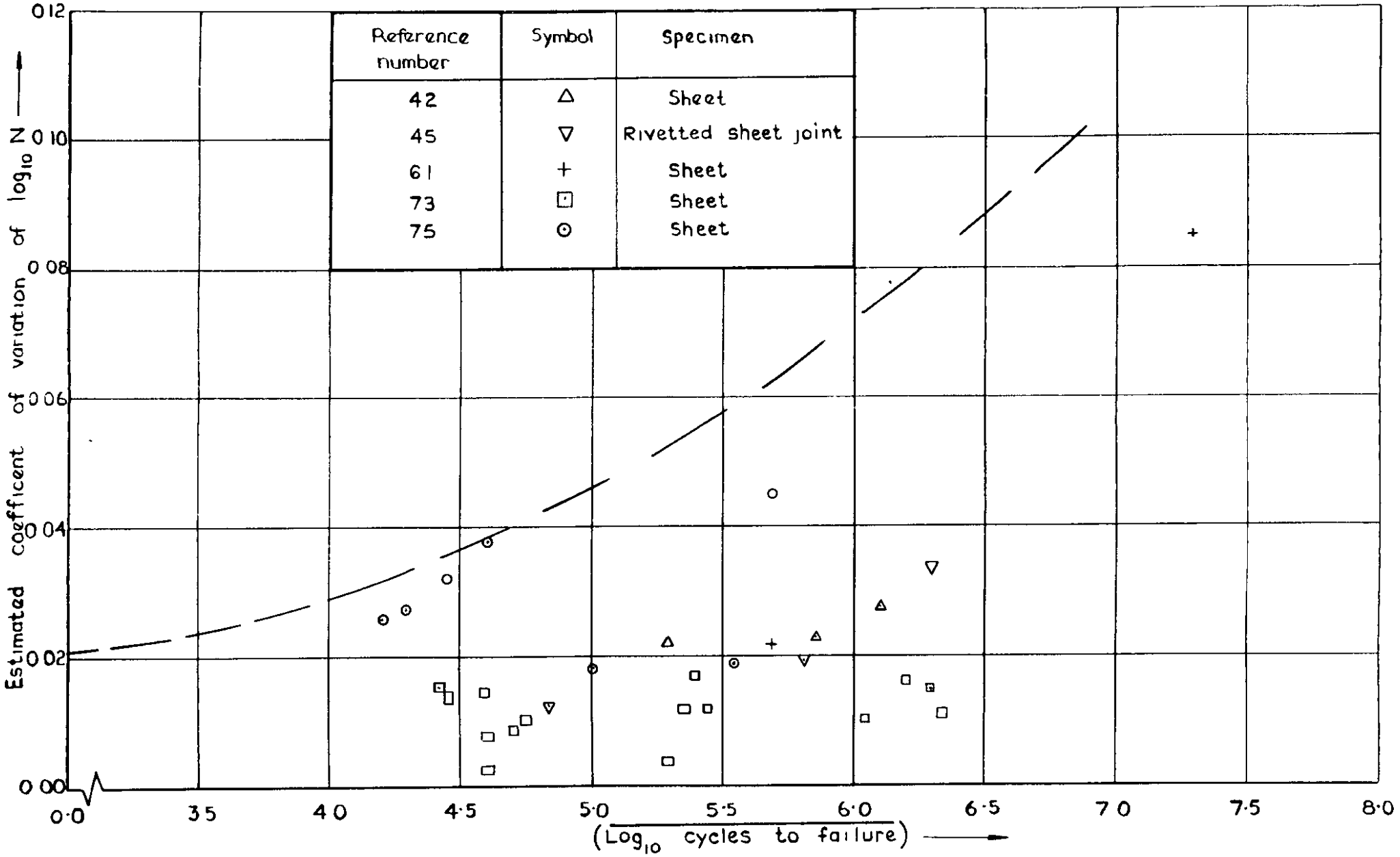

Fig.23 Constant amplitude, axial load unnotched 2024 material sheet form

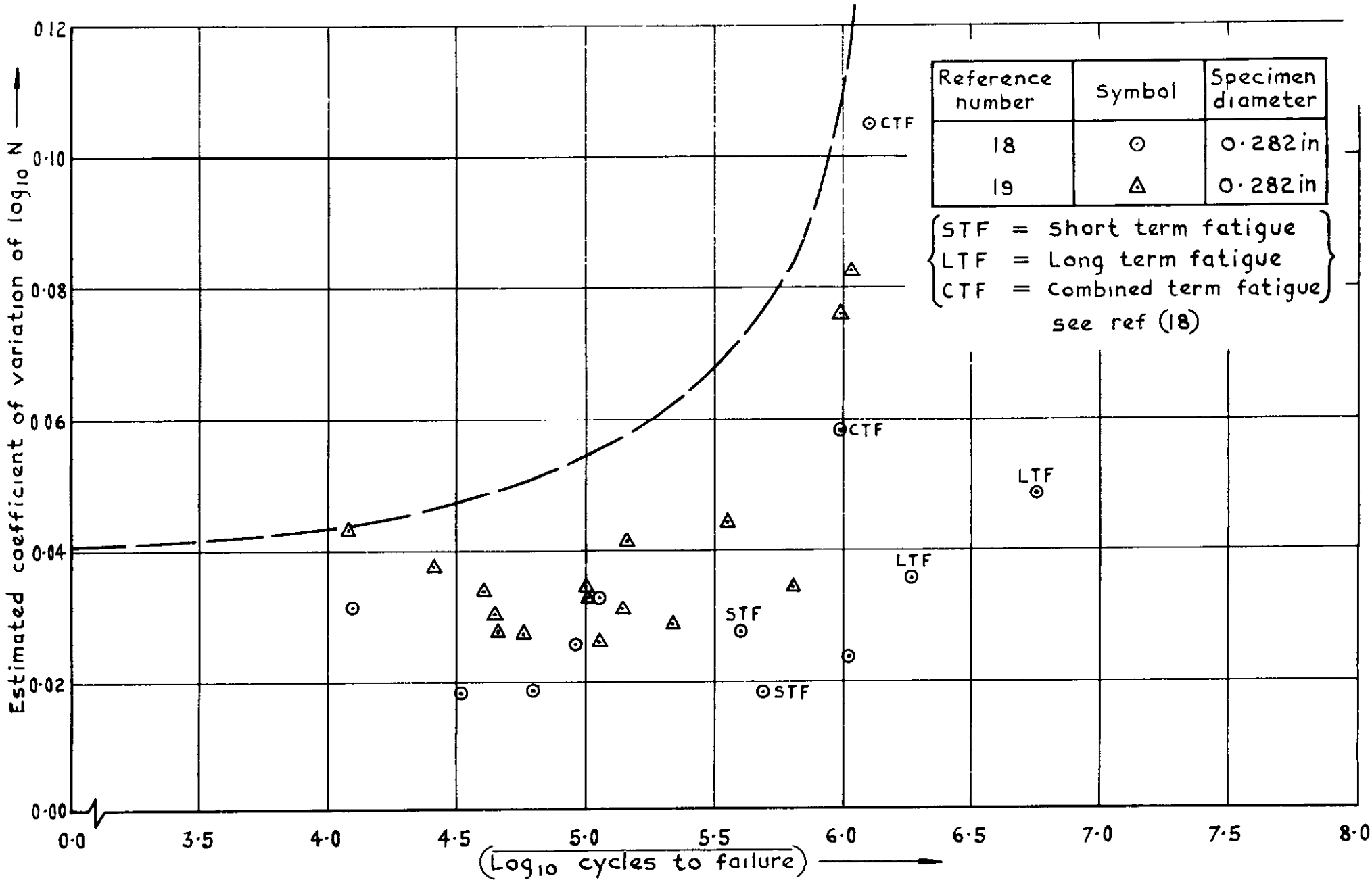

Fig.24 Constant amplitude, axial load, unnotched 2024 material bar form

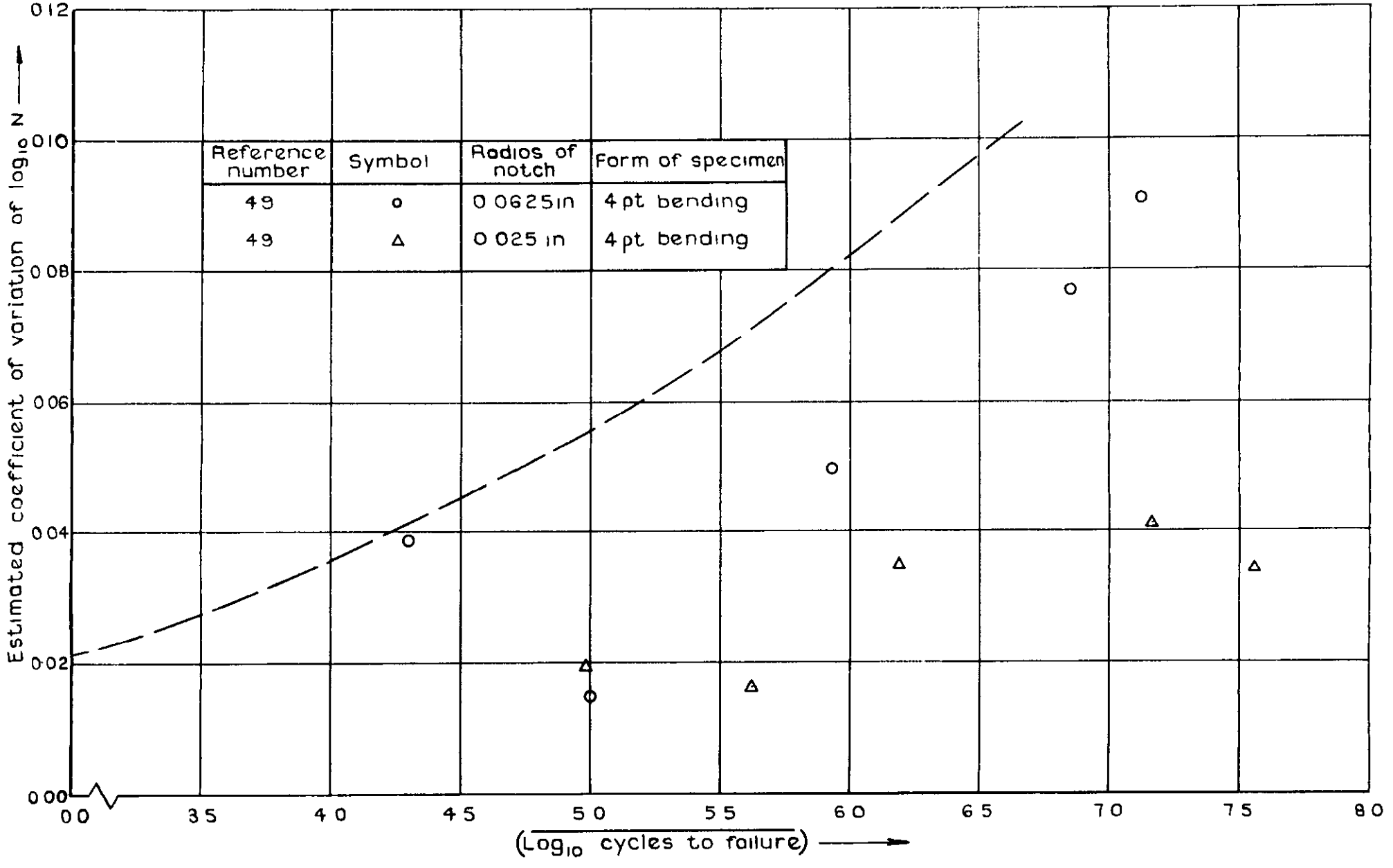

Fig. 25 Constant amplitude, rotating beam notched 2024 material bar form

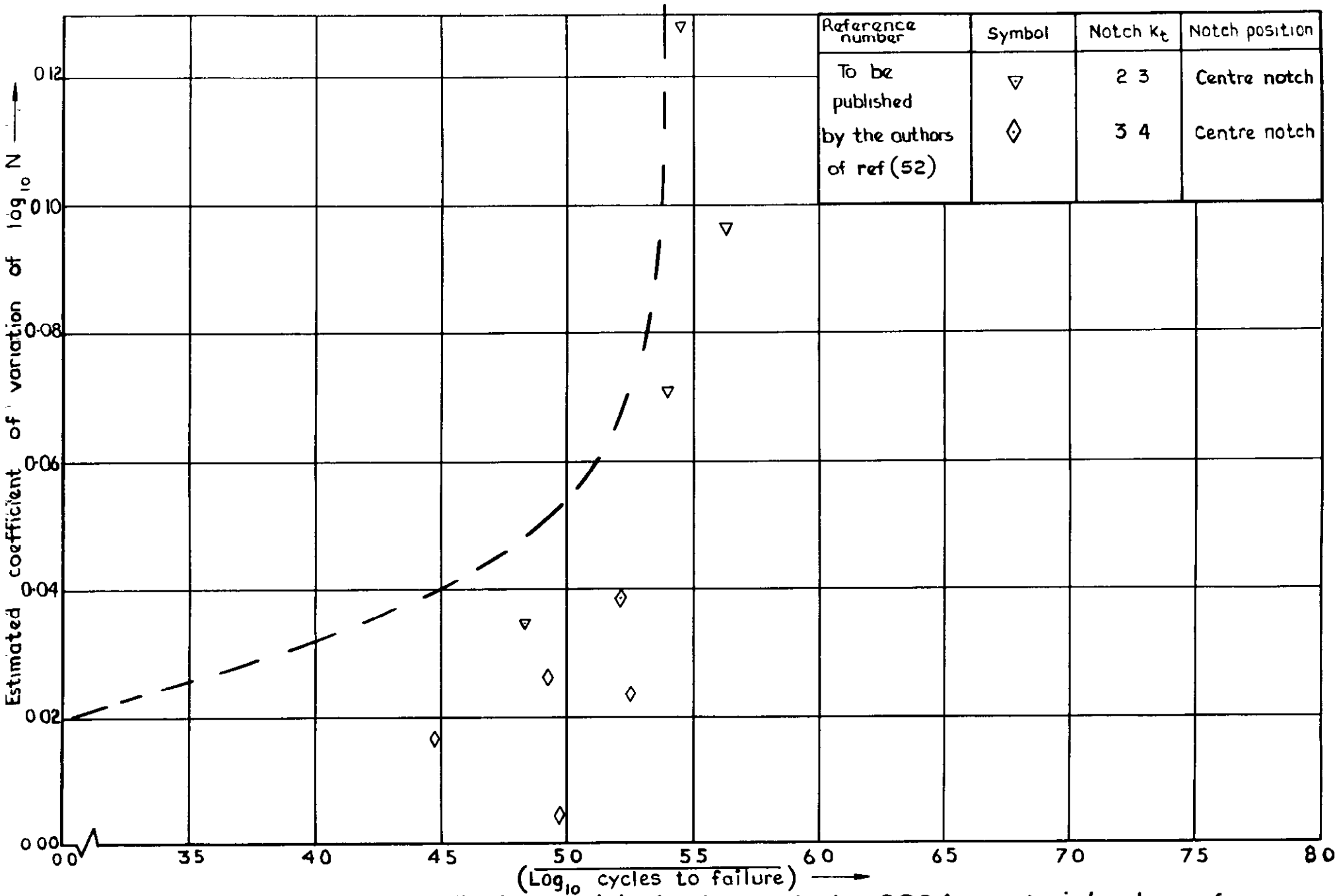

Fig 26 Constant amplitude, axial load notched 2024 material bar form

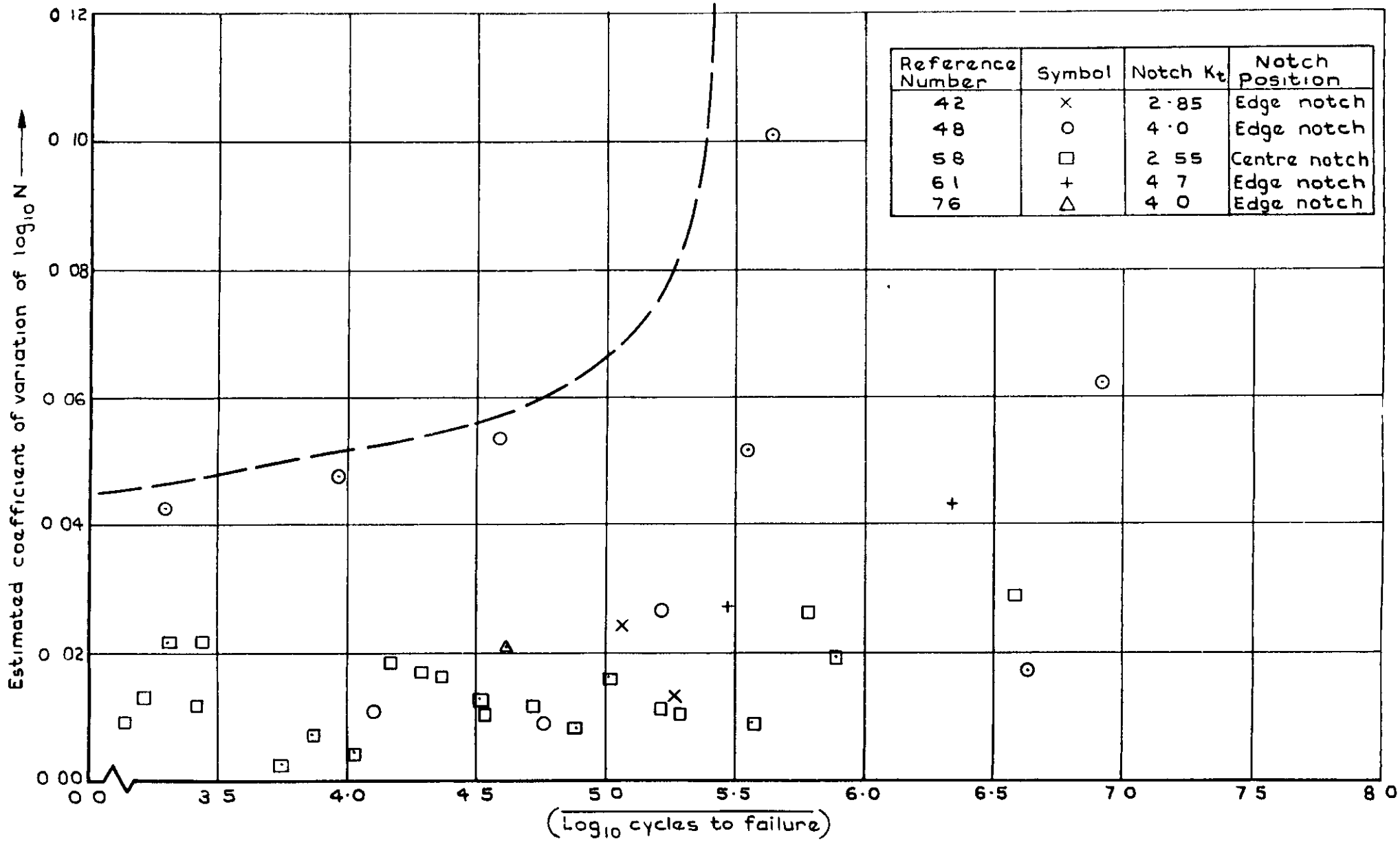

Fig.27 Constant amplitude, axial load notched 2024 material, sheet form

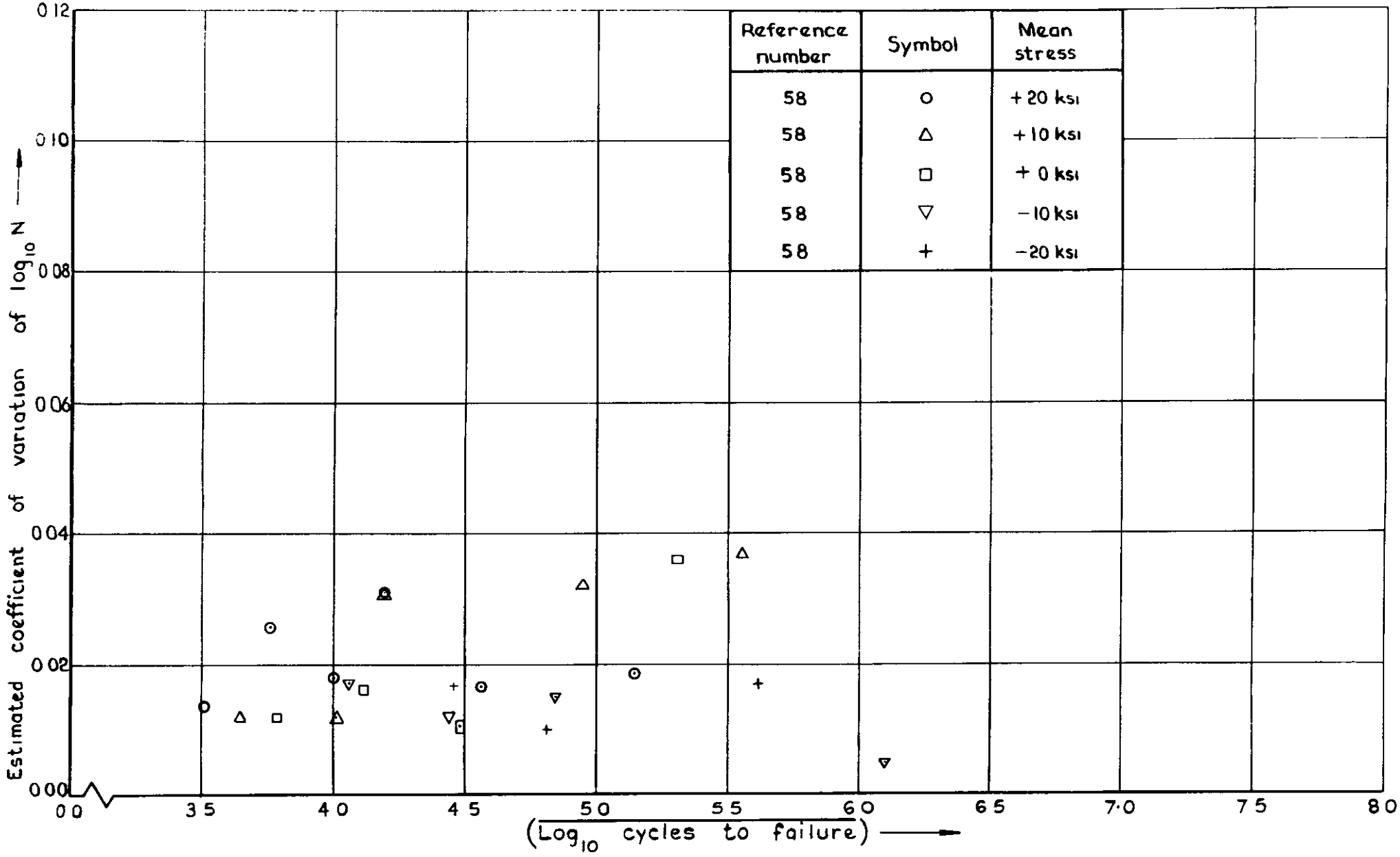

Fig. 28 Constant amplitude, axial load ref (58) centre notched 7075 material 0·032 inches thick sheet $K_t = 2·55$

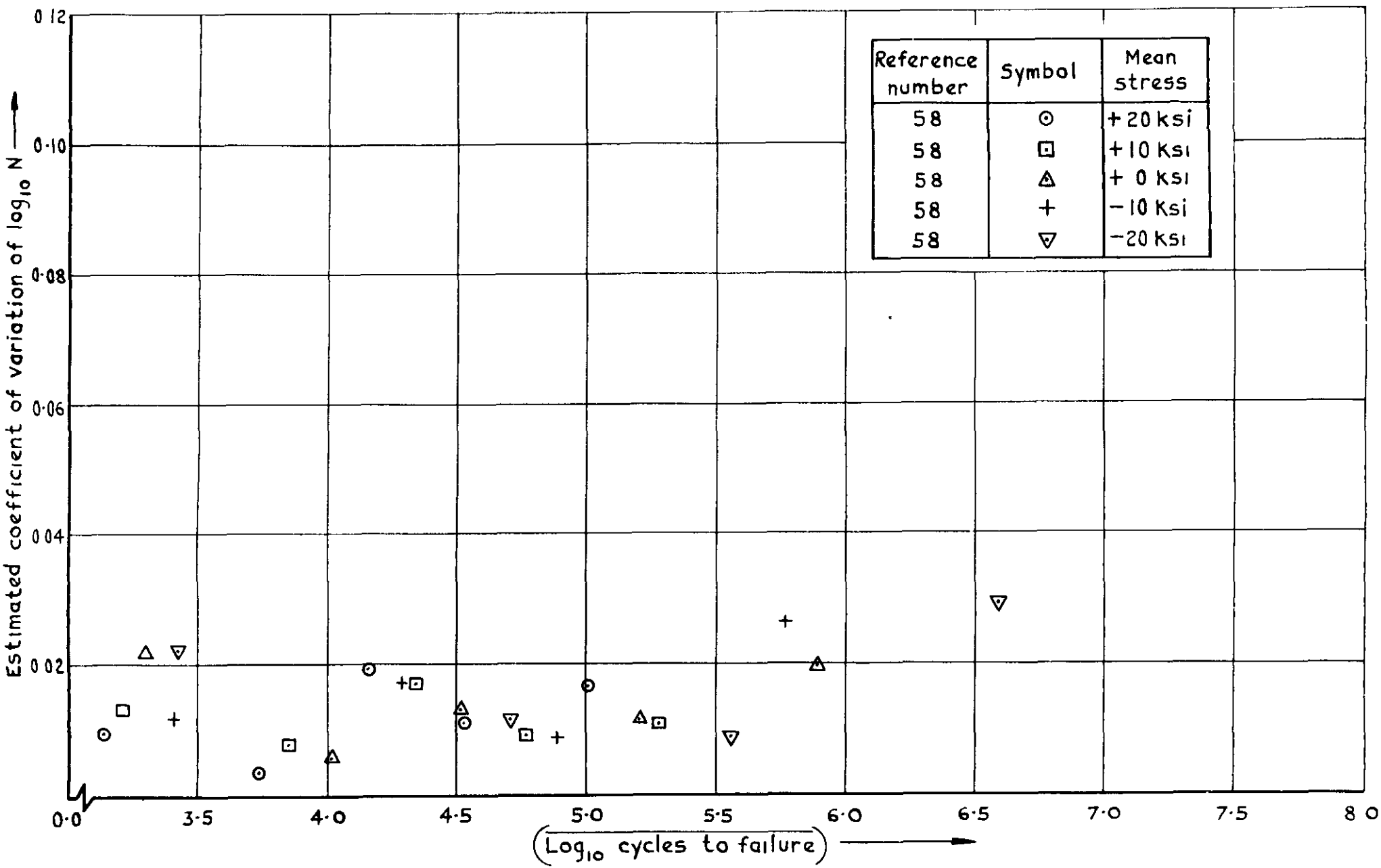

Fig. 29 Constant amplitude, axial load ref(58), centre notched 2024 material 0·032 in thick sheet $K_t = 2{\cdot}55$

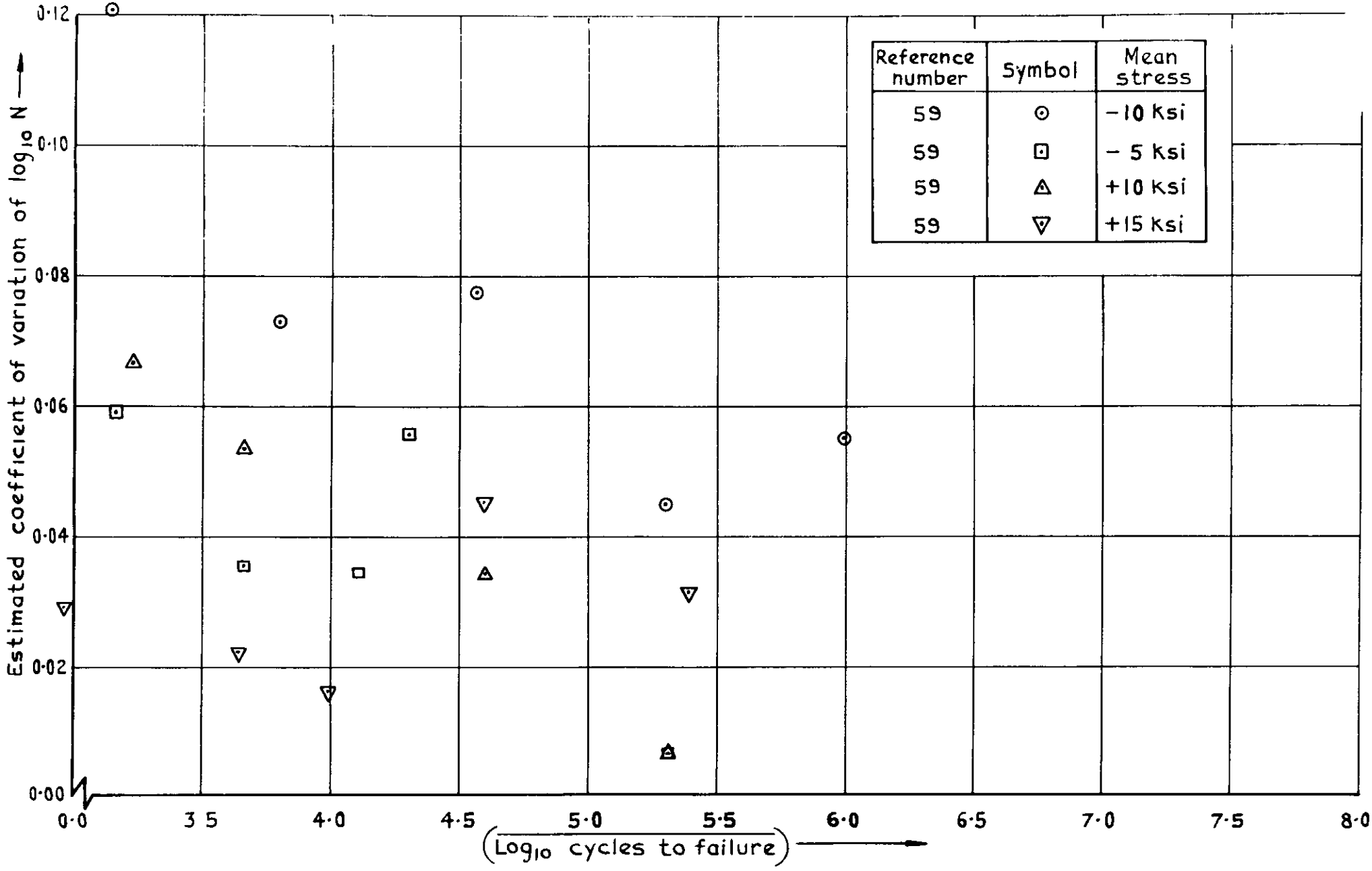

Fig. 30 Constant amplitude, axial load ref(59), notched 7075 material coupon $K_t = 3$

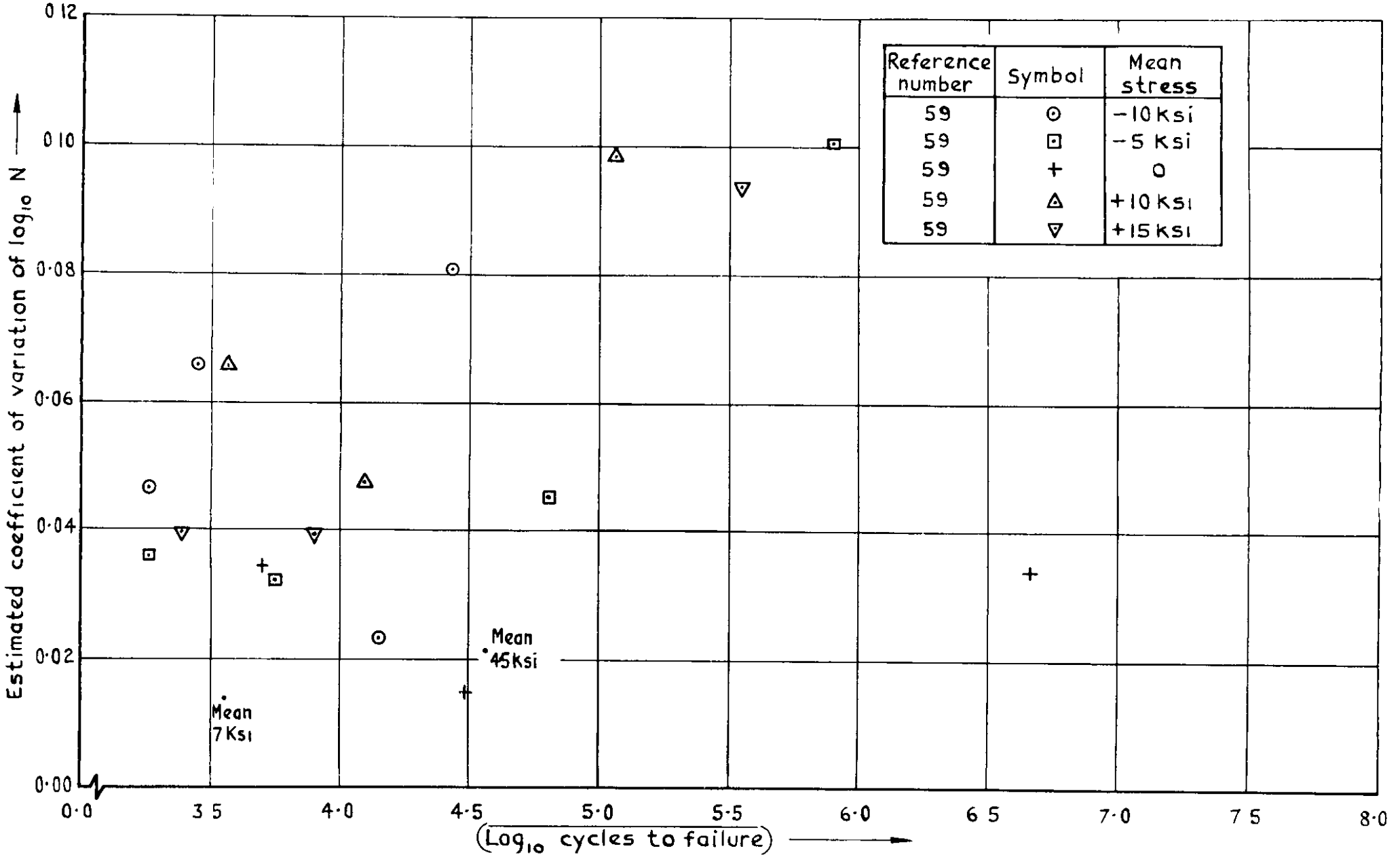

Fig.31 Constant amplitude, axial load ref (59), notched 7075 material coupon $K_t = 4{\cdot}0$

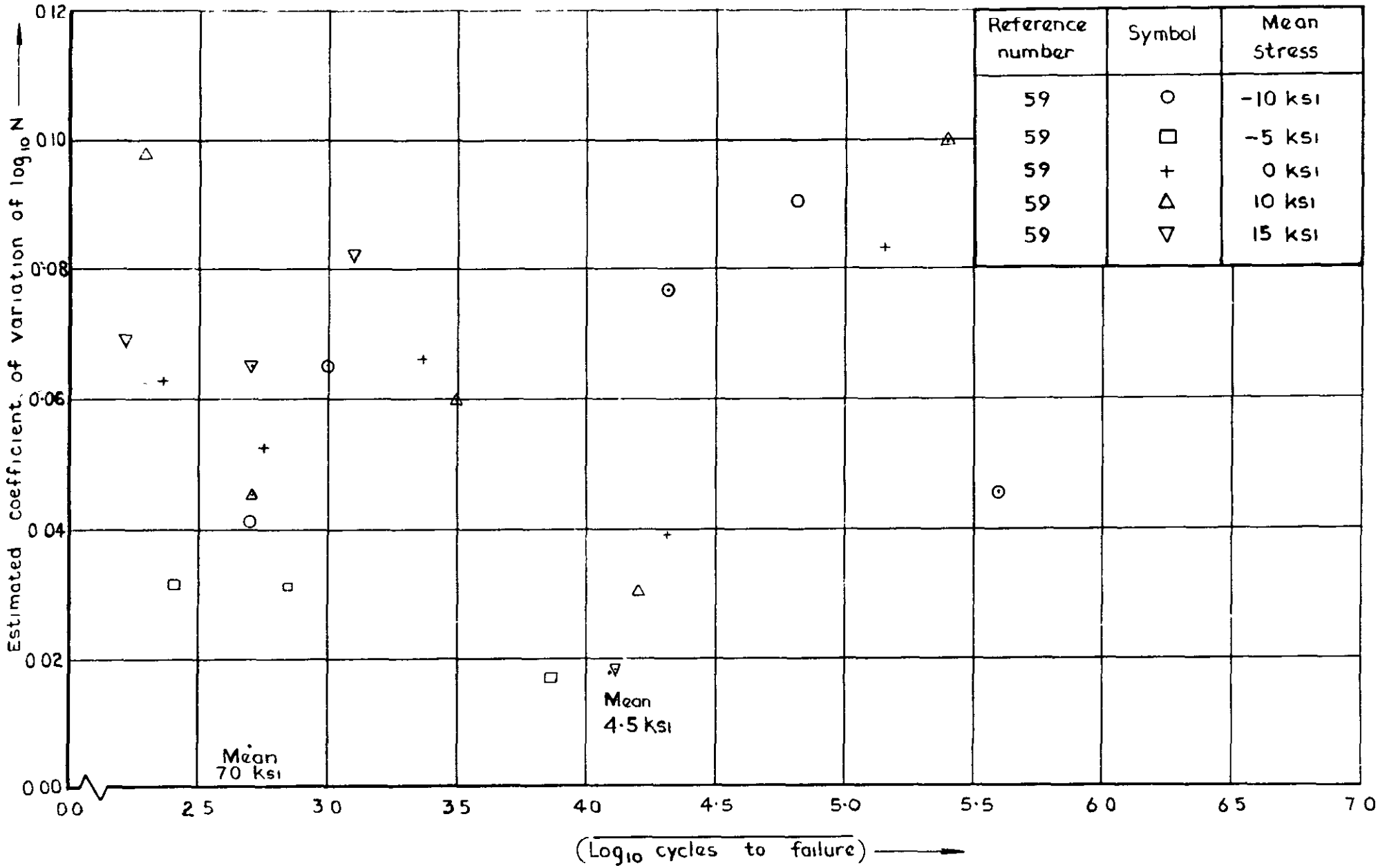

Fig 32 Constant amplitude, axial load ref (59) notched 7075 material coupon $K_t = 7.0$

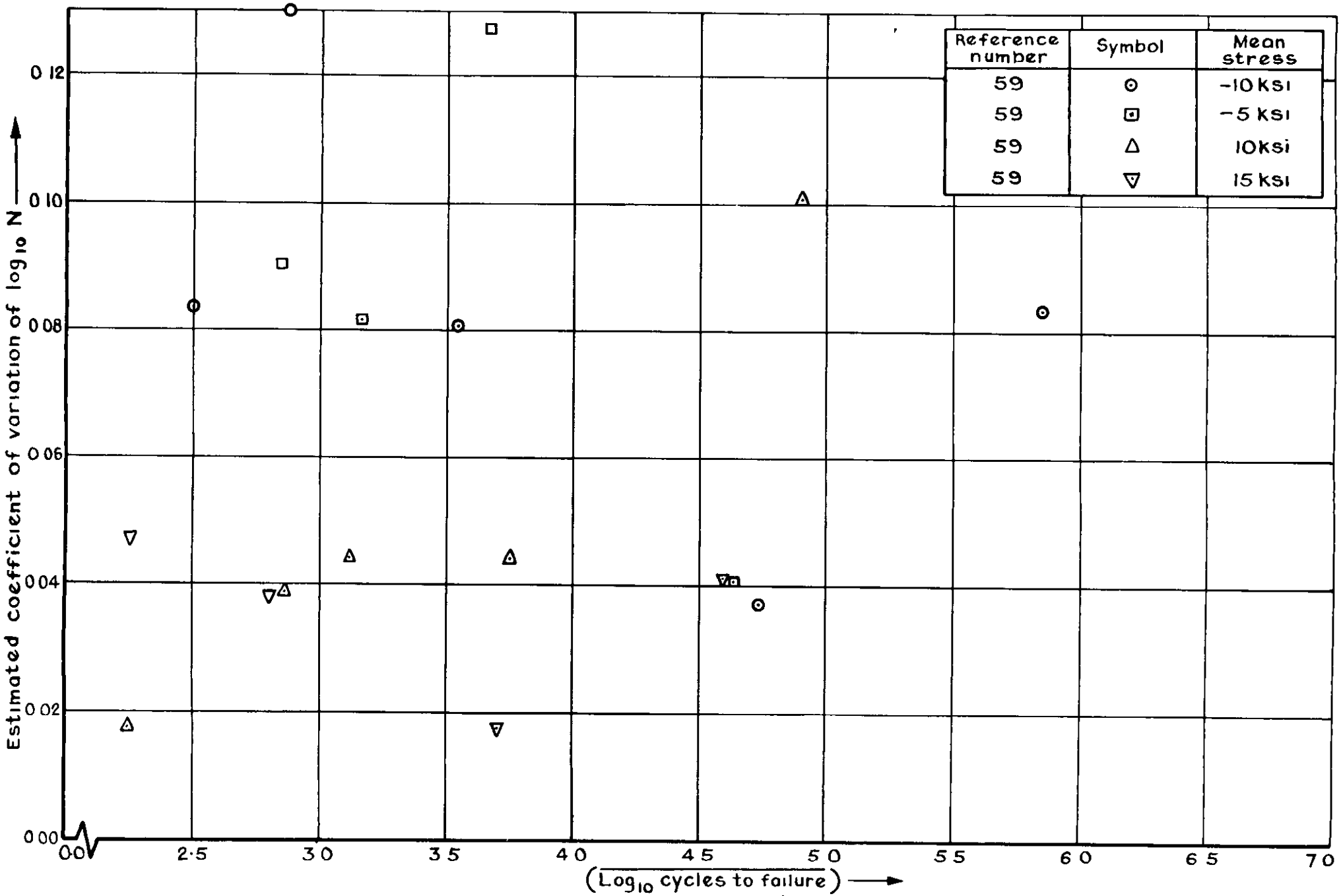

Fig. 33 Constant amplitude axial load ref (59) notched 7075 material coupon K_t=10 0

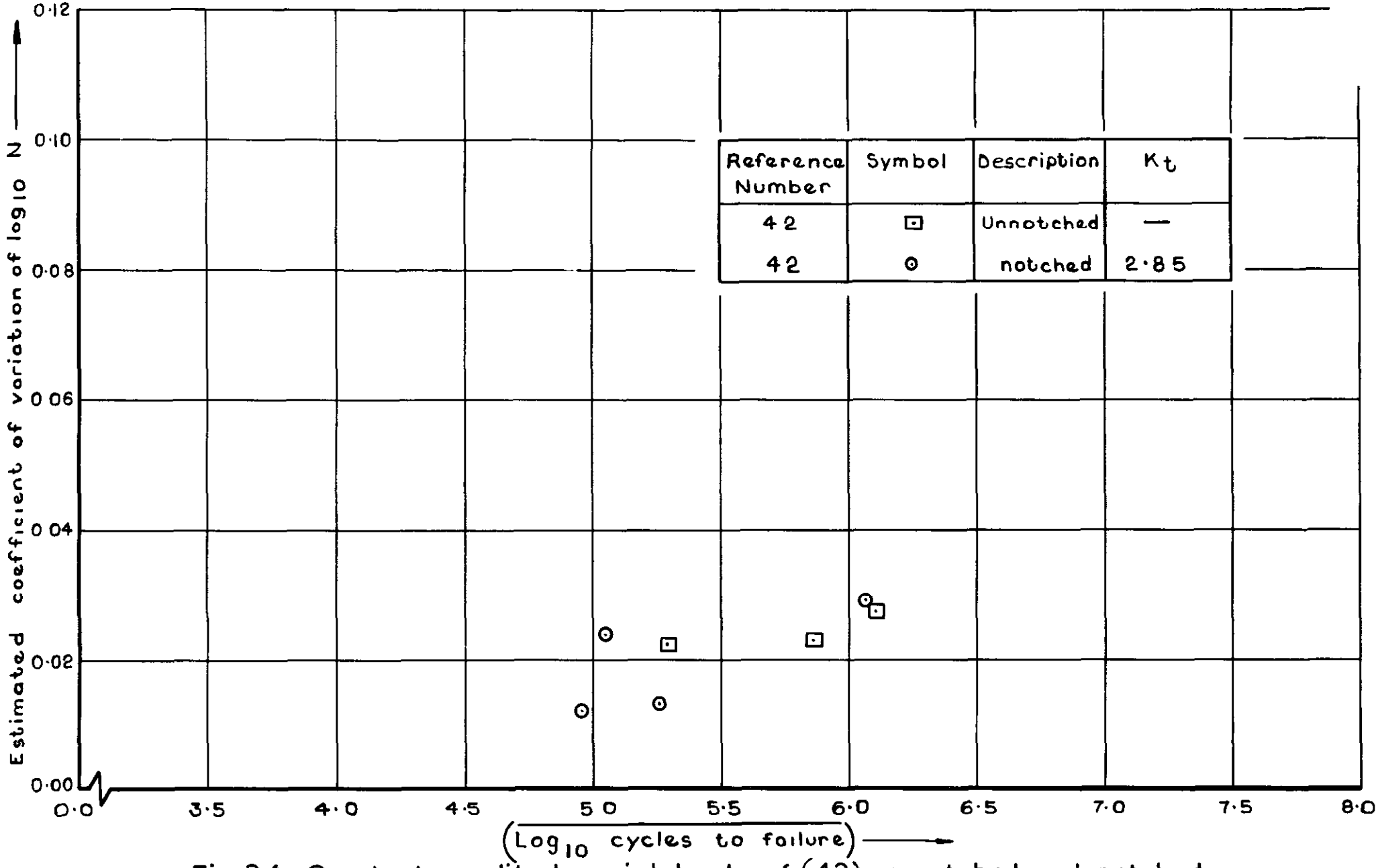

Fig 34 Constant amplitude axial load ref (42) unnotched and notched 2024 sheet material R=O

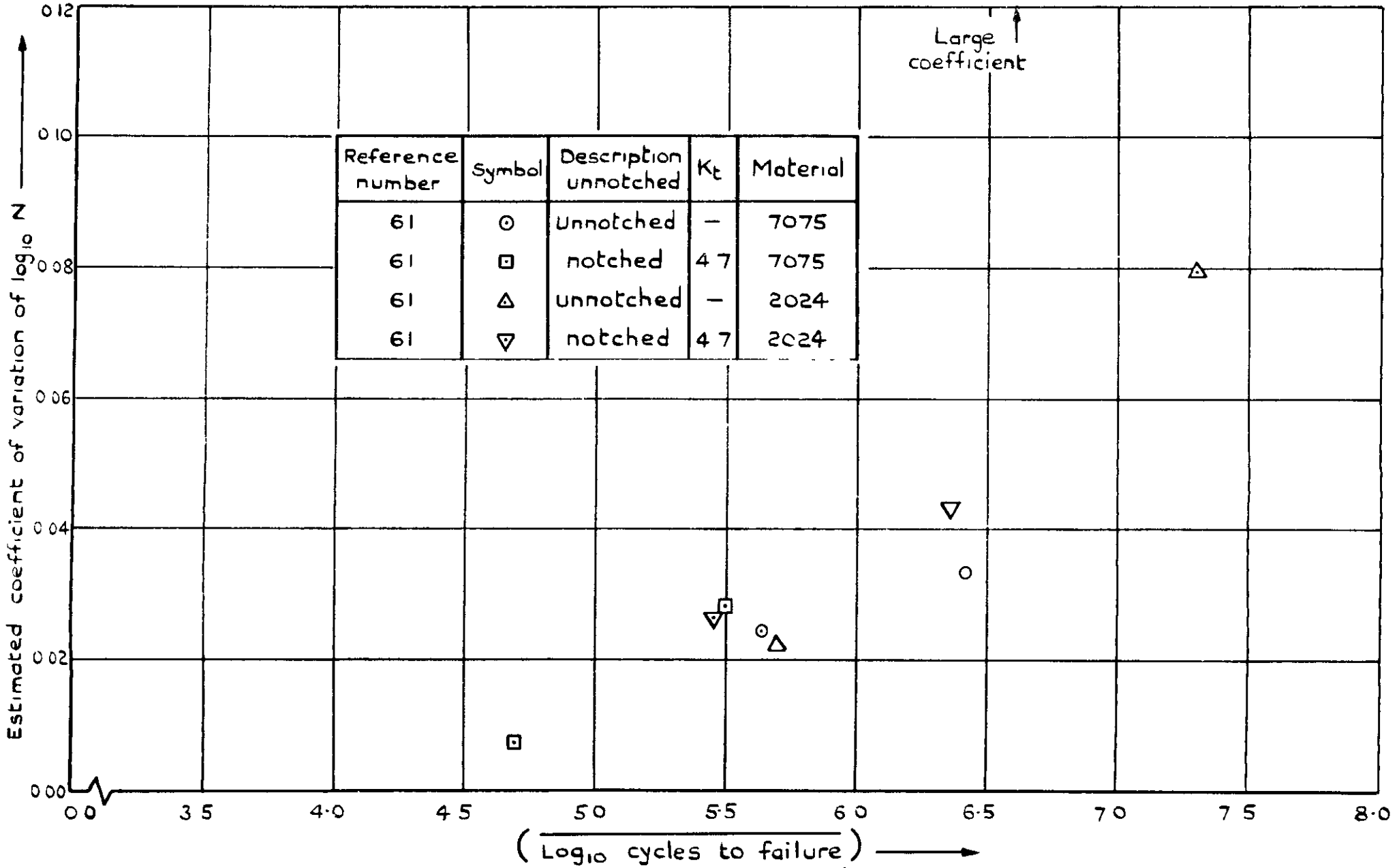

Fig. 35 Constant amplitude axial load ref (61) unnotched and notched 7075 and 2024 sheet material

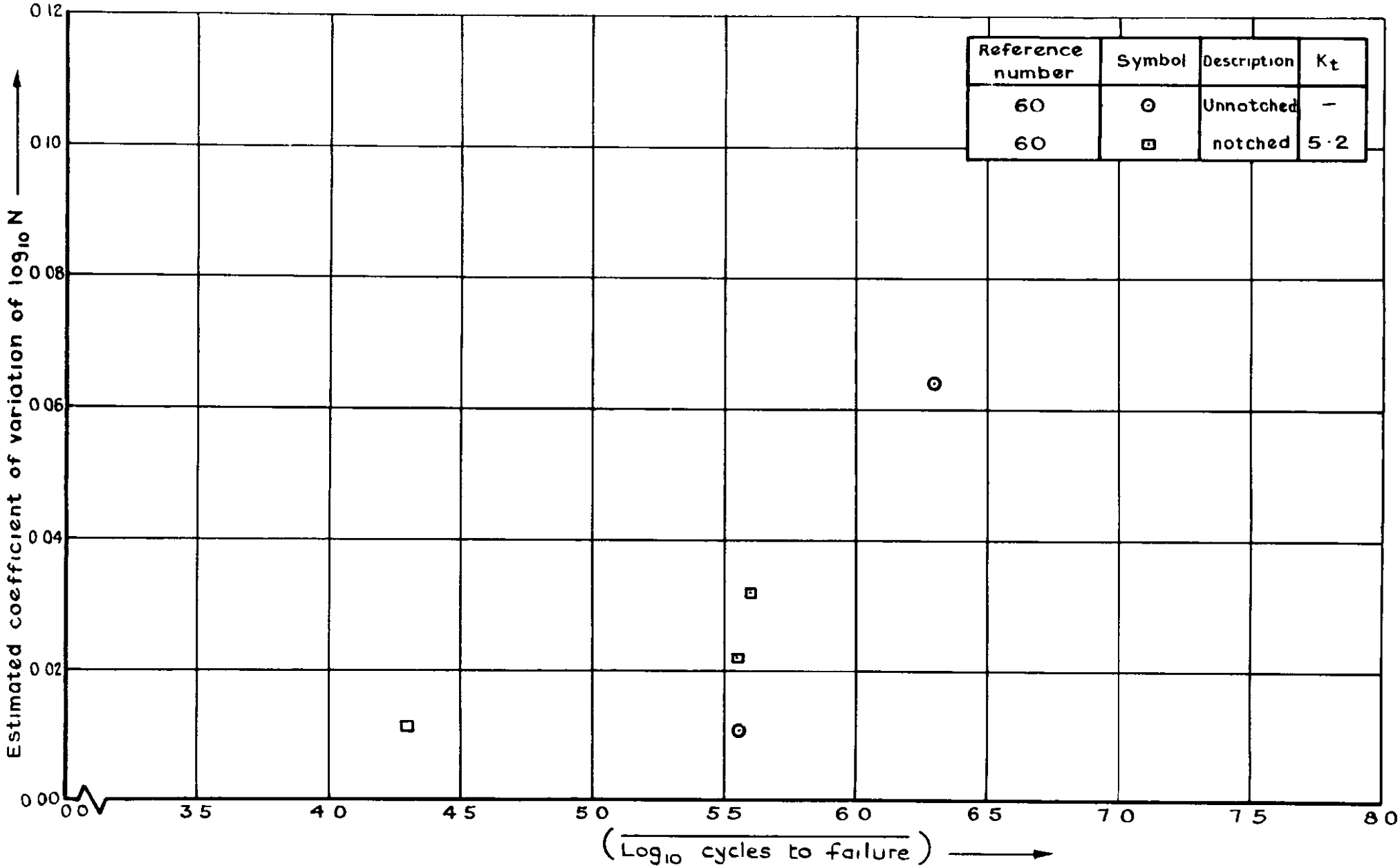

Fig.36 Constant amplitude rotating bending ref (60) unnotched and notched 2024 material bar form $\frac{1}{4}$" dia

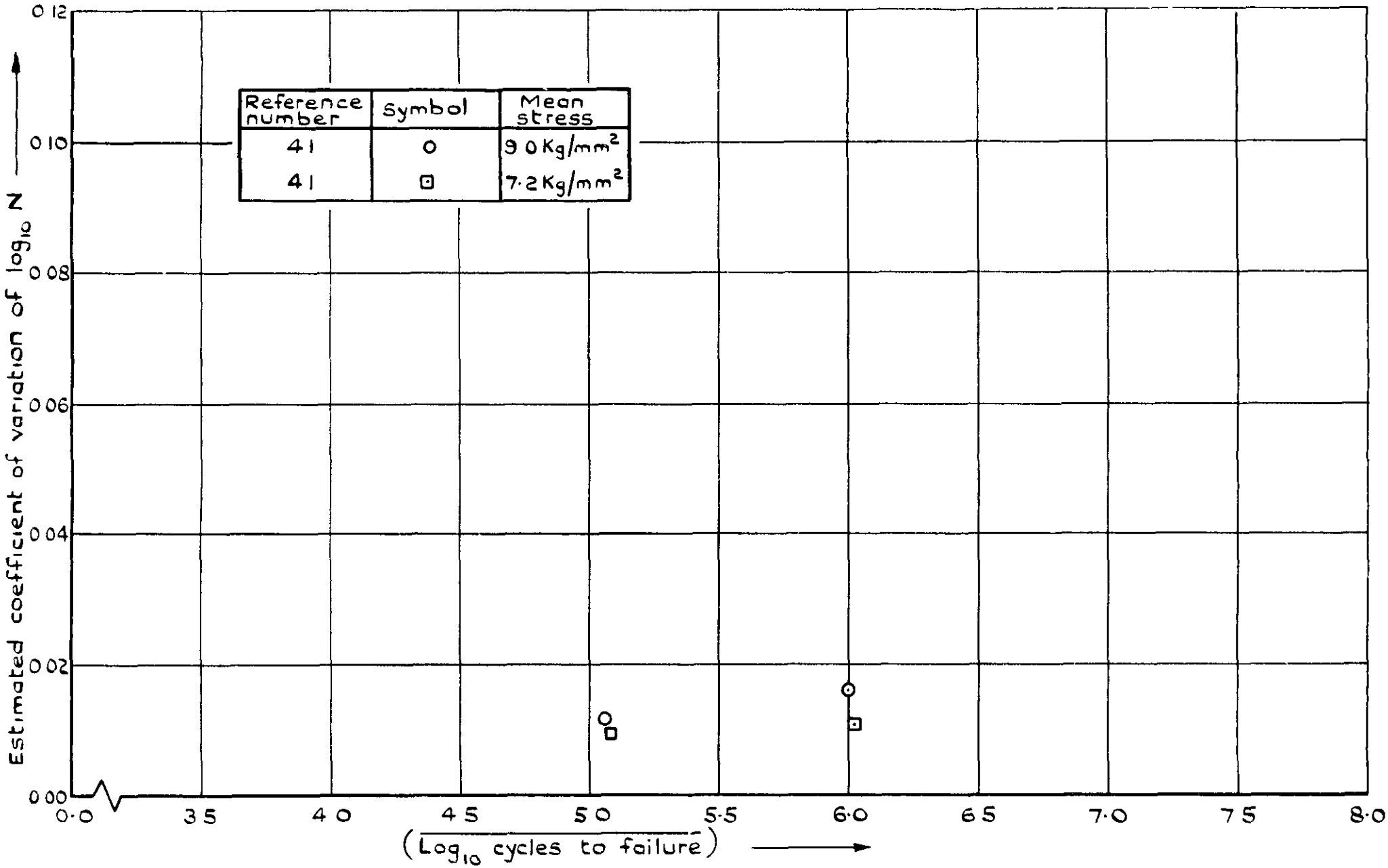

Fig 37 Constant amplitude axial load ref (41) riveted joint of 2024 material

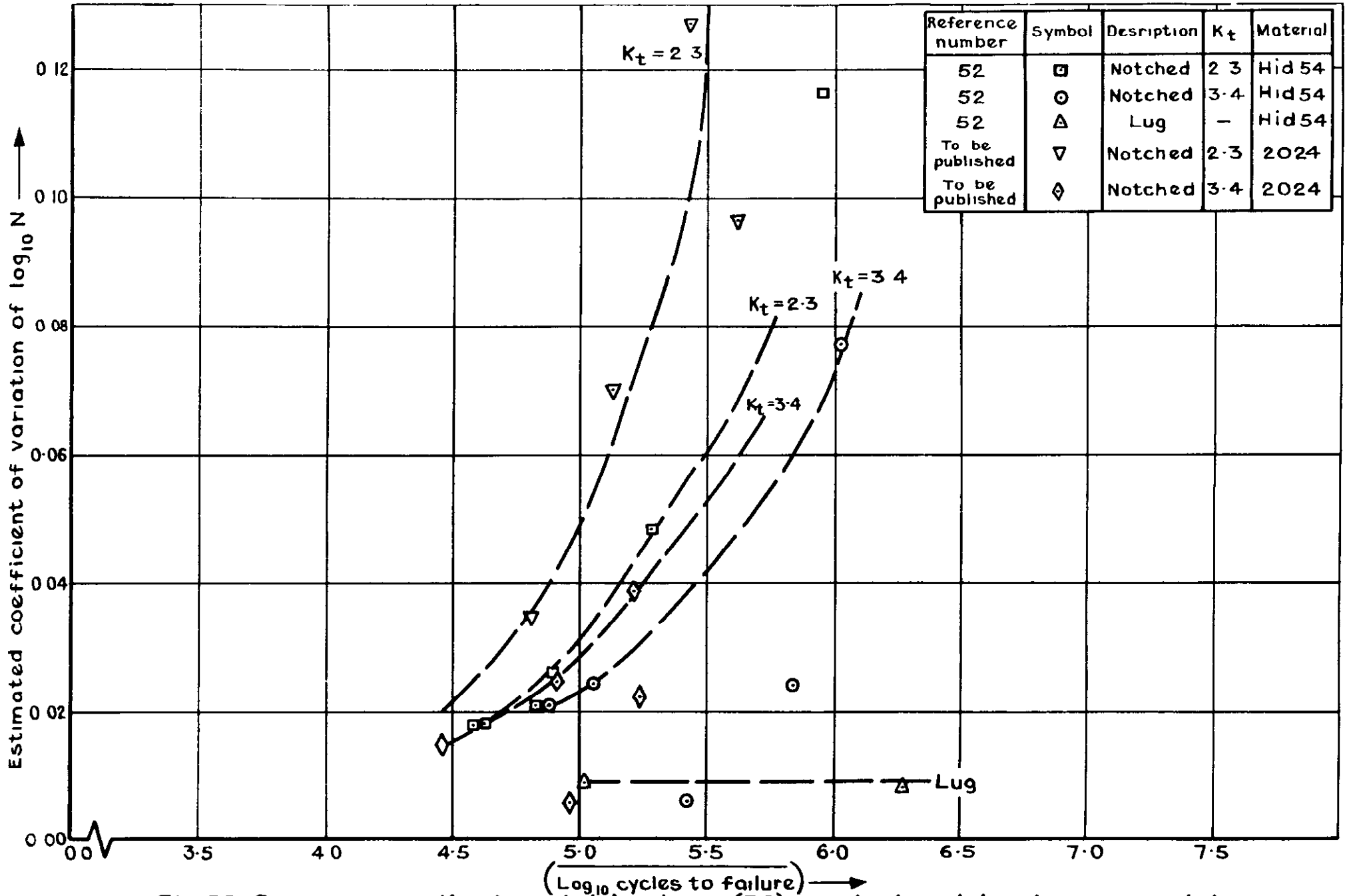

Fig. 38 Constant amplitude axial load ref (52) notched and lug bar material

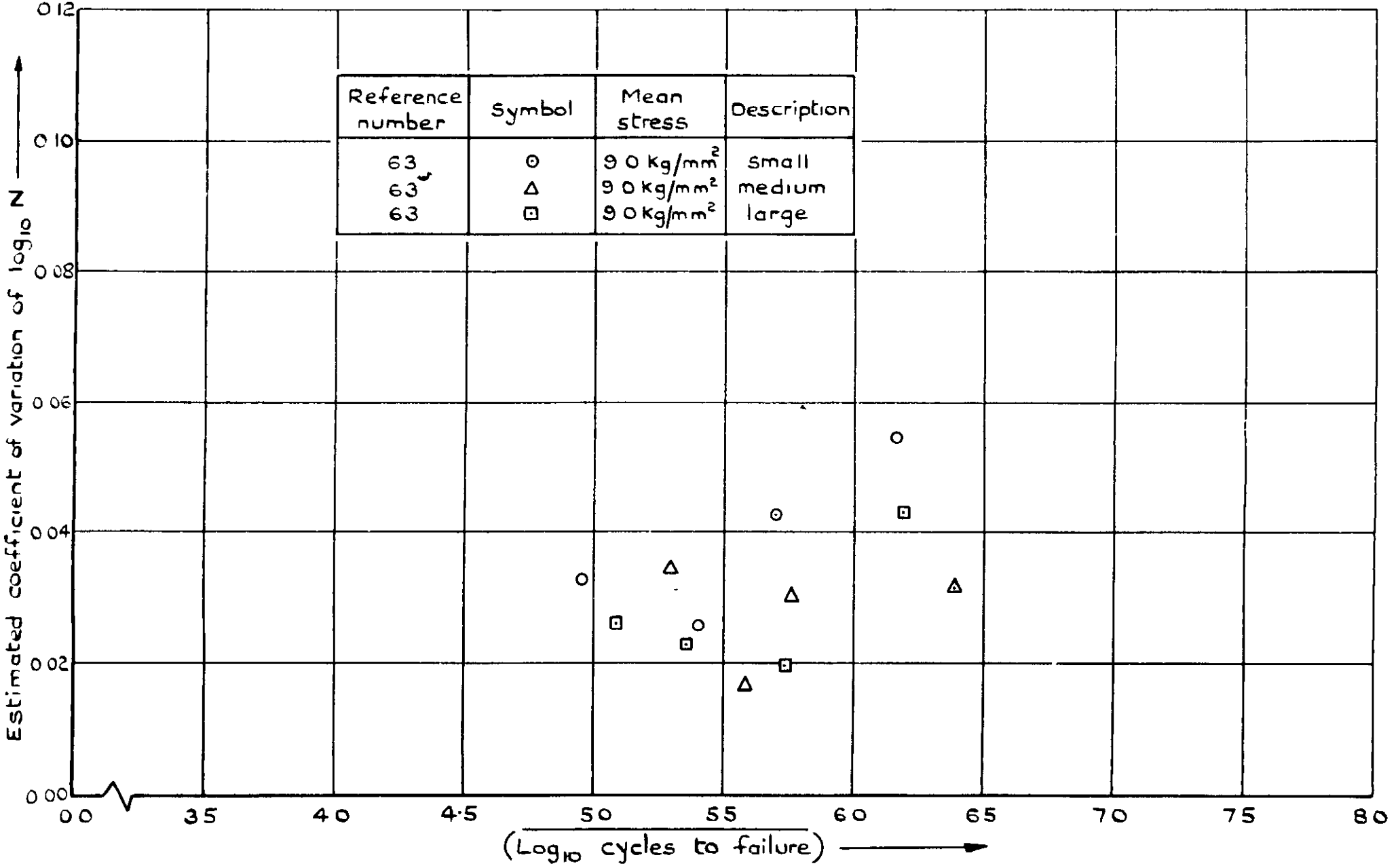

Fig. 39 Constant amplitude axial load ref (63) riveted joint of 2024 sheet material

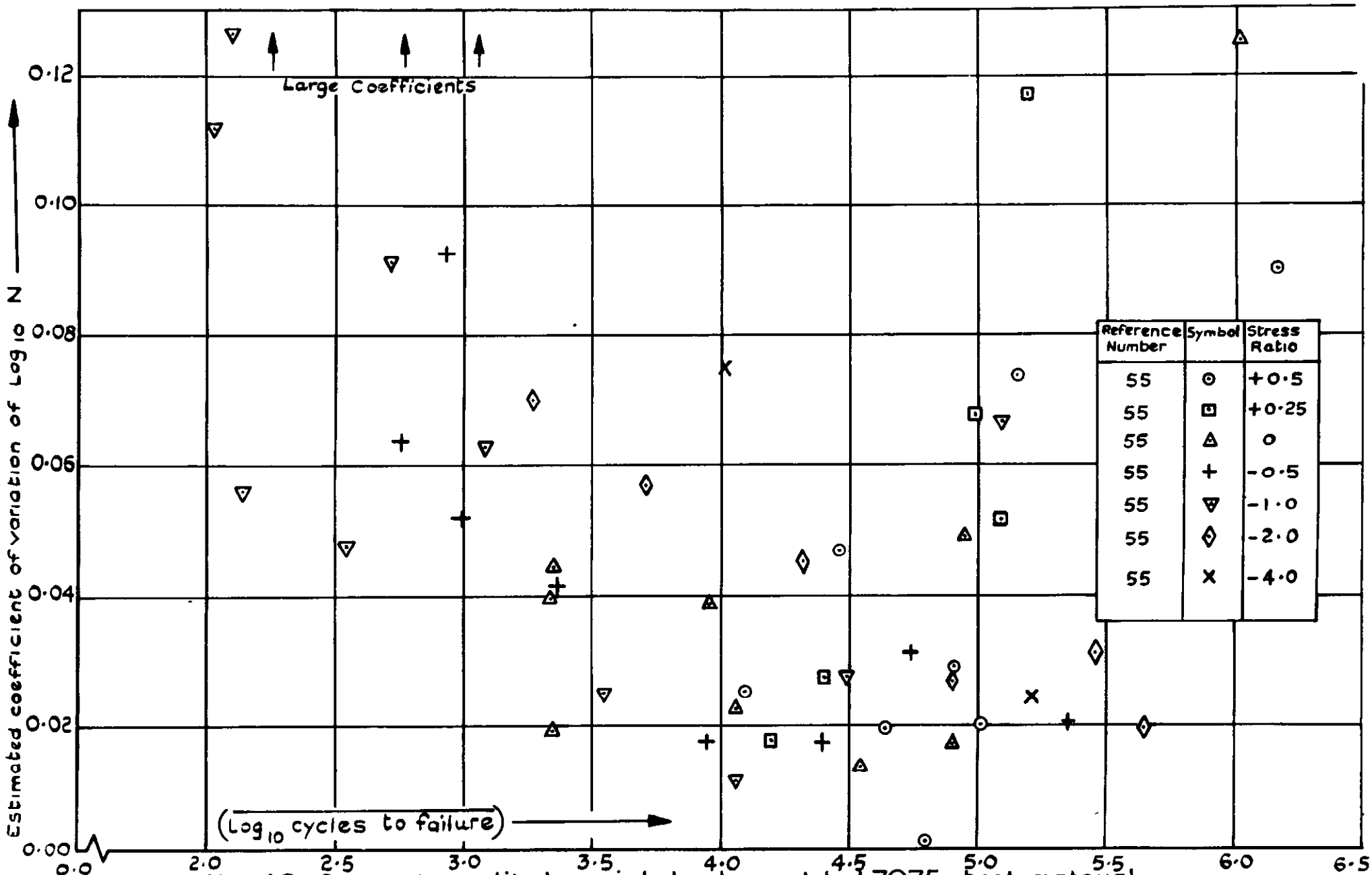

Fig. 40 Constant amplitude axial load unnotched 7075 sheet material
(Sets of tests conducted at constant stress ratio = $\frac{\text{minimum stress}}{\text{maximum stress}}$)

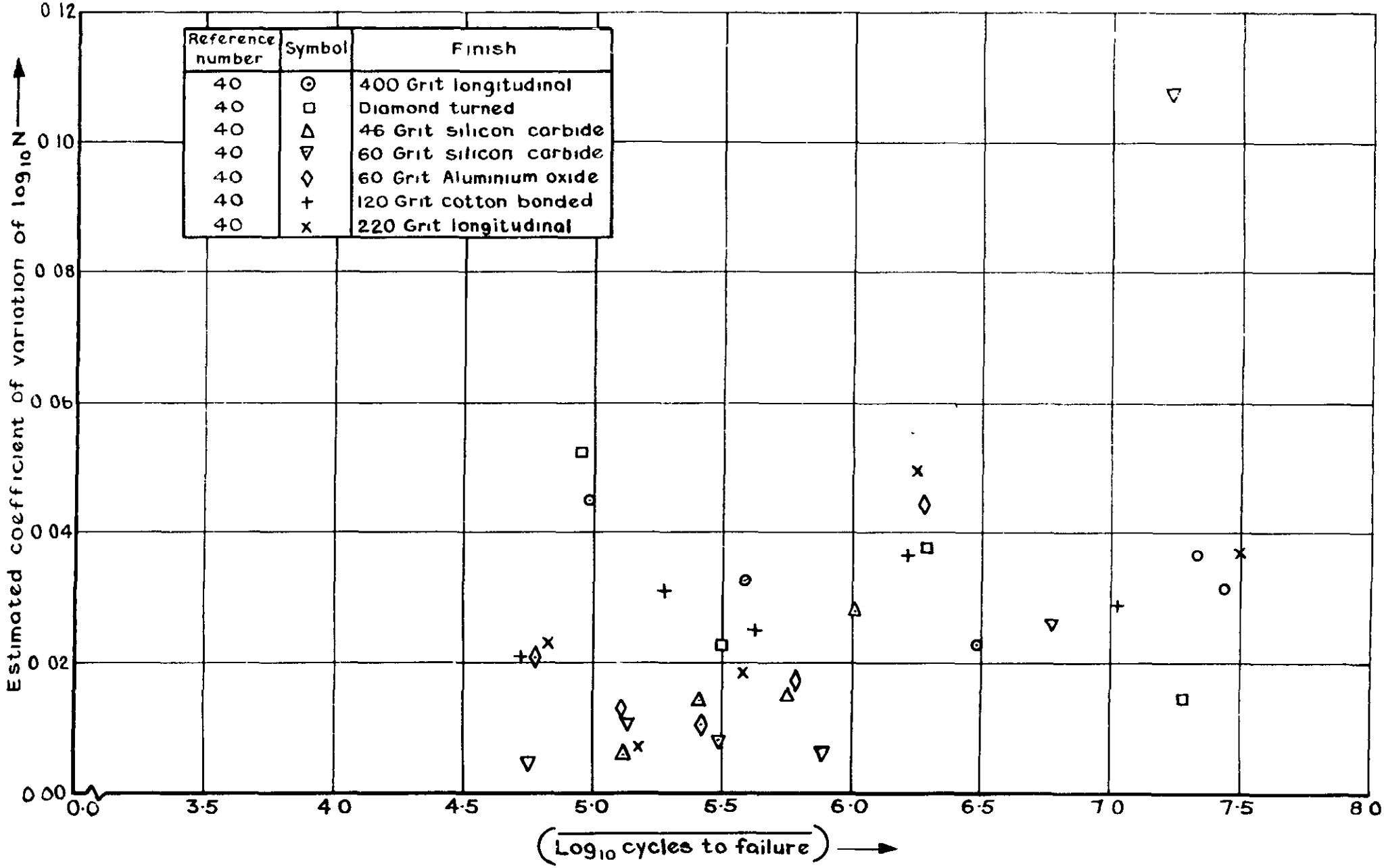

Fig. 41 Constant amplitude rotating bending ref (40) unnotched 2024 material

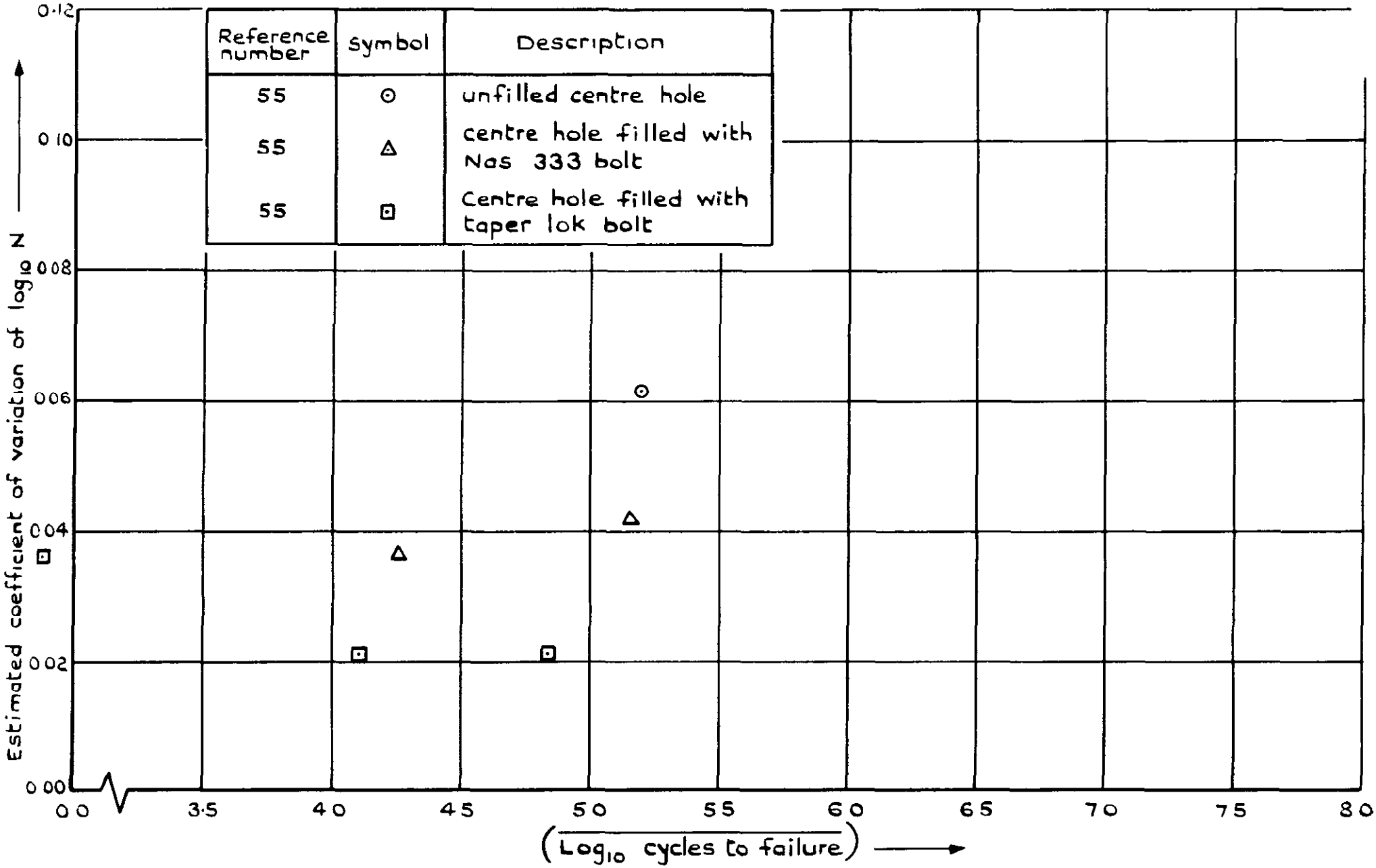

Fig. 42 Constant amplitude axial load ref (55) notched 7075 material sheet form

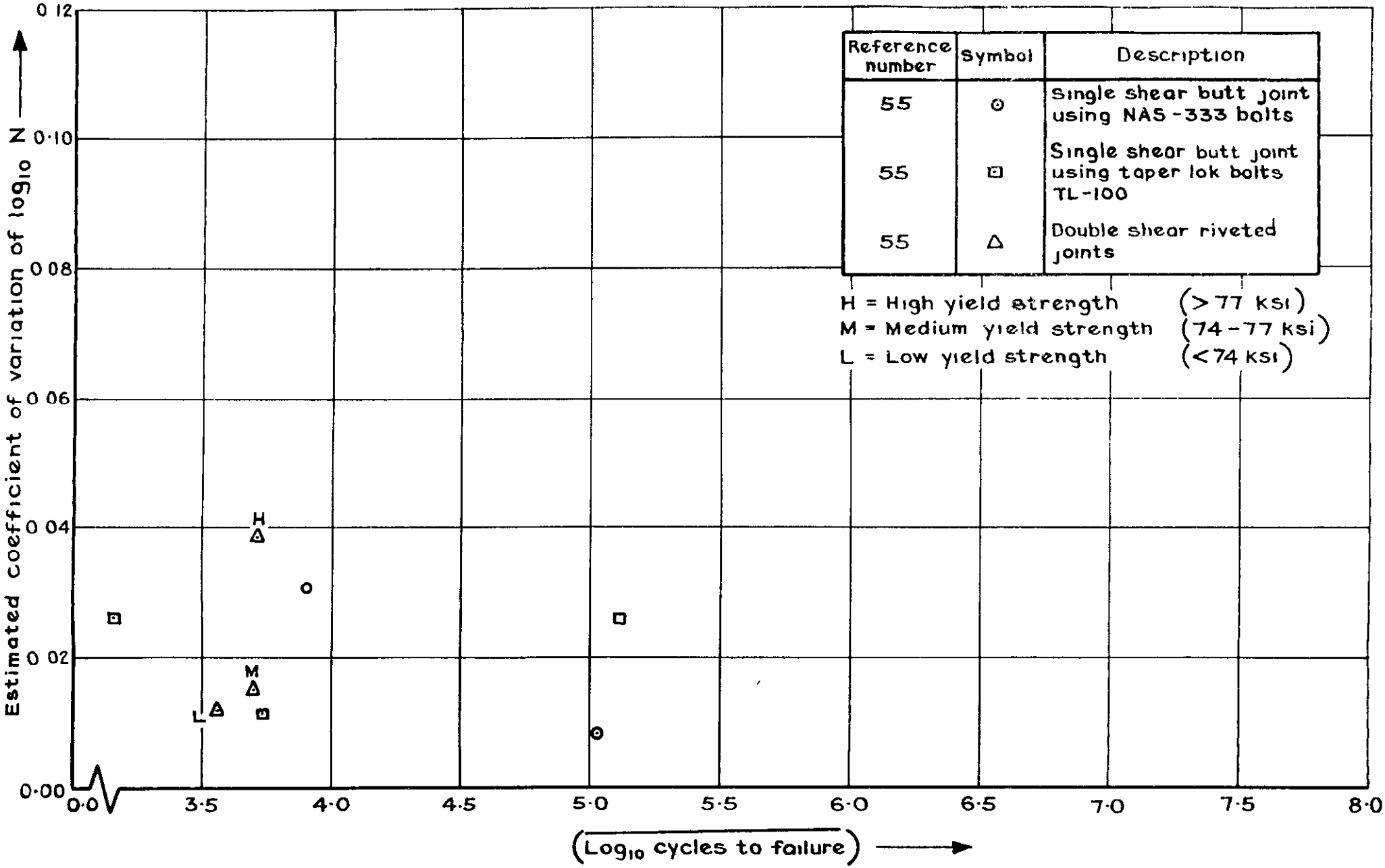

Fig. 43 Constant amplitude axial load ref (55) butt joints of 7075-sheet material

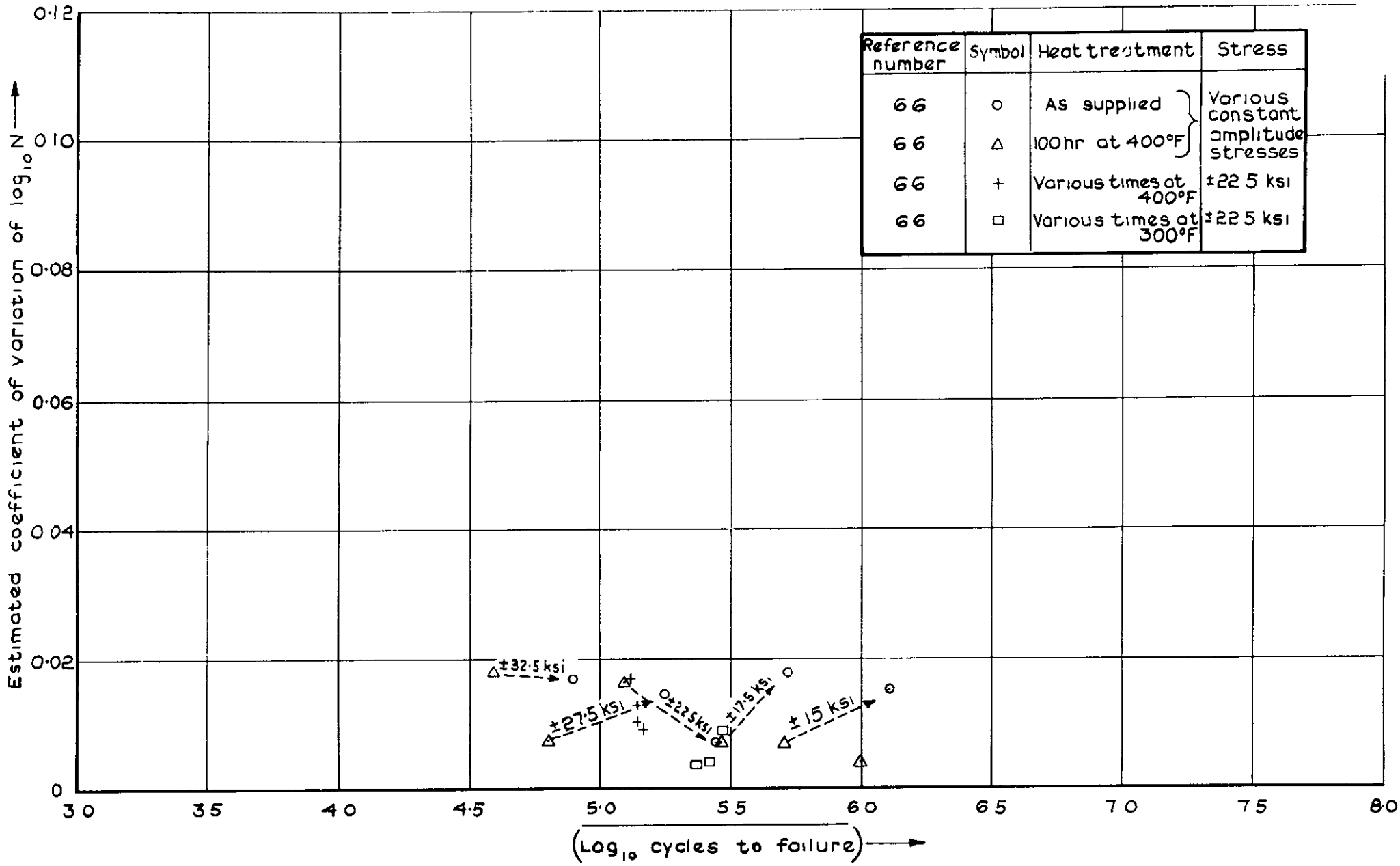

Fig. 44 Constant amplitude reversed bending unnotched 2024 material

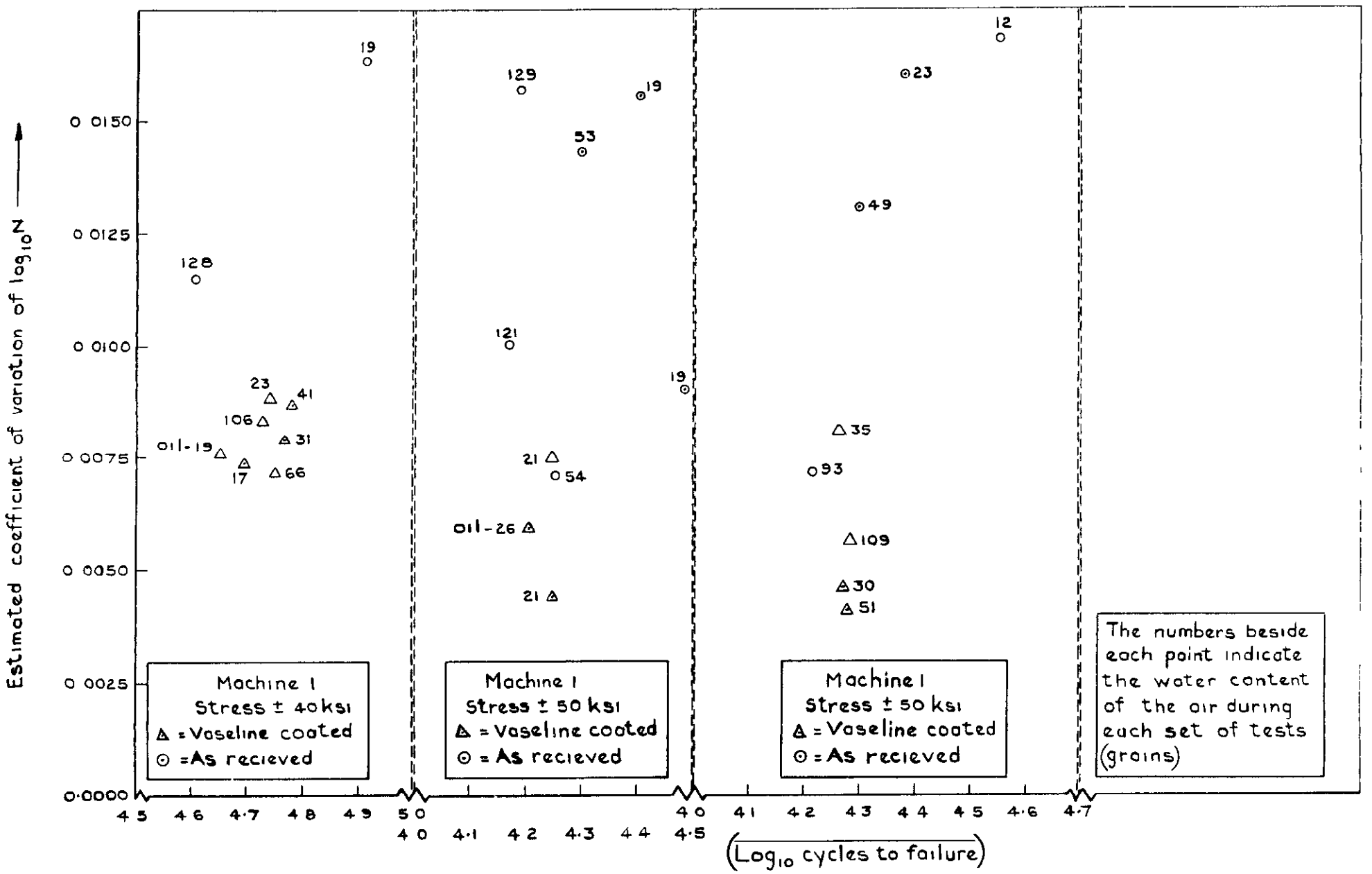

Fig. 45 Constant amplitude rotating bending ref 15 unnotched wire specimens of 7075 material

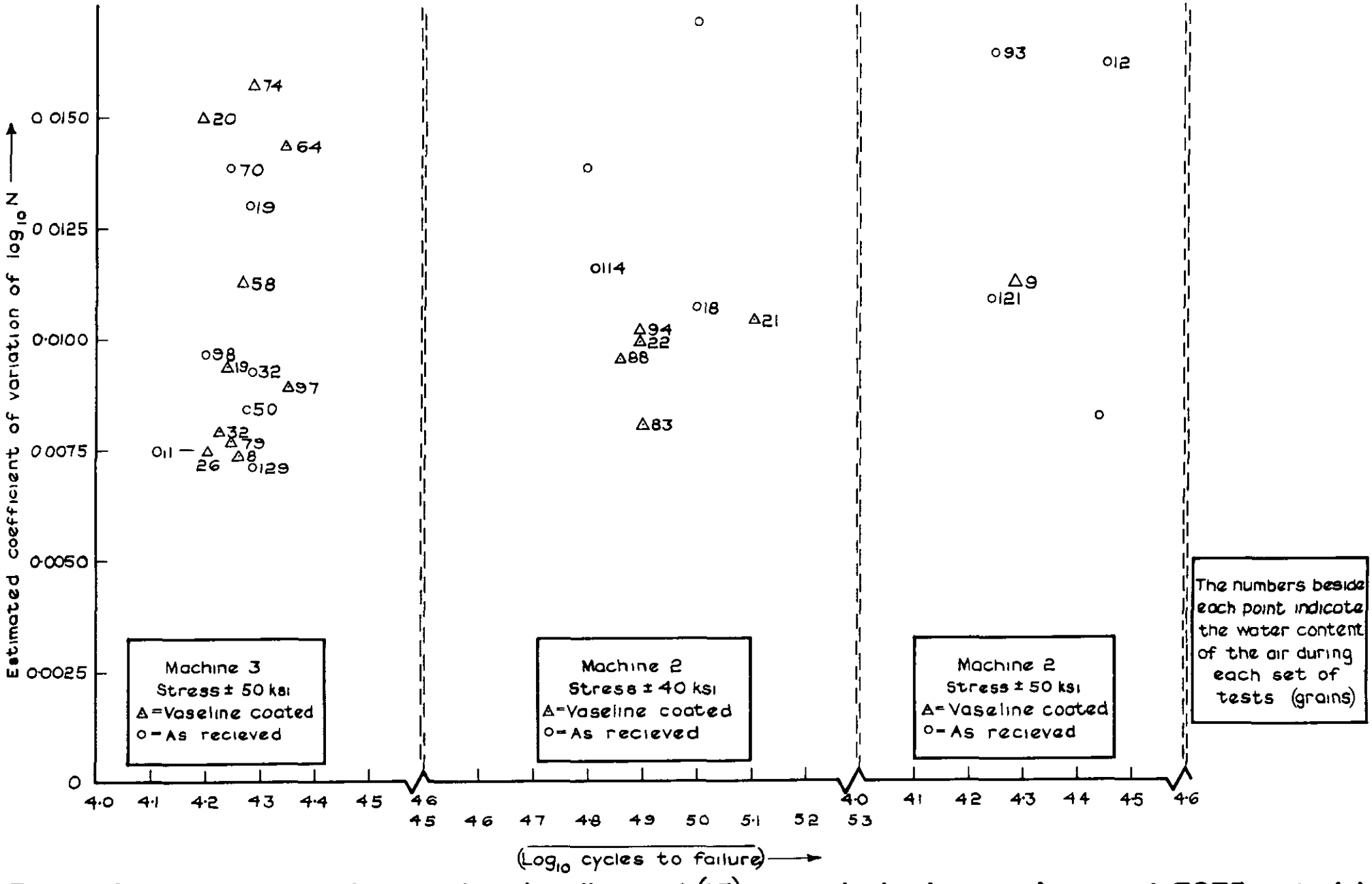

Fig.46 Constant amplitude rotating bending ref (15) unnotched wire specimens of 7075 material

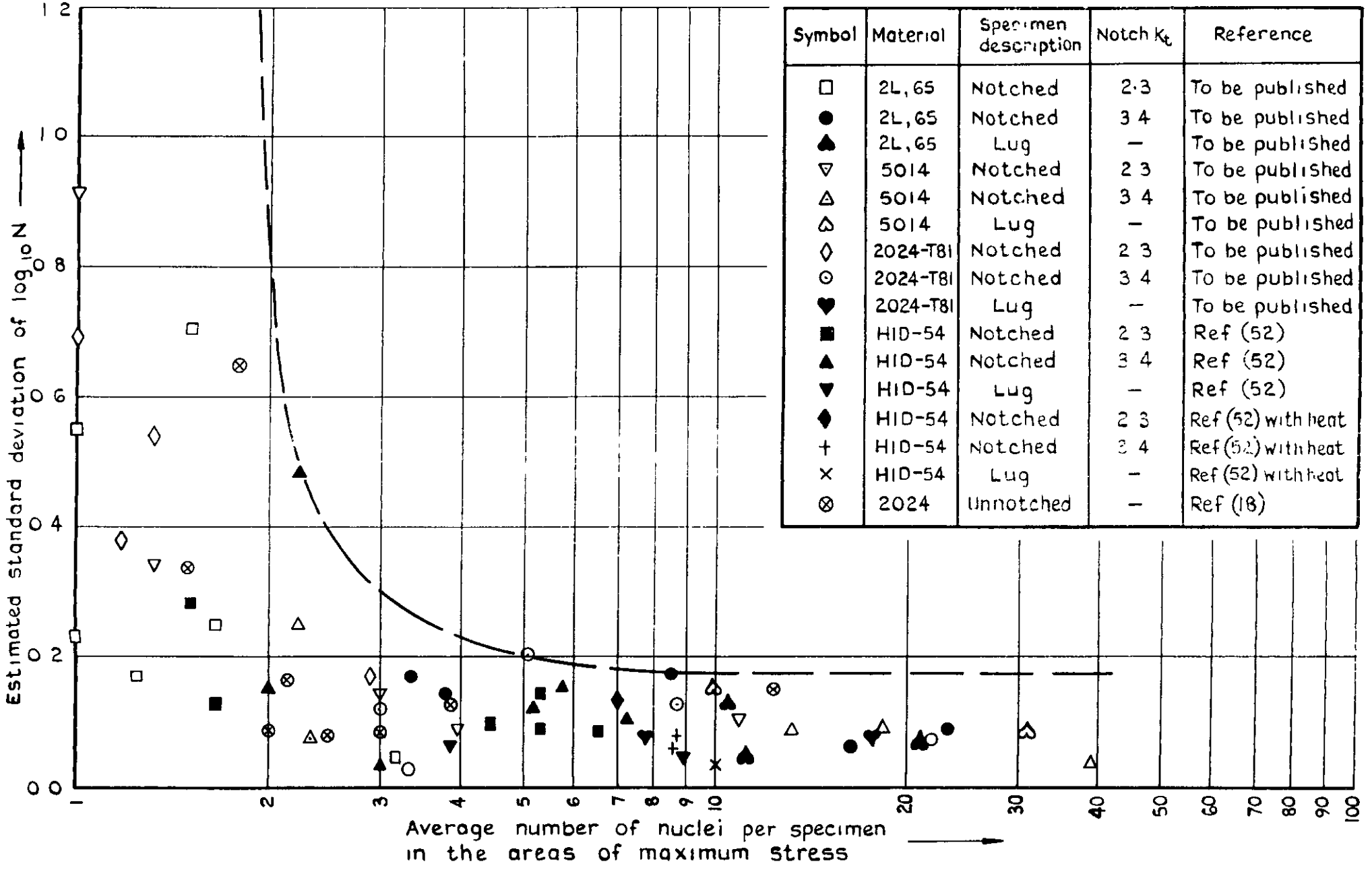

Symbol	Material	Specimen description	Notch K_t	Reference
□	2L,65	Notched	2·3	To be published
●	2L,65	Notched	3 4	To be published
▲	2L,65	Lug	—	To be published
▽	5014	Notched	2 3	To be published
△	5014	Notched	3 4	To be published
⌓	5014	Lug	—	To be published
◇	2024-T81	Notched	2 3	To be published
⊙	2024-T81	Notched	3 4	To be published
♥	2024-T81	Lug	—	To be published
■	HID-54	Notched	2 3	Ref (52)
▲	HID-54	Notched	3 4	Ref (52)
▼	HID-54	Lug	—	Ref (52)
◆	HID-54	Notched	2 3	Ref (52) with heat
+	HID-54	Notched	3 4	Ref (52) with heat
×	HID-54	Lug	—	Ref (52) with heat
⊗	2024	Unnotched	—	Ref (18)

Fig.47 Constant amplitude, axial load, several materials. Correlation of scatter with the number of crack nuclei

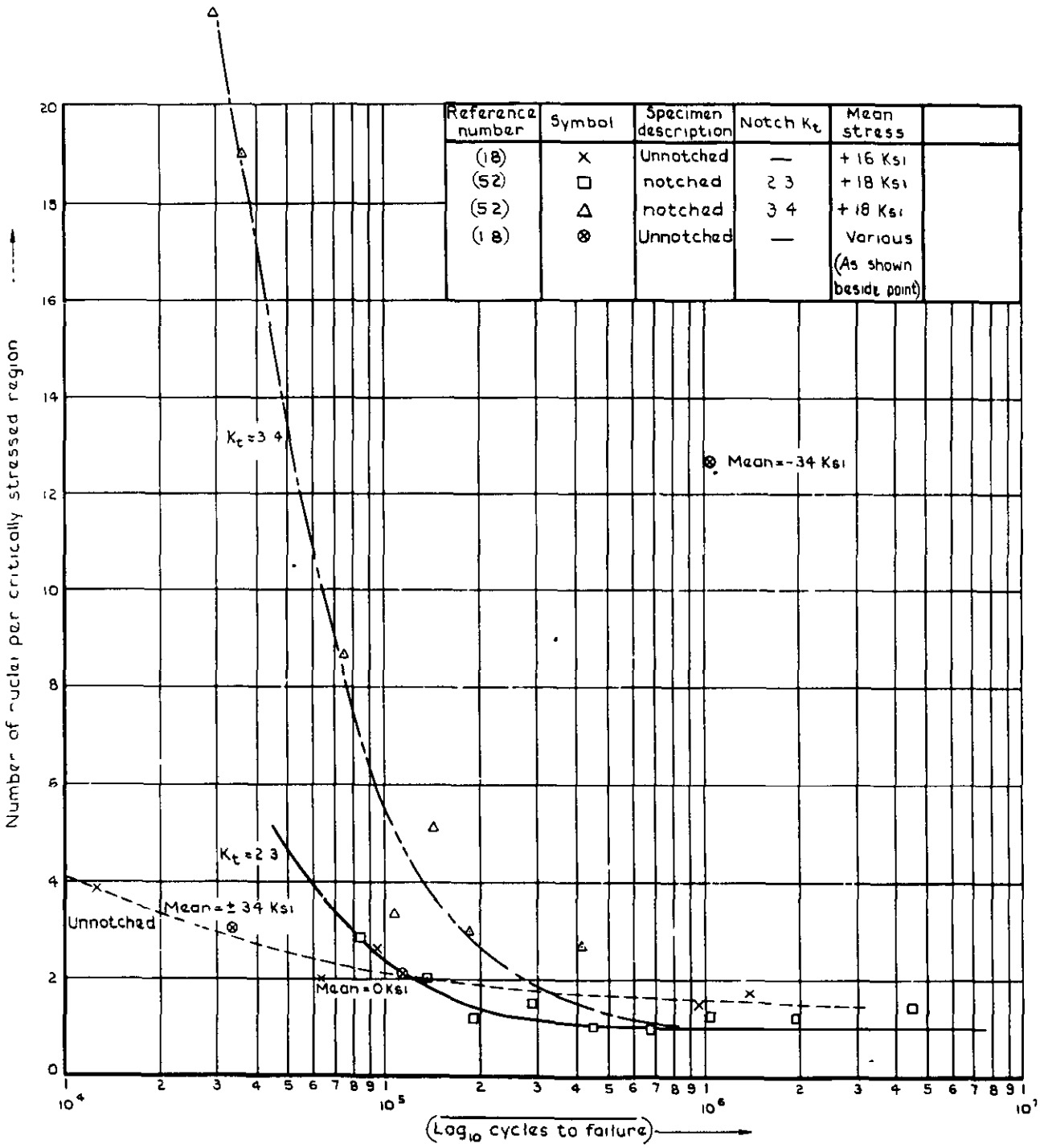

Fig 48 Constant amplitude, number of nuclei per specimen against life; bar specimens of 2024 material

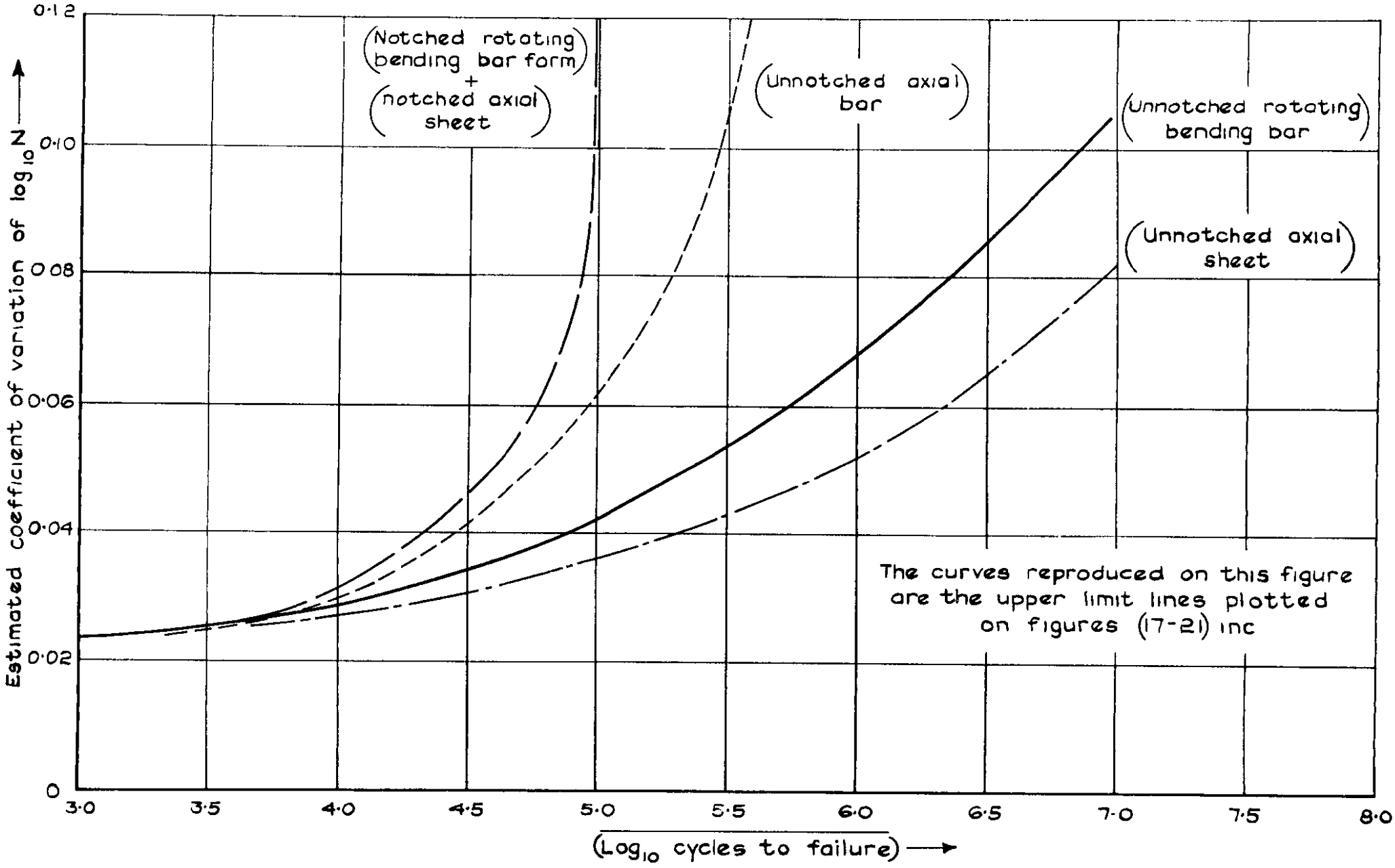

Fig. 49 Constant amplitude 7075 material

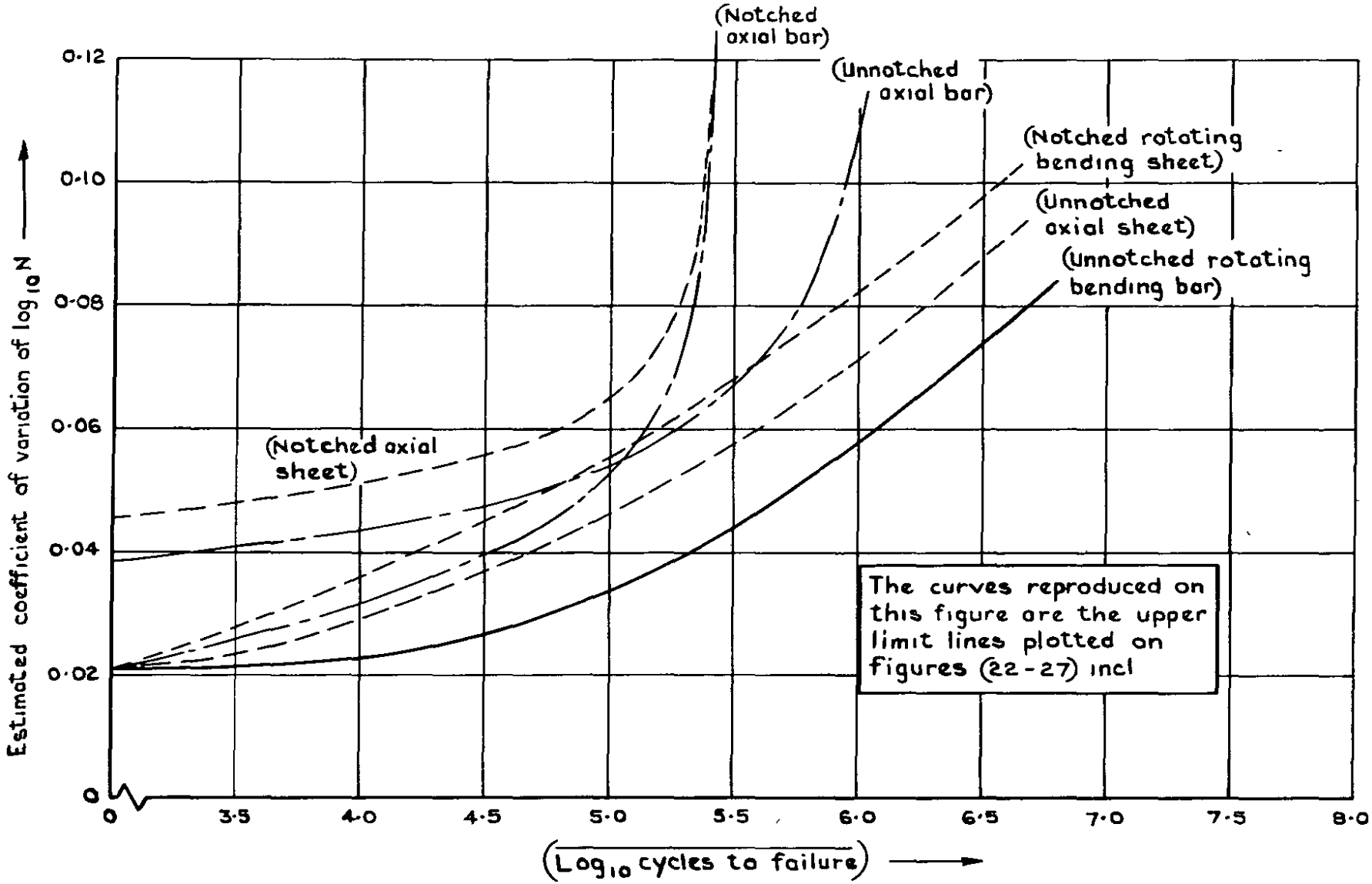

Fig.50 Constant amplitude 2024 material

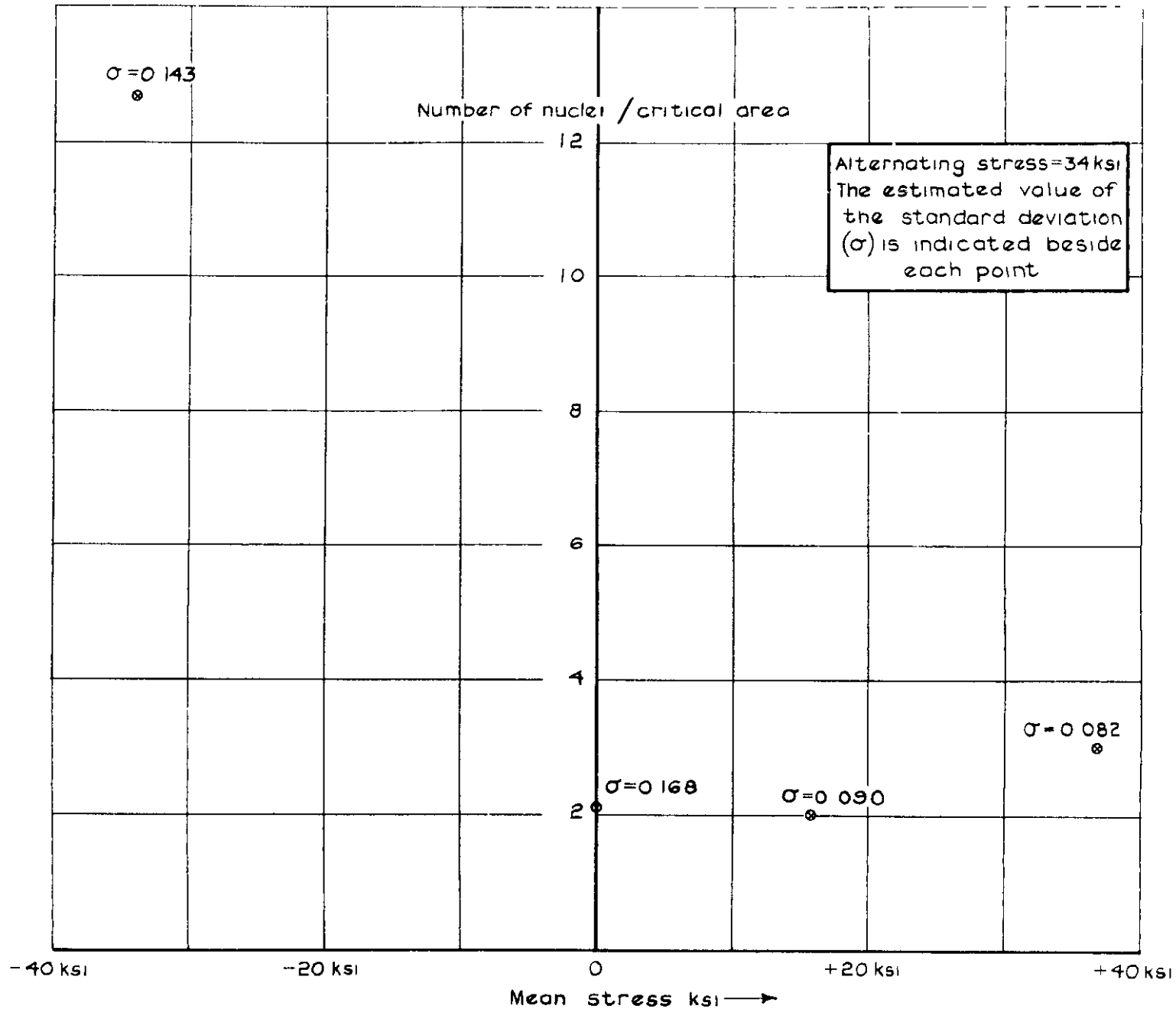

Fig. 51 Constant amplitude axial load ref (18) unnotched 2024 material bar form

Printed in England for Her Majesty's Stationery Office by the Royal Aircraft Establishment, Farnborough. Dd.146915. K.4.

DETACHABLE ABSTRACT CARD

A.R.C. C.P. No. 1093
April 1969

620.178.3 :
539.431 :
669.715

Stagg, A. M.

AN INVESTIGATION OF THE SCATTER IN CONSTANT AMPLITUDE FATIGUE TEST RESULTS OF ALUMINIUM ALLOYS 2024 AND 7075

A brief review of some of the investigations that have been conducted in the past into the form of the distribution of constant amplitude fatigue test results is presented and is followed by an analysis of a large amount of constant amplitude data for 2024 and 7075 materials collected from a variety of sources. This analysis, in terms of a log-normal distribution of life, confirms that the amount of scatter obtained in fatigue results increases with a decrease in the alternating stress amplitude. Further a comparison of the scatter for the two materials is made and the effects on the scatter of such parameters as notch acuity and mean stress are investigated. The discussion is in terms of a simplified model of the

(over)

A.R.C. C.P. No. 1093
April 1969

620.178.3 :
539.431 :
669.715

Stagg, A. M.

AN INVESTIGATION OF THE SCATTER IN CONSTANT AMPLITUDE FATIGUE TEST RESULTS OF ALUMINIUM ALLOYS 2024 AND 7075

A brief review of some of the investigations that have been conducted in the past into the form of the distribution of constant amplitude fatigue test results is presented and is followed by an analysis of a large amount of constant amplitude data for 2024 and 7075 materials collected from a variety of sources. This analysis, in terms of a log-normal distribution of life, confirms that the amount of scatter obtained in fatigue results increases with a decrease in the alternating stress amplitude. Further a comparison of the scatter for the two materials is made and the effects on the scatter of such parameters as notch acuity and mean stress are investigated. The discussion is in terms of a simplified model of the

(over)

fatigue mechanism and indicates a possible correlation between the amount of scatter and the number of crack nuclei present in a specimen.

fatigue mechanism and indicates a possible correlation between the amount of scatter and the number of crack nuclei present in a specimen.

Published by
HER MAJESTY'S STATIONERY OFFICE

To be purchased from
49 High Holborn, London W C 1
13a Castle Street, Edinburgh EH 2 3AR
109 St. Mary Street, Cardiff CF1 1JW
Brazennose Street, Manchester 2
50 Fairfax Street, Bristol BS1 3DE
258 Broad Street, Birmingham 1
7 Linenhall Street, Belfast BT2 8AY
or through any bookseller

C.P. No. 1093

SBN 11 470293 4